CHAPTER 6

METEOROLOGY AND HYDROLOGY

CONTENTS

6. METEOROLOGY AND HYDROLOGY

6.1 Summary

Bhutan is situated between latitude 26.7° and 28.4°N, and longitude 22.7° and 92.2°E. The area is 46,620 km^2. Maximum north-south distance is 170 km and east-west distance is 300 km. The northern end of Bhutan forms the border with China and its altitude is over 7,000 m. There are some glaciers and glacier lakes over 4,000 m area of the region. On the other hand, the southern end of Bhutan forms the border with India and its altitude is less than 200 m.

The Punatsangchhu originates in the Himalayas of northwestern Bhutan and flows down to south. The river is formed by the Mochhu and the Phochhu which join at Punakha and flows into the Brahmaputra river at Assam State in India. The Punatsangchhu is called the "Sankosh River" in India, and the total length is approximately 320 km.

Based on the isohyetal map issued by SoB, annual precipitation of the upstream area ranges from 400 to 600 mm, and the midstream area including Punakha and Wangdue Phodrang ranges from 700 to 900 mm in the Punatsangchhu basin. However there are some areas whose annual precipitations are over 2,000 mm on the steep slope from midstream to upstream of the basin. The downstream area near the border with India belongs to subtropical zones and its annual precipitation ranges 3,000 to 5,000 mm. The rainy season affected by monsoon is 4 months ranging from June to September in the basin.

The highest temperature is over 30°C in August as against the lowest one of approximately 0°C in January in the midstream area including the project site near Wangdue Phodrang. The largest discharge is approximately 1,200 m^3/s in rainy season as against the smallest one of 60 m^3/s in dry season at the project site.

6.2 Meteorological and Hydrological Stations

6.2.1 Meteorological Stations

Meteorological observation has been carried out by DoP in the Punatsangchhu basin. The data of 10 meteorological stations, Gasa, Punakha, Shelgana, Wangdi, Gaselo, Basochhu, Tashithang, Damphu, Sonkosh, Drujeygang are available.

The locations of these stations are shown in Fig. 6.1. Table 6.1 shows the period and kind of the data of each station.

Wangdi and Damphu are Class A stations which were installed in 1991 when BHUTAN POWER SYSTEM MASTER PLAN (hereinafter referred to as "Master Plan") financed by IBRD had been carried out.

Wind velocity and direction, evaporation, sunshine duration and soil temperature in addition to rainfall, air temperature and humidity have been observed at the Class A stations. Wangdi meteorological station is located about 10 km upstream and nearest from the damsite of this project.

The hydrometeorological observation network has been established with installing SEBA's hydrological and meteorological equipment made in Germany during the Master Plan study in Bhutan.

6.2.2 Hydrological Stations

Discharge measurements have been carried out by DoP at 6 hydrological stations in the Punatsangchhu basin as shown in Fig. 6.1. There are 4 stations, Yebesa, Wangdi Rapids, Dubani and Kerabari on the main stream and 2 stations, Maza Fall and Toshiding on the tributaries.

Discharge data of Yebesa, Wangdi Rapids, Dubani and Maza Fall were collected for this study. Suspended load have been measured at Yebesa, Wangdi Rapids and Dubani. These data were also collected. The period and kind of data are shown in Table 6.1. Wangdi Rapids station is located about 9 km upstream and nearest from the damsite.

6.3 Discharge at the Project Site

6.3.1 Verification of Discharge Data at Wangdi Rapids Station

As shown in Fig. 6.1 Wangdi Rapids GS (Gauging Station) is located about 9 km upstream and nearest from the damsite. Therefore, discharge at the damsite was to be calculated using its data basically. The perfect discharge data for 8 years (1992-1999) are available at Wangdi Rapids GS. Average monthly discharges for a year are shown in Fig. 6.2.

To verify the consistency of the discharge data, the double mass curve with rainfall data in the basin was used. As shown in Fig. 6.3, it is not found any significant change of gradient and consequently the consistency of the discharge data was verified.

Further, in order to verify the climatic cycle, the spectrum analysis on rainfall data of 13 years was carried out, and the result is shown in Fig. 6.4. Power spectrum is not remarkable except for the

point of around frequency=0.08 (1/12). This shows that annual cycle is excelled compared with the cycle for several years; and thus long cycle for several years was not recognized.

6.3.2 Discharge at Damsite

As large tributaries aren't joining main stream of the Punatsangchhu between Wangdi Rapids GS and the damsite, discharge at the damsite was converted from the catchment area ratio of following formula.

$$Q_d = Q_g \cdot A_d/A_g$$

where,

Q_d : discharge at the damsite (m^3/s)

Q_g : discharge at Wangdi Rapids gauging station (m^3/s)

A_d : catchment area at the damsite (km^2)

A_g : catchment area at Wangdi Rapids gauging station (km^2)

	Wangdi Rapids GS	Damsite
Catchment Area : A (km^2)	5,640	5,796
Average Discharge : Q (m^3/s)	290	298

Firm discharge (95%) at the damsite was calculated to be 64.0 m^3/s.

6.4 Flood Discharge at the Project Site

6.4.1 Probable Flood

Based on maximum daily discharge for 8 years of 1992-1999, frequency analysis was carried out using the Gumbel distribution. The results are summarized in the tables below.

Probable Flood

Return Period (year)	5	10	20	50	100	200	1,000
Flood Discharge (m^3/s)	1,469	1,630	1,784	1,984	2,134	2,283	2,628

6.4.2 Probable Maximum Flood (PMF)

(1) General

As it is considered that this project will play a very important role for economical and social development of Bhutan, it will be appropriate to adopt the Probable Maximum Flood (PMF) in the design of the Punatsangchhu dam. PMF is defined as the flood that may be caused under the theoretical combination of the most severe meteorological and hydrological conditions.

PMF is calculated by following procedure.

- Calculation of Probable Maximum Precipitation (PMP)
- Preparation of Unit Hydrograph
- Distribution of PMP
- Synthesis of Unit Hydrographs
- Determination of Baseflow

(2) Calculation of Probable Maximum Precipitation (PMP)

PMP is generally classified as non-orographic and orographic precipitations. The form of precipitation in the Punatsangchhu basin is considered to have typical orographic characters. Because it is observed that precipitation caused by monsoon from the south is concentrated at the southern slope of the Himalayan range, while precipitation in the flat area as well as north of the Himalayan range is extremely small. Following are the process of estimating PMP in this study. (ref. Manual for Estimation of Probable Maximum Precipitation :WMO* No.332)

*WMO : World Meteorological Organization

1) Preparation of ground profile

The principal ground profiles at southern slope of the Himalayan range in the Punatsangchhu basin are prepared dividing 1/50,000 maps into meshes as shown in Fig. 6.6. Elevation therein is changed into the atmospheric pressure (hPa) for convenience of succeeding calculation (Fig. 6.7).

2) Setting of air streamlines

Air streamlines are figured at intervals of 50 hPa and the nodal surface which is not affected by the topographic conditions is set at 300 hPa. Precipitation between streamlines is given by the following formula.

$$R = \frac{\overline{V}_1 \cdot \Delta p_1 \left(\overline{q}_1 - \overline{q}_2 \right)}{Y} \cdot \frac{1}{g\rho}$$

where

R	:	Precipitation (cm/sec)
$\overline{V}_1$	:	Mean inflow wind speed (cm/sec)
Δp_1	:	Inflow pressure difference (hPa)
$\overline{q}_1 \cdot \overline{q}_2$	:	Mean specific humidities at inflow and outflow (g/kg)
Y	:	Horizontal distance (cm)
g	:	Acceleration of gravity (cm/sec^2)
ρ	:	Density of water (g/cm^3)

When mixing ratio (w) in place of mean specific humidity and dimensions indicated in respective data are applied, the above formula will be modified as follow.

$$R = \frac{0.8813 \times \overline{V}_1 \cdot \Delta p_1 \left(\overline{w}_1 - \overline{w}_2 \right)}{Y}$$

where

R	:	Daily precipitation (mm/day)
$\overline{V}_1$	:	Mean inflow wind speed (m/sec)
Δp_1	:	Inflow pressure difference (hPa)
$\overline{w}_1 \cdot \overline{w}_2$	:	Mean mixing ratio at inflow and outflow (g/kg)
Y	:	Horizontal Distance (km)

3) Selection of meteorological data (boundary condition)

Atmospheric temperature, relative humidity and wind velocity recorded at Wangdi meteorological station (EL.1,180m, 1991 – 1997) located 10 km upstream from the damsite are applied. As the data availablility at present is indicated in daily values, PMP is also to be estimated at daily basis. The representative values of respective meteorological data are assumed as follows.

Temperature (γ):

The maximum value of 31°C is adopted referring to monthly average value of daily maximum temperature. Decrement of temperature by altitude is estimated at minus 0.6°C/100m.

Relative humidity (RH):

The lower value of humidities between two records observed each day is selected as daily representative humidity and the maximum value (91%) of these representative humidities is adopted. Variation of humidity by altitude is assumed to be linear upto 50% at 300 hPa referring to measurement in Japan.

Wind velocity (V):

The maximum value of 4.2 m/s is adopted referring to the daily mean velocities during the monsoon season (June – September). Variation of wind velocity by altitude is also assumed to be linear upto 50 m/s at 300 hPa referring to measurement records in Japan.

4) Setting of Freezing Level

Based on decrement of temperature by altitude previously stated, the freezing level is set at 450 hPa. Above or below this level, it snows or rains.

5) Preparation of Precipitation Trajectories

Precipitation trajectories are to be prepared at every 10 km as shown in Fig. 6.7. Computation of the precipitation trajectory is shown in Table 6.3.

6) Calculation of Precipitation

Precipitation between each trajectory is to be calculated with the formula previously stated and the results are shown in 6.4.

Based on the above, the daily average value of PMP on the southern slope of the Himalayan range in the drainage area at Punatsangchhu damsite is estimated to be 358 mm/day as shown in Table 6.5.

(3) Preparation of Unit Hydrograph

As unit hydrographs of the Punatsangchhu basin are not available at present, basin lag, peak flow, etc of unit hydrograph are estimated by the Snyder method in this study. The shape of unit hydrograph is expressed in a function of $t^{2.4}$ at ascending portion and exponential function at descending portion, and is graded in every 6 hours and rainfall density of 1 cm as shown Fig. 6.8.

(4) Distribution of PMP

Since unit hydrograph is graded in every 6 hours, it is required to distribute the PMP values previously estimated in every 6 hours also. The following formula showing the relationship between time and precipitation for the world's greatest observed point rainfall are applied for this purpose.

$R = 422 \cdot D^{0.475}$

where

R: Rainfall (mm)

D: Duration (hr)

The result of caluculation are shown in Table 6.6, in which "Arrange" means the arrangement so as to cause the maximum discharge and the effective precipitation is the value arranged minus hourly retention loss of 2 mm/hr.

(5) Synthesis of Unit Hydrographs

The flood hydrograph synthesized with the effective precipitation and unit hydrographs is as shown in Table 6.7 and Fig. 6.9. As a result of the synthesis, peak discharge of 13,524 m^3/s is calculated.

(6) Determination of Baseflow and PMF

And base flow of 376 m^3/s is determined based on the discharge of 95% probability during monsoon season (July – September). Therefore, PMF discharge at Punatsangchhu damsite is estimated to be 13,900 m^3/s.

(7) Comparison with other Projects in Bhutan

Design flood discharges of Chhukha HPP and Tala HPP were calculated as SPF (Standard probable Flood) discharges. SPF discharges usually equal 40 to 60% of the PMF for the same basin. Assuming that SPF discharge equals 50% of the PMF discharge, PMF discharges of Chhukha (CA=3,550 km^2) and Tala (CA=4,028 km^2) are calculated to be 11,320 m^3/s and 12,500 m^3/s respectively. These values and 13,900 m^3/s of Punatsangchhu's PMF discharge (CA=5,796 km^2) are plotted on the curves obtained by Creager's equation as shown in Fig. 6.10.

As a result of plotting on the graph, these three discharges were confirmed to be plotted near C (regional coefficient) =100 line.

6.4.3 Glacier Lake Outburst Flood (GLOF)

(1) General

The occurrence of Glacier Lake Outburst Flood (GLOF) is often reported in the areas such as the Himalayas, Alaska, European Alps, etc. where rivers have their origins in glacial ranges. In the Himalayas region, the occurrence is often reported in Nepal, Pakikistan, Tibet besides Bhutan.

The mechanism of GLOF occurrence is as follows:

1) Process of Forming Glacier Lake

Glacier lakes are generally classified into the following 3 categories according to the materials forming dams.

- Moraine dammed lake
- Glacier ice dammed lake
- Ice-core moraine dammed lake

In the Nepal and Bhutan Himalayan area, many glacier lakes which are dammed by moraine or moraine with ice-core are widely distributed; and that is the main source of GLOF.

The process of creating glacier lakes of this kind is presumed to take the following steps;

(i) Advancement of large glacier and formation of a large sized moraine deposit at its end
(ii) Recession of glacier due to climatic conditions
(iii) Formation of glacier lake by damming water inside the moraine

Some of big moraines have a height of more than 100 m and volume of glacier lake formed by dam of this size will become as large as $10^6 m^3$ or even up to $10^7 m^3$ sometimes. Moraines are divided into ice-cored moraine type or simple moraine type, depending on inclusion of remains of ice body therein.

While, the phenomena of forming glacier lakes due to river closure by glacier itself are observed quite often at many places in the world such as Alaska, European Alps, etc. In the case of the surge of glacier (abrupt forward movement of glacier presumably caused by earthquake, heavy snowfall in short time, avalanche, ice-fall, sudden change of temperature, etc.), there is a heigh possibility of desastrous damage caused therefrom.

2) Causes of Failure of Glacier Lake made by Moraine Dam

The causes of failure of glacier lake can be devided into a failure of dam body by external force like earthquake or an erosion of dam body by piping, overtopping, etc. Among the factors indicated above, it is considered that the piping in moraine dam including ice-cored one and the overtopping due to icefall at the end of glacier are the prevailing factors for trigging GLOFs observed in the Himalayan area.

Causes for piping depend upon quality and thickness of moraine, and further, temperature in the case of ice-cored moraine. Since the failures of glacier lakes are frequently observed during the monsoon season from July to September, the following serial processes of dam failure will be presumed.

With increase of inflow to glacier lake due to melting of glacier by rainfall and/or high temperature, the surface of glacier lake will rise up resulting in eventual overtopping or increase of seepage water through moraine.

Under the above-stated conditions that the lake surface is kept at high elevation due to continuous supply of water from the upstream and loosening of moraine dam body is considerably progressed and further, if over topping of considerable amount of water takes place due to heavy rainfall, icefall, etc., then the moraine dam will dash toward erosion failure as can be imagined.

3) Features of GLOF

Different from the case of ordinary flood caused by rainfall, the hydrograph of GLOF is characterized by sharp rise to and fall from its peak.

The propagation of flood toward downstream basin is greatly governed by configuration of riverbed portion and is characterized by continuous river scoring and deposition of debris and subsequent flood detention and release.

As observed in the past records, peak discharge attenuates as it goes downstream. Further, a large quantity of sediment transportation is also one of the features of GLOF.

(2) Past Records

According to [The Raphstreng Lake, Lunana, (Bhutan) Report on Flood Mitigatory measures (Phase 1-1996) by WAPCOS], following 4 floods are reported about the Punatsangchhu.

1950 Flood : This flood was caused due to the outburst of a proglacial lake in the western Lunana area. It was during summer and lasted for about 24hurs.

1960 Flood : This flood was caused due to bursting some lakes in the Eastern Lunana. It lasted for 5 days.

1968 Flood : The original bridge of Wangdue Phodrang was washed away by this flood which occurred in the Punatsangchhu due to heavy rain.

1994 Flood : This flood was caused due to bursting some lakes in the eastern Lunana.

The Punatsangchhu is formed by the Mochhu and the Phochhu which join at Punakha. There are 2 large glacier lakes in the Lunana area where is the most upstream area of the Phochhu. As stated above, most of floods were caused by the outburst of glacier lakes in this area.

(3) Satellite Image Analysis

Glacier lakes in the upstream area from the project site including the Lunana area were extracted from the satellite imagery data in the first. Then the location, surface area and transition (especially before and after 1994's GLOF) for each lake were identified to be the basic data for hydrological analysis of GLOF.

1) Satellite Image Data

LANDSTAT-TM and RADARSAT images which have wide swatch width were selected as the satellite images.

LANDSAT-TM image is effective on condition that there is no cloud in a target area. The data are managed by NRCT (National Research Council of Thailand). The target area is covered with Path 138, Row041 of LANDSAT-No.4, No.5.

Since the newest LANDSAT-TM image was not available in good condition, the RADARSAT image was adopted for the newest data. The RADARSAT image is obtained by the radar satellite with micro wave and can be observed in all-weather. The radar satellite has been used since 1996. The data are managed by RADARSAT International Satellite Data Distribution Center.

The satellite image data adopted for this analysis are as follows:

No. 1	24th	November,	1988	(LANDSAT-TM)
No. 2	25th	January,	1994	(LANDSAT-TM)
No. 3	27th	October,	1995	(LANDSAT-TM)
No. 4	1st	September,	1998	(RADARSAT)

2) Extraction of Glacier Lakes

The distribution and the transition of glacier lakes extracted using above 4 satellite image data based on some conditions such as temperature, altitude, water area, etc are shown in Fig. 6.11 and Table 6.9. It is clear that 2 glacier lakes (Raphstreng Lake and Luggye Lake) in the most upstream area of the Phochhu are the largest glacier lakes in the whole area.

The distances from the damsite, altitudes and surface areas of these lakes are shown in following table.

Lake	Distance from the Damsite (km)	Altitude (m)	Water Surface Area (km^2)	
			1994	1995
Raphstreng	117	4,440	1.2	1.3
Luggye	121	4,560	1.1	0.9

3) The Cause of 1994's GLOF

Fig. 6.12 shows the transition of glacier lakes in the eastern Lunana area before and after GLOF in October 1994. According to [Geology, Environmental Hazards and Remedial Measures of the Lunana Area, Gasa, Dzongkhag: Report of 1995 Indo-Bhutan Expedition by Gedological Survey of India Bhutan Unit] (hereinafter referred to as 1995's Report), the study team concluded that 1994's GLOF was caused due to the outburst of the Luggye Lake and the Tshopda Lake. The scale of the Luggye Lake's water surface in 1995 is smaller than in 1994's as shown in Fig. 6.12. Therefore, it is considered that 1994's GLOF was caused due to the outburst of the Luggye Lake, the same as 1995's Report concluded.

According to the record of discharge of GLOF observed on 7th October 1994 at Wangdi Rapids GS, the flood volume was calculated to be 25 MCM.

Based on the satellite images of 1994 and 1995, the surface area of the Luggye Lake is 1.0 km^2 on average. Therefore, it is presumed that the water existing from the surface to 25 m in depth was spilled out.

(4) Analysis of GLOF

1) Simulation of 1994 GLOF

Photo 6.1 – 6.4 (provided by Dr. Motegi, JICA expert in Bhutan) shows GLOF in Punatsangchhu which occurred in October 1994. The discharge of GLOF has been recorded evely 15 minutes at Wangdi Rapids GS at that time. At first the simulation of 1994 GLOF was carried our with the DAMBRK developed by US National Weather Service (NWS) for the analysis of the hydrograph of prospective GLOF.

The DAMBRK is a computer program for the calculation of hydrographs at downstream sections in a dam breaching. The flood hydrograph of the moraine dam will be calculated by some data such as reservoir capacity of the glacier lake, height, breaching width, breaching time of the moraine dam and so on. Further, the flood hydrographs at

some downstream sections will be calculated based on the information of the river such as some main cross sections with its altitude, distance from the dam and so on.

The principal data used in the simulation of 1994 GLOF are as follows. Details of these data and results of the simulation are contained in Appendix.

- Water level : EL 4,560 m
- Area of Luggye Lake : 1.1 km^2
- Height of Moraine Dam : 25 m
- Breach Width of Moraine Dam : 35 m
- Representative Cross Sections : 4 sections (Luggye Lake – Wangdi Rapids GS)
- Altitude of Cross Sections : (Wangdi Rapids GS : EL 1,170 m)
- Distance from Luggye Lake : (Wangdi Rapids GS : 111 km)

The DAMBRK is different from common calculation program for non-uniform flow, and can correspond supercritical flow. The river flow is apparently supercritical between the Luggye Lake and Wangdi Rapids GS because the average gradient is approximately 1/30.

Actually the subcritical flow would appear partly in the section on gentle slope from Punakha to Wangdue Phodrang. However, the large difference of gradient would make the calculation insecure in the DAMBRK. Therefore, the calculation was carried out with smoothing gradient as shown in Fig. 6.13 on condition that river flow of all sections were supercritical.

The lateral inflow was considered to make the initial inflow about 300 m^3/s at Wangdi Rapids GS based on the discharge record. The data about the glacier lake was set to make the GLOF volume 25 MCM.

Among those data by changing the width and time of the moraine dam breaching, as parameters as a result of trial and error, it was proved that the calculated result followed the observed data well on condition that the breaching width was 35 m and breaching time was 3.5 hr. This result is shown in Fig. 6.14. The calculated result well indicates the peak discharge and ascending and descending shapes of the hydrograph.

Fig. 6.15 shows hydrographs at Wangdi Rapids GS and at just downstream section of the Luggye Lake on the same time axis. According to the calculated result, it is presumed that the discharge at Wangdi Rapids GS located 111 km downstream begun

increasing at 3.5 hr later from the Luggye Lake's outburst, and became a peak at 5.5 hr later.

The river flow of this section seems to be of supercritical and has lateral inflows from the Mochhu, etc. Therefore, it is considered that the peak of hydrograph was transmitted to downstream without attenuation.

2) Estimation of GLOF Scale

GLOF from the Raphstreng Lake or the Luggye Lake are to be the target on this study, judging from the scale, the location and the past outburst of glacier lakes. It is presumed that GLOF from the Luggye Lake will be same scale as the past one (1994's GLOF) owing to the topographical and the physical conditions.

On the other hand the 1995's report says that the GLOF scale from the Rapstreng Lake will be 31 MCM if the moraine dam with a height of 26 m and a width of 300 m collapses. Flood mitigatory measures such as lowering the lake surface, deepening of the natural channel, etc. have been taken for around these lakes since 1996. Therefore, as it is presumed that the GLOF whose volume are more than the values mentioned above hardly occur. However there is the possibility that the Raphstreng Lake (the lower lake) will collapse due to the outburst of the Luggye Lake (the upper lake) continuously because the distance between two lakes is only about 5 km.

On the assumption in such a situation, it is presumed that GLOF of following volumes will occur with a time lag.

- GLOF volume from the Luggye Lake : 25 MCM
- GLOF volume from the Raphstreng Lake : 31 MCM

3) Simulation of Prospective GLOF

The simulation of GLOF due to the Luggye and Raphstreng Lake outbursts was carried out using parameters used in 1994's GLOF simulation.

In view of the relation of two lakes' locations as shown in Fig. 6.13 (longitudinal section), it is considered that first the Luggye Lake outburst will cause the Raphstreng Lake outburst with a time lag in case of GLOF occurred by two lakes. This time lag was set up 1.5 hr as half of the time that Luggye Lake outburst gets to the peak. Base flow was considered the same as PMF's, and set up to be about 400 m^3/s at the damsite by adjusting of the initial flow and lateral inflow.

The DAMBRK cannot correspond the calculation for a flood due to two dams outbrust. Therefore, the hydrograph at Punatsangchhu damsite was to be made by synthesis of two respective results. The GLOF volumes from the Luggye Lake and the Raphstreng Lake were set up to be 25 MCM and 31 MCM respectively inputting area of the water surface, length of reservoir, etc. based on the satellite image analysis. The parameters related to river character of 1994's GLOF simulation were to be used in the calculation.

Breaching width and breach time of moraine dam affects a peak and shape of the hydrograph. However it is almost impossible to estimate these parameters accurately. Therefore, breach width = 35m and breach time = 3.5 hr, combination of which well followed the hydrograph of 1994's GLOF was adopted in this study.

The simulation result on above conditions is shown in Fig. 6.16. Details of input data and calculation result are contained in Appendix.

The peak discharge due to two lakes (Luggye and Raphstreng) was calculated to be 4,600 m^3/s based on this hydrograph. Further, it is presumed that the discharge at the damsite located 120km downstream will begin increasing at 3.5 hr later from the Luggye Lake outburst, and will have its peak at 7 hr later.

GLOF hydrographs from respective glacier lakes are collected in Fig. 6.17. The prospective peak flood discharges are as follows.

Source of GLOF	GLOF Discharge at Damsite (m^3/s)
Luggye Lake	2,500
Raphstreng Lake	3,100
Luggye Lake & Raphstreng Lake	4,600

(5) Warning System against GLOF

1) General

To cope with GLOF, various measures such as reduction of glacier lake, construction of protective structures and also monitoring of GLOF for advance prevention of damages have to be investigated. The outline of the protective measures are shown below:

• Lowering of glacier lake surface	- Controlled breaching
	- Construction of control outlet
	- Pumping out of lake water
	- Tunnelling through moraine or debris barrier
• Construction of protective structures against GLOF surge	- Regulation dam for flood, high speed lifting of spillway gate, reinforced pier structure, sudden closure of intake gate
• Monitoring system	- Measurement of river surface, constant lake surveillance (by satellite and airplane), emergency communication system

Among the above, two measures have been applied in Nepal, namely, manual breaching through moraine dyke and construction of drainage facilities at the end moraine with flexible materials such as gabions. Further, warning equipment for informing GLOF occurrence financed by World Bank, were installed on river side.

2) Protective Measures for Punatsangchhu Project

In order to cope with GLOF in the Punatsangchhu basin, it can be said that one of the most effective measures is to lower the water level of glacier lakes. On the other hand the important element in protecting the river constructions like dam from damages by GLOF is to first provide gauging stations, sensors, etc. in the upstream basin and then to directly connect these facilities with the gate operation system for data transmission, so that the reservoir water level can be lowered prior to the arrival of GLOF surge. Further, considering the case of malfunction of control system for spillway gates or mistake of the operation, the dam should be designed to permit overtopping.

6.5 Sedimentation

6.5.1 Estimation of Sediment Load

The suspended load data of Wangdi Rapids station are shown in Table 6.10. Annual average suspended load of 8 years (1992-1999) is 1,354,569 m^3/year. The bed load and total load are calculated to be 338,642 m^3/year and 1,693,211 m^3/year respectively on the assumption that the bed load equals 25% of the suspended load. The specific total load is 300 m^3/year/km^2 in the project area.

In connection with the ratio of trapped sediment to the reservoir capacity, the following figure devised by Brune is generally applied.

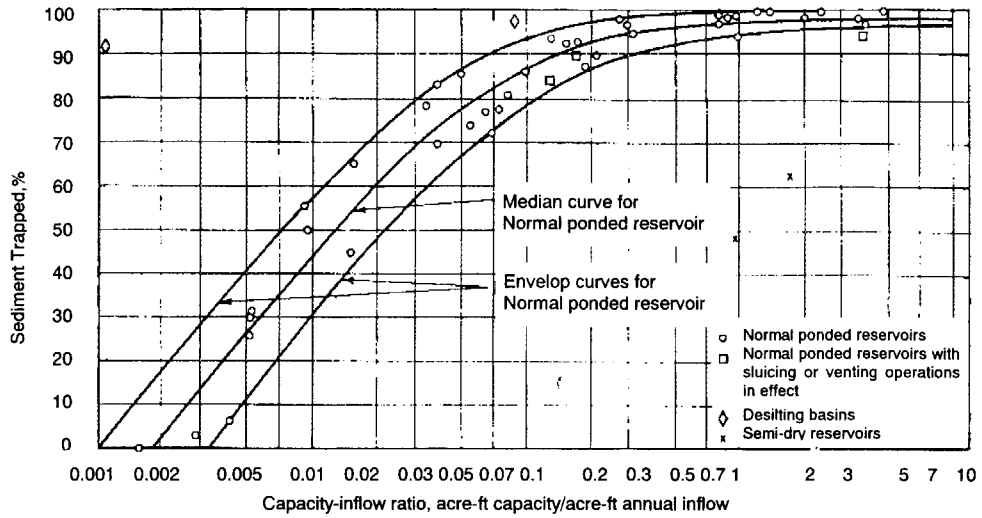

Trap efficiency as related to capacity-inflow ratio.

According to this figure, the capacity - inflow ratio for the gross reservoir capacity of 12.6 MCM versus annual inflow of approximately 9,400 MCM is given to be only 0.13%, which indicates that the most of suspended load flows down through the dam without being trapped. It is considered that this phenomenon is true in theory. The case of this project comes under this phenomenon. On the other hand there were few cases that the ratio of trapped sediment was less than 0.2. Therefore, the ratio of 0.2 is applied in this study. However it is assumed that the bed load is entirely trapped. Annual sediment load is summarized below.

- Suspended Load : 1,354,569 × 0.20 = 271×10^3 m^3/year.
- Bed Load : 1,354,569 × 0.25 = 339×10^3 m^3/year.
- Total : 610×10^3 m^3/year.

6.5.2 Calculation of Deposit Shape

The approximate value of the deposit in the reservoir is estimated as per the above paragraphs and the following indicates the results of simulation analysis to calculate the shape of deposit. (EPDC/KCC FLOW 500 MODEL)

(1) Calculation Process

i) Non-uniform flow calculation for the initial river sections

ii) Calculation of friction velocities (u*) at respective sections

iii) Calculation of sediment load based on the Lane-Kalinske formula

iv) Estimate of riverbed movement by equation of continuity and then surface elevation of deposit

v) Related calculation of the above on daily basis

(2) Prerequisite for Calculation

i) Diameter of Particle

Uniform diameter was adopted in this calculation. d=0.65 mm was adopted to make annual sediment load approximately $610 \times 10^3 m^3$/year in the Lane-Kalinske formula, and then the porosity of 0.4 was used.

ii) River Discharge

The river discharge at Wangdi Rapids GS was used.

iii) Reservoir Elevation

The reservoir surface used for the calculation is set at 1,154.5 m.

(3) Simulation of Deposit Shape

According to the result of calculation as shown in Fig. 6.19, it is considered that the front of deposit will reach near the damsite in 20 years. Further, as the effective storage capacity will be decreased by deposit at the upstream end of the reservoir, it is required to move this deposit into the reservoir by adequate flushing operation.

Since spillway gates (sill level of spillway gate : EL 1,142m) equipped at the dam will be operated throughout the period of wet season, it is considered that the surface of deposit will keep equilibrium at the dotted line shown in Fig. 6.19, still it will be required to perform flushing operation every year in order to remove the deposit at the upstream end of the reservoir which will be formed continuously.

However, the sediment load due to GLOF is not considered in this analysis. The sediment load due to GLOF is supposed to be extremely large according to the past cases. However it is difficult to estimate the quantity accurately. Therefore in the future, periodic topographical survey of the river and a comparison between before and after of GLOF is recommended to be done to estimate the sediment load due to GLOF.

There is a possibility that the deposit will progress faster than calculated simulation because of the deposit of GLOF. Therefore it is necessary to pay attention to this point when designing the structures.

6.6 Calculation of Backwater during Flood

Backwater at the upstream area of the damsite during a flood was to be calculated based on the simulation of the deposit shape. GLOF with estimated peak discharge 4,600 m^3/s was adopted for the target flood for this calculation. Two cases of the backwater calculation of which conditions are that the river situations were set up before and after the dam construction were carried out respectively. The conditions for the calculations are shown in the table below. Further, as a condition of the water level at the damsite after the dam construction, the overflow water level (EL 1,168.2 m) at the top of spillway gate was set up as the initial water level for this calculation in case of the urgent malfunction of gate control system during GLOF.

	Flood Discharge (m^3/s)	Water Level at the Damsite
Before the dam construction	4,600	EL.1,103.0 m
After the dam construction (considering sedimentation)	4,600	EL.1,168.2 m

The result of the calculation is shown in Fig. 6.19. Water surfaces before and after the dam construction begin to approach each other at 4 km upstream from the damsite and are closer at more upstream.

The following table shows the result of the calculation. The difference between the water levels is about 1-2 m at about 8 km upstream from the damsite. This shows that there is little difference about scales of inundated areas due to the dam existence the flood.

Calculation Result of Backwater during Flood

Calculation Point	Before the dam construction Water Level (EL m)	After the dam construction Water Level (EL m)	Difference (m)
Damsite	1,103.0	1,168.2	65.2
500 m	1,116.8	1,168.5	51.7
1,000 m	1,126.0	1,168.5	42.5
1,500 m	1,132.8	1,168.5	35.7
2,000 m	1,142.5	1,168.6	26.1
2,500 m	1,152.5	1,171.7	19.2
3,000 m	1,165.3	1,173.4	8.1
3,500 m	1,174.1	1,177.7	3.6
4,000 m	1,181.3	1,184.4	3.1
4,500 m	1,182.3	1,185.1	2.8
5,000 m	1,184.8	1,186.7	1.9
5,500 m	1,186.2	1,188.3	2.1
6,000 m	1,187.3	1,190.2	2.9
6,500 m	1,188.9	1,191.9	3.0
7,000 m	1,194.4	1,194.7	0.3
7,500 m	1,195.1	1,196.1	1.0
8,000 m	1,198.3	1,200.0	1.7

Table 6.1 Availability of Data

Meteorological Station

Station Name	1985	1986	1987	1988	1989	1990	1991	1992	1993	1994	1995	1996	1997	1998	1999	Data
Gasa											-			-		**R,T,H**
Punakha				-												**R,T,H**
Shelgana																**R,T,H**
Wangdi	-	-	-	-	-											**R,T,H,W,E,S,D**
Gaselo	-								-	-	-					**R,T,H**
Basochhu	-	-	-	-	-											**R,T,H**
Tashithang									-							**R,T,H**
Sonkosh													-			**R,T,H**
Drujeygang																**R,T,H**
Damphu	-	-	-	-	-	-	-	-	-	-	-					**R,T,H,W,E,S,D**

LEGEND **R** : Rainfall, **T** : Temperature, **H** : Humidity, **W** : Wind Speed/Direction, **E** : Evapolation, **S** : Soi l Temperature, **D** : Duration of Sunshine

Hydrological Station

Station Name	1985	1986	1987	1988	1989	1990	1991	1992	1993	1994	1995	1996	1997	1998	1999	Data
Yebesa																Discharge, Suspended Load
Wangdi Rapids																Discharge, Suspended Load
Dubani							-									Discharge, Suspended Load
Maza Fall																Discharge

LEGEND : Available - : No Data

Table 6.2 Monthly Discharge at Dam Site

(unit : m^3/s)

Y/M	JAN	FEB	MAR	APR	MAY	JUN	JUL	AUG	SEP	OCT	NOV	DEC	MAX	MIN	AVE
1991	-	-	-	-	-	-	-	-	696.9	256.2	133.3	92.3	696.9	92.3	294.7
1992	71.7	62.3	91.3	123.7	168.4	325.2	602.9	727.0	447.9	229.2	126.5	87.3	727.0	62.3	255.3
1993	71.1	67.9	62.9	104.7	232.2	239.3	546.9	831.9	546.5	297.6	150.8	103.5	831.9	62.9	271.3
1994	78.9	67.2	78.2	103.0	206.5	418.6	447.8	621.4	474.9	304.1	125.5	89.3	621.4	67.2	251.3
1995	71.0	67.1	87.7	115.5	255.4	532.3	773.2	697.8	486.0	295.7	173.7	95.9	773.2	67.1	304.3
1996	78.0	66.1	81.5	124.8	228.9	449.3	833.8	730.8	678.5	326.5	156.0	103.9	833.8	66.1	321.5
1997	77.4	66.5	87.2	104.8	212.1	463.7	663.5	693.8	603.0	237.4	132.1	95.2	693.8	66.5	286.4
1998	74.4	64.0	69.0	119.4	238.1	577.1	956.1	1128.8	516.8	298.3	147.3	99.1	1128.8	64.0	357.4
1999	75.8	64.8	63.5	108.2	226.2	501.5	749.3	899.2	631.4	369.5	174.4	111.9	899.2	63.5	331.3
MAX	78.9	67.9	91.3	124.8	255.4	577.1	956.1	1128.8	696.9	369.5	174.4	111.9	1128.8	67.9	386.1
MIN	71.0	62.3	62.9	103.0	168.4	239.3	447.8	621.4	447.9	229.2	125.5	87.3	621.4	62.3	222.2
AVE	74.8	65.7	77.7	113.0	221.0	438.4	696.7	791.3	564.6	290.5	146.6	97.6	791.3	65.7	298.2

Firm Discharge (95%) = $64m^3/s$

Annual Inflow (10^9m^3) 9.403

Table 6.3 Computation of Rain and Snow Drift for Computing Precipitation Trajectories

P (hPa)	V (m/s)	Vav (m/s)	Vav△P	DRR (km)	Σ DRIFT(DRR) (km)	DRS (km)	Σ DRIFT(DRS) (km)
300	50.0						
350	46.0	48.0	2,401	1.1	6.9	5.3	32.7
400	42.1	44.1	2,203	1.0	5.8	4.9	27.4
450	38.1	40.1	2,006	0.9	4.7	4.4	22.6
500	34.2	36.2	1,808	0.8	3.8	4.0	18.1
550	30.2	32.2	1,610	0.7	3.0	3.6	14.1
600	26.3	28.2	1,412	0.7	2.2	3.1	10.6
650	22.3	24.3	1,215	0.6	1.6	2.7	7.5
700	18.4	20.3	1,017	0.5	1.0	2.2	4.8
750	14.4	16.4	819	0.4	0.5	1.8	2.5
775	12.4	13.4	335	0.2	0.2	0.7	0.7

Legend

DRR = Vav△P/2,160 :Horizontal rain drift (2,160hPa/hr = falling velocity of rain)

DRS = Vav△P/453 :Horizontal snow drift (453hPa/hr = falling velocity of snow)

Table 6.4 (1/4) Computation of PMP

10～20km

P (hPa)	γ (°C)	R.H (%)	V (m/s)	Vav (m/s)	Vav△P	Ws (g/kg)	WI (g/kg)	Pc (hPa)	γc (°C)	P_{LT} (hPa)	W_{LT} (g/kg)	P_{UT} (hPa)	W_{UT} (g/kg)	WIav (g/kg)	W_{LT}av (g/kg)	W_{UT}av (g/kg)	ΔW_{LT}av =WIav-W_{LT}av	Vav△p·ΔW_{LT}a	ΔW_{UT}av =WIav-W_{UT}av	Vav△p·ΔW_{UT}av
350.0	-9.9	53.5	46.0			5.0	2.7	310.0	-19.5	350.0	2.7	350.0	2.7							
400.0	-3.9	57.1	42.1	44.1	2203.3	7.0	4.0	355.0	-13.0	399.0	4.0	395.0	4.0	3.4	3.4	3.4	0.0	0.0	0.0	0
450.0	0.9	60.6	38.1	40.1	2005.6	9.5	5.8	405.0	-6.5	447.0	5.8	440.0	5.8	4.9	4.9	4.9	0.0	0.0	0.0	0
500.0	5.7	64.2	34.2	36.2	1807.8	12.0	7.7	440.0	-1.3	495.0	7.7	483.0	7.7	6.8	6.8	6.8	0.0	0.0	0.0	0
550.0	9.3	67.7	30.2	32.2	1610.1	13.0	8.8	500.0	1.7	542.0	8.8	528.0	8.8	8.3	8.3	8.3	0.0	0.0	0.0	0
600.0	12.9	71.2	26.3	28.2	1412.3	16.0	11.4	555.0	6.7	590.0	11.4	572.0	11.4	10.1	10.1	10.1	0.0	0.0	0.0	0
650.0	17.7	74.8	22.3	24.3	1214.6	21.0	15.7	610.0	13.0	638.0	15.7	616.0	15.7	13.6	13.6	13.6	0.0	0.0	0.0	0
700.0	20.1	78.3	18.4	20.3	1016.8	22.0	17.2	687.0	16.2	684.0	17.2	660.0	17.2	16.5	16.5	16.5	0.0	0.0	0.0	0
750.0	23.7	81.9	14.4	16.4	819.1	26.0	21.3	720.0	20.0	739.0	21.3	704.0	20.6	19.3	19.3	18.9	0.0	0.0	0.4	287
775.0	24.9	83.6	12.4	13.4	335.4	27.0	22.6	742.0	21.3	756.0	22.6	728.0	22.0	22.0	22.0	21.3	0.0	0.0	0.7	218

Legend
P : Atmospheric pressure
γ : Atmospheric temperature
R.H : Relative humidity
V : Wind velocity
av : average
Ws : Saturation mixing ratio
WI : Mixing ratio at inflow =R.H×Ws
Pc, γc : Condensation pressure, temperature
$_{LT}$: Lower precipitation trajectory
$_{UT}$: Upper precipitation trajectory

TOTAL =	0		505
24hr Volume(mm(km)) = 0.8813×TOTAL	0	=A	445 =B
Unit Horizontal Area (km)=	10	=C	20 =D
24hr Average Rainfall Over Last Leg =	(B-A)/(D-C) =		44 mm

20～30km

P (hPa)	γ (°C)	R.H (%)	V (m/s)	Vav (m/s)	Vav△P	Ws (g/kg)	WI (g/kg)	Pc (hPa)	γc (°C)	P_{LT} (hPa)	W_{LT} (g/kg)	P_{UT} (hPa)	W_{UT} (g/kg)	WIav (g/kg)	W_{LT}av (g/kg)	W_{UT}av (g/kg)	ΔW_{LT}av =WIav-W_{LT}av	Vav△p·ΔW_{LT}a	ΔW_{UT}av =WIav-W_{UT}av	Vav△p·ΔW_{UT}av
350.0	-9.9	53.5	46.0			5.0	2.7	300.0	-19.5	350.0	2.7	347.0	2.7							
400.0	-3.9	57.1	42.1	44.1	2203.3	7.0	4.0	355.0	-13.0	395.0	4.0	390.0	4.0	3.4	3.4	3.4	0.0	0.0	0.0	0
450.0	0.9	60.6	38.1	40.1	2005.6	9.5	5.8	405.0	-6.5	440.0	5.8	435.0	5.8	4.9	4.9	4.9	0.0	0.0	0.0	0
500.0	5.7	64.2	34.2	36.2	1807.8	12.0	7.7	440.0	-1.3	483.0	7.7	480.0	7.7	6.8	6.8	6.8	0.0	0.0	0.0	0
550.0	9.3	67.7	30.2	32.2	1610.1	13.0	8.8	500.0	1.7	528.0	8.8	522.0	8.8	8.3	8.3	8.3	0.0	0.0	0.0	0
600.0	12.9	71.2	26.3	28.2	1412.3	16.0	11.4	555.0	6.7	572.0	11.4	570.0	11.4	10.1	10.1	10.1	0.0	0.0	0.0	0
650.0	17.7	74.8	22.3	24.3	1214.6	21.0	15.7	610.0	13.0	616.0	15.7	613.0	15.7	13.6	13.6	13.6	0.0	0.0	0.0	0
700.0	20.1	78.3	18.4	20.3	1016.8	22.0	17.2	687.0	16.2	660.0	17.2	659.0	17.1	16.5	16.5	16.4	0.0	0.0	0.1	51
750.0	23.7	81.9	14.4	16.4	819.1	26.0	21.3	720.0	20.0	704.0	20.6	703.0	20.5	19.3	18.9	18.8	0.4	286.7	0.4	369
775.0	24.9	83.6	12.4	13.4	335.4	27.0	22.6	742.0	21.3	728.0	22.0	727.0	21.9	22.0	21.3	21.2	0.7	218.0	0.8	252

Legend
P : Atmospheric pressure
γ : Atmospheric temperature
R.H : Relative humidity
V : Wind velocity
av : average
Ws : Saturation mixing ratio
WI : Mixing ratio at inflow =R.H×Ws
Pc, γc : Condensation pressure, temperature
$_{LT}$: Lower precipitation trajectory
$_{UT}$: Upper precipitation trajectory

TOTAL =	505		671
24hr Volume(mm(km)) = 0.8813×TOTAL	445	=A	591 =B
Unit Horizontal Area (km)=	20	=C	30 =D
24hr Average Rainfall Over Last Leg =	(B-A)/(D-C) =		15 mm

Table 6.4 (2/4) Computation of PMP

30～40km

P (hPa)	γ (°C)	R.H (%)	V (m/s)	Vav (m/s)	Vav△P	Ws (g/kg)	WI (g/kg)	Pc (hPa)	γc (°C)	P_{LT} (hPa)	W_{LT} (g/kg)	P_{UT} (hPa)	W_{UT} (g/kg)	WIav (g/kg)	W_{LT}av (g/kg)	W_{UT}av (g/kg)	ΔW_{LT}av =WIav-W_{LT}av	Vav△p·ΔW_{LT}a	ΔW_{UT}av =WIav-W_{UT}av	Vav△p·ΔW_{UT}av
350.0	-9.9	53.5	46.0			5.0	2.7	300.0	-19.5	347.0	2.7	345.0	2.7							
400.0	-3.9	57.1	42.1	44.1	2203.3	7.0	4.0	355.0	-13.0	390.0	4.0	390.0	4.0	3.4	3.4	3.4	0.0	0.0	0.0	0
450.0	0.9	60.6	38.1	40.1	2005.6	9.5	5.8	405.0	-6.5	435.0	5.8	427.0	5.8	4.9	4.9	4.9	0.0	0.0	0.0	0
500.0	5.7	64.2	34.2	36.2	1807.8	12.0	7.7	440.0	-1.3	480.0	7.7	460.0	7.7	6.8	6.8	6.8	0.0	0.0	0.0	0
550.0	9.3	67.7	30.2	32.2	1610.1	13.0	8.8	500.0	1.7	522.0	8.8	500.0	8.8	8.3	8.3	8.3	0.0	0.0	0.0	0
600.0	12.9	71.2	26.3	28.2	1412.3	16.0	11.4	555.0	6.7	570.0	11.4	536.0	10.6	10.1	10.1	9.7	0.0	0.0	0.4	565
650.0	17.7	74.8	22.3	24.3	1214.6	21.0	15.7	610.0	13.0	613.0	15.7	570.0	14.0	13.6	13.6	12.3	0.0	0.0	1.3	1518
700.0	20.1	78.3	18.4	20.3	1016.8	22.0	17.2	687.0	16.2	659.0	17.1	608.0	14.5	16.5	16.4	14.3	0.1	50.8	2.2	2237
750.0	23.7	81.9	14.4	16.4	819.1	26.0	21.3	720.0	20.0	703.0	20.5	645.0	18.5	19.3	18.8	16.5	0.4	368.6	2.8	2252
775.0	24.9	83.6	12.4	13.4	335.4	27.0	22.6	742.0	21.3	727.0	21.9	666.0	19.6	22.0	21.2	19.1	0.8	251.5	2.9	973

Legend P : Atmospheric pressure
γ : Atmospheric temperature
R.H : Relative humidity
V : Wind velocity
av : average
Ws : Saturation mixing ratio
WI : Mixing ratio at inflow =R.H×Ws
Pc, γc : Condensation pressure, temperature
LT : Lower precipitation trajectory
UT : Upper precipitation trajectory

TOTAL =	671	7545
24hr Volume(mm(km)) = 0.8813×TOTAL	591 =A	6650 =B
Unit Horizontal Area (km)=	30 =C	40 =D
24hr Average Rainfall Over Last Leg =	(B-A)/(D-C) =	606 mm

40～50km

P (hPa)	γ (°C)	R.H (%)	V (m/s)	Vav (m/s)	Vav△P	Ws (g/kg)	WI (g/kg)	Pc (hPa)	γc (°C)	P_{LT} (hPa)	W_{LT} (g/kg)	P_{UT} (hPa)	W_{UT} (g/kg)	WIav (g/kg)	W_{LT}av (g/kg)	W_{UT}av (g/kg)	ΔW_{LT}av =WIav-W_{LT}av	Vav△p·ΔW_{LT}a	ΔW_{UT}av =WIav-W_{UT}av	Vav△p·ΔW_{UT}av
350.0	-9.9	53.5	46.0			5.0	2.7	300.0	-19.5	345.0	2.7	344.0	2.7							
400.0	-3.9	57.1	42.1	44.1	2203.3	7.0	4.0	355.0	-13.0	390.0	4.0	380.0	4.0	3.4	3.4	3.4	0.0	0.0	0.0	0
450.0	0.9	60.6	38.1	40.1	2005.6	9.5	5.8	405.0	-6.5	427.0	5.8	410.0	5.8	4.9	4.9	4.9	0.0	0.0	0.0	0
500.0	5.7	64.2	34.2	36.2	1807.8	12.0	7.7	440.0	-1.3	460.0	7.7	440.0	7.7	6.8	6.8	6.8	0.0	0.0	0.0	0
550.0	9.3	67.7	30.2	32.2	1610.1	13.0	8.8	500.0	1.7	500.0	8.8	467.0	7.7	8.3	8.3	7.7	0.0	0.0	0.6	886
600.0	12.9	71.2	26.3	28.2	1412.3	16.0	11.4	555.0	6.7	536.0	10.6	500.0	9.4	10.1	9.7	8.6	0.4	564.9	1.6	2189
650.0	17.7	74.8	22.3	24.3	1214.6	21.0	15.7	610.0	13.0	570.0	14.0	529.0	12.6	13.6	12.3	11.0	1.3	1518.2	2.6	3097
700.0	20.1	78.3	18.4	20.3	1016.8	22.0	17.2	687.0	16.2	608.0	14.5	559.0	13.0	16.5	14.3	12.8	2.2	2237.0	3.7	3711
750.0	23.7	81.9	14.4	16.4	819.1	26.0	21.3	720.0	20.0	645.0	18.5	590.0	16.4	19.3	16.5	14.7	2.8	2252.5	4.6	3727
775.0	24.9	83.6	12.4	13.4	335.4	27.0	22.6	742.0	21.3	666.0	19.6	609.0	17.7	22.0	19.1	17.1	2.9	972.6	4.9	1643

Legend P : Atmospheric pressure
γ : Atmospheric temperature
R.H : Relative humidity
V : Wind velocity
av : average
Ws : Saturation mixing ratio
WI : Mixing ratio at inflow =R.H×Ws
Pc, γc : Condensation pressure, temperature
LT : Lower precipitation trajectory
UT : Upper precipitation trajectory

TOTAL =	7545	15253
24hr Volume(mm(km)) = 0.8813×TOTAL	6650 =A	13443 =B
Unit Horizontal Area (km)=	40 =C	50 =D
24hr Average Rainfall Over Last Leg =	(B-A)/(D-C) =	679 mm

Table 6.4 (3/4) Computation of PMP

50～60km

P (hPa)	γ (°C)	R.H (%)	V (m/s)	Vav (m/s)	VavΔP	Ws (g/kg)	WI (g/kg)	Pc (hPa)	γc (°C)	P_{LT} (hPa)	W_{LT} (g/kg)	P_{UT} (hPa)	W_{UT} (g/kg)	WIav (g/kg)	W_{LT}av (g/kg)	W_{UT}av (g/kg)	ΔW_{LT}av =WIav-W_{LT}av	VavΔp·ΔW_{LT}a	ΔW_{UT}av =WIav-W_{UT}av	VavΔp·ΔW_{UT}av
350.0	-9.9	53.5	46.0			5.0	2.7	300.0	-19.5	344.0	2.7	339.0	2.7							
400.0	-3.9	57.1	42.1	44.1	2203.3	7.0	4.0	355.0	-13.0	380.0	4.0	370.0	4.0	3.4	3.4	3.4	0.0	0.0	0.0	0
450.0	0.9	60.6	38.1	40.1	2005.6	9.5	5.8	405.0	-6.5	410.0	5.8	396.0	5.5	4.9	4.9	4.8	0.0	0.0	0.2	301
500.0	5.7	64.2	34.2	36.2	1807.8	12.0	7.7	440.0	-1.3	440.0	7.7	422.0	7.2	6.8	6.8	6.4	0.0	0.0	0.4	723
550.0	9.3	67.7	30.2	32.2	1610.1	13.0	8.8	500.0	1.7	467.0	7.7	450.0	7.0	8.3	7.7	7.1	0.6	885.5	1.2	1852
600.0	12.9	71.2	26.3	28.2	1412.3	16.0	11.4	555.0	6.7	500.0	9.4	479.0	8.7	10.1	8.6	7.9	1.6	2189.1	2.3	3178
650.0	17.7	74.8	22.3	24.3	1214.6	21.0	15.7	610.0	13.0	529.0	12.6	508.0	11.8	13.6	11.0	10.3	2.6	3097.2	3.3	4008
700.0	20.1	78.3	18.4	20.3	1016.8	22.0	17.2	687.0	16.2	559.0	13.0	538.0	12.2	16.5	12.8	12.0	3.7	3711.4	4.5	4525
750.0	23.7	81.9	14.4	16.4	819.1	26.0	21.3	720.0	20.0	590.0	16.4	565.0	15.5	19.3	14.7	13.9	4.6	3726.8	5.4	4423
775.0	24.9	83.6	12.4	13.4	335.4	27.0	22.6	742.0	21.3	609.0	17.7	585.0	16.8	22.0	17.1	16.2	4.9	1643.4	5.8	1945

Legend
P : Atmospheric pressure
γ : Atmospheric temperature
R.H : Relative humidity
V : Wind velocity
av : average
Ws : Saturation mixing ratio
WI : Mixing ratio at inflow =R.H×Ws
Pc, γc : Condensation pressure, temperature
LT : Lower precipitation trajectory
UT : Upper precipitation trajectory

TOTAL =	15253	20954
24hr Volume(mm(km)) = 0.8813×TOTAL	13443 =A	18467 =B
Unit Horizontal Area (km)=	50 =C	60 =D
24hr Average Rainfall Over Last Leg =	(B-A)/(D-C) =	502 mm

60～70km

P (hPa)	γ (°C)	R.H (%)	V (m/s)	Vav (m/s)	VavΔP	Ws (g/kg)	WI (g/kg)	Pc (hPa)	γc (°C)	P_{LT} (hPa)	W_{LT} (g/kg)	P_{UT} (hPa)	W_{UT} (g/kg)	WIav (g/kg)	W_{LT}av (g/kg)	W_{UT}av (g/kg)	ΔW_{LT}av =WIav-W_{LT}av	VavΔp·ΔW_{LT}a	ΔW_{UT}av =WIav-W_{UT}av	VavΔp·ΔW_{UT}av
350.0	-9.9	53.5	46.0			5.0	2.7	300.0	-19.5	339.0	2.7	330.0	2.7							
400.0	-3.9	57.1	42.1	44.1	2203.3	7.0	4.0	355.0	-13.0	370.0	4.0	360.0	4.0	3.4	3.4	3.4	0.0	0.0	0.0	0
450.0	0.9	60.6	38.1	40.1	2005.6	9.5	5.8	405.0	-6.5	396.0	5.5	389.0	5.2	4.9	4.8	4.6	0.2	300.8	0.3	602
500.0	5.7	64.2	34.2	36.2	1807.8	12.0	7.7	440.0	-1.3	422.0	7.2	416.0	7.0	6.8	6.4	6.1	0.4	723.1	0.7	1175
550.0	9.3	67.7	30.2	32.2	1610.1	13.0	8.8	500.0	1.7	450.0	7.0	445.0	6.9	8.3	7.1	7.0	1.2	1851.6	1.3	2093
600.0	12.9	71.2	26.3	28.2	1412.3	16.0	11.4	555.0	6.7	479.0	8.7	472.0	8.5	10.1	7.9	7.7	2.3	3177.7	2.4	3390
650.0	17.7	74.8	22.3	24.3	1214.6	21.0	15.7	610.0	13.0	508.0	11.8	501.0	11.7	13.6	10.3	10.1	3.3	4008.1	3.5	4190
700.0	20.1	78.3	18.4	20.3	1016.8	22.0	17.2	687.0	16.2	538.0	12.2	530.0	11.9	16.5	12.0	11.8	4.5	4524.9	4.7	4728
750.0	23.7	81.9	14.4	16.4	819.1	26.0	21.3	720.0	20.0	565.0	15.5	558.0	15.2	19.3	13.9	13.6	5.4	4423.0	5.7	4669
775.0	24.9	83.6	12.4	13.4	335.4	27.0	22.6	742.0	21.3	585.0	16.8	577.0	16.5	22.0	16.2	15.9	5.8	1945.2	6.1	2046

Legend
P : Atmospheric pressure
γ : Atmospheric temperature
R.H : Relative humidity
V : Wind velocity
av : average
Ws : Saturation mixing ratio
WI : Mixing ratio at inflow =R.H×Ws
Pc, γc : Condensation pressure, temperature
LT : Lower precipitation trajectory
UT : Upper precipitation trajectory

TOTAL =	20954	22893
24hr Volume(mm(km)) = 0.8813×TOTAL	18467 =A	20175 =B
Unit Horizontal Area (km)=	60 =C	70 =D
24hr Average Rainfall Over Last Leg =	(B-A)/(D-C) =	171 mm

Table 6.4 (4/4) Computation of PMP

70～80km

P (hPa)	γ (°C)	R.H (%)	V (m/s)	Vav (m/s)	Vav△P	Ws (g/kg)	WI (g/kg)	Pc (hPa)	γc (°C)	P_{LT} (hPa)	W_{LT} (g/kg)	P_{UT} (hPa)	W_{UT} (g/kg)	WIav (g/kg)	W_{LT}av (g/kg)	W_{UT}av (g/kg)	ΔW_{LT}av =WIav-W_{LT}av	Vav△p・ΔW_{LT}a	ΔW_{UT}av =WIav-W_{UT}av	Vav△p・ΔW_{UT}av
350.0	-9.9	53.5	46.0			5.0	2.7	300.0	-19.5	330.0	2.7	329.0	2.7							
400.0	-3.9	57.1	42.1	44.1	2203.3	7.0	4.0	355.0	-13.0	360.0	4.0	358.0	4.0	3.4	3.4	3.4	0.0	0.0	0.0	0
450.0	0.9	60.6	38.1	40.1	2005.6	9.5	5.8	405.0	-6.5	389.0	5.2	386.0	5.1	4.9	4.6	4.6	0.3	601.7	0.4	702
500.0	5.7	64.2	34.2	36.2	1807.8	12.0	7.7	440.0	-1.3	416.0	7.0	411.0	6.8	6.8	6.1	6.0	0.7	1175.1	0.8	1446
550.0	9.3	67.7	30.2	32.2	1610.1	13.0	8.8	500.0	1.7	445.0	6.9	435.0	6.7	8.3	7.0	6.8	1.3	2093.1	1.5	2415
600.0	12.9	71.2	26.3	28.2	1412.3	16.0	11.4	555.0	6.7	472.0	8.5	460.0	8.0	10.1	7.7	7.4	2.4	3389.6	2.8	3884
650.0	17.7	74.8	22.3	24.3	1214.6	21.0	15.7	610.0	13.0	501.0	11.7	475.0	10.7	13.6	10.1	9.4	3.5	4190.3	4.2	5101
700.0	20.1	78.3	18.4	20.3	1016.8	22.0	17.2	687.0	16.2	530.0	11.9	510.0	11.2	16.5	11.8	11.0	4.7	4728.2	5.5	5593
750.0	23.7	81.9	14.4	16.4	819.1	26.0	21.3	720.0	20.0	558.0	15.2	538.0	14.5	19.3	13.6	12.9	5.7	4668.7	6.4	5242
775.0	24.9	83.6	12.4	13.4	335.4	27.0	22.6	742.0	21.3	577.0	16.5	555.0	15.6	22.0	15.9	15.1	6.1	2045.8	6.9	2314

Legend
P : Atmospheric pressure
γ : Atmospheric temperature
R.H : Relative humidity
V : Wind velocity
av : average
Ws : Saturation mixing ratio
WI : Mixing ratio at inflow =R.H×Ws
Pc, γc : Condensation pressure, temperature
LT : Lower precipitation trajectory
UT : Upper precipitation trajectory

TOTAL =	22893		26697
24hr Volume(mm(km)) = 0.8813×TOTAL	20175	=A	23528 =B
Unit Horizontal Area (km)=	70	=C	80 =D
24hr Average Rainfall Over Last Leg =	(B-A)/(D-C) =		335 mm

80～90km

P (hPa)	γ (°C)	R.H (%)	V (m/s)	Vav (m/s)	Vav△P	Ws (g/kg)	WI (g/kg)	Pc (hPa)	γc (°C)	P_{LT} (hPa)	W_{LT} (g/kg)	P_{UT} (hPa)	W_{UT} (g/kg)	WIav (g/kg)	W_{LT}av (g/kg)	W_{UT}av (g/kg)	ΔW_{LT}av =WIav-W_{LT}av	Vav△p・ΔW_{LT}a	ΔW_{UT}av =WIav-W_{UT}av	Vav△p・ΔW_{UT}av
350.0	-9.9	53.5	46.0			5.0	2.7	300.0	-19.5	329.0	2.7	328.0	2.7							
400.0	-3.9	57.1	42.1	44.1	2203.3	7.0	4.0	355.0	-13.0	358.0	4.0	355.0	4.0	3.4	3.4	3.4	0.0	0.0	0.0	0
450.0	0.9	60.6	38.1	40.1	2005.6	9.5	5.8	405.0	-6.5	386.0	5.1	380.0	4.8	4.9	4.6	4.4	0.4	702.0	0.5	1003
500.0	5.7	64.2	34.2	36.2	1807.8	12.0	7.7	440.0	-1.3	411.0	6.8	404.0	6.6	6.8	6.0	5.7	0.8	1446.3	1.1	1898
550.0	9.3	67.7	30.2	32.2	1610.1	13.0	8.8	500.0	1.7	435.0	6.7	426.0	6.3	8.3	6.8	6.5	1.5	2415.1	1.8	2898
600.0	12.9	71.2	26.3	28.2	1412.3	16.0	11.4	555.0	6.7	460.0	8.0	450.0	7.6	10.1	7.4	7.0	2.8	3883.9	3.2	4449
650.0	17.7	74.8	22.3	24.3	1214.6	21.0	15.7	610.0	13.0	475.0	10.7	473.0	10.5	13.6	9.4	9.1	4.2	5101.2	4.5	5466
700.0	20.1	78.3	18.4	20.3	1016.8	22.0	17.2	687.0	16.2	510.0	11.2	499.0	10.9	16.5	11.0	10.7	5.5	5592.5	5.8	5847
750.0	23.7	81.9	14.4	16.4	819.1	26.0	21.3	720.0	20.0	538.0	14.5	523.0	13.9	19.3	12.9	12.4	6.4	5242.1	6.9	5611
775.0	24.9	83.6	12.4	13.4	335.4	27.0	22.6	742.0	21.3	555.0	15.6	540.0	15.1	22.0	15.1	14.5	6.9	2314.1	7.5	2499

Legend
P : Atmospheric pressure
γ : Atmospheric temperature
R.H : Relative humidity
V : Wind velocity
av : average
Ws : Saturation mixing ratio
WI : Mixing ratio at inflow =R.H×Ws
Pc, γc : Condensation pressure, temperature
LT : Lower precipitation trajectory
UT : Upper precipitation trajectory

TOTAL =	26697		29670
24hr Volume(mm(km)) = 0.8813×TOTAL	23528	=A	26148 =B
Unit Horizontal Area (km)=	80	=C	90 =D
24hr Average Rainfall Over Last Leg =	(B-A)/(D-C) =		262 mm

Table 6.5 Average PMP of the Punatsangchhu Basin

SECTION (km)	PMP (mm/day)	AREA (km^2)	PMP×AREA
10-20	44	473	20,812
20-30	15	593	8,895
30-40	606	649	393,294
40-50	679	868	589,372
50-60	502	869	436,238
60-70	171	837	143,127
70-80	335	833	279,055
80-90	262	418	109,516
Total		5,540	1,980,309
		A	B
Average	358 mm =B/A		

Table 6.6 PMP Distribution and Effective Rainfall

Time (hour)	Max. Rain (mm)	Rate	PMP (mm)	6hour increment (mm)	Arrange (mm)	Retention Loss (mm)	Effective Rainfall (mm)
6	988	0.518	185	185	24	12	12
12	1,374	0.719	258	73	27	12	15
18	1,666	0.872	312	54	31	12	19
24	1,909	1.000	358	46	36	12	24
30	2,123	1.112	398	40	46	12	34
36	2,315	1.212	434	36	73	12	61
42	2,491	1.304	467	33	185	12	173
48	2,654	1.390	498	31	54	12	42
54	2,807	1.470	526	28	40	12	28
60	2,951	1.545	553	27	33	12	21
66	3,087	1.617	579	26	28	12	16
72	3,218	1.685	603	24	26	12	14

Table 6.7 Synthesis of Unit Hydrographs

Time (hr)	Rainfall (cm)	Loss (cm)	Effectiv e (cm)	Time (hour Unit (m^3/s)	0	6	12	18	24	30	36	42	48	54	60	66	72	78	84	90	96	102	108	114	120	126	132	138	144	Discharge (m^3/s)
0	0	0	0.0		0																									0
6	2.4	1.2	1.2		0	0																								0
12	2.7	1.2	1.5		0	19	0																							19
18	3.1	1.2	1.9		0	24	98	0																						122
24	3.6	1.2	2.4		0	30	123	262	0																					415
30	4.6	1.2	3.4		0	38	156	327	522	0																				1,043
36	7.3	1.2	6.1		0	54	197	414	653	474	0																			1,792
42	18.5	1.2	17.3		0	98	279	523	827	593	384	0																		2,703
48	5.4	1.2	4.2		0	277	500	741	1,044	751	480	302	0																	4,095
54	4.0	1.2	2.8		0	67	1,419	1,330	1,479	948	608	378	230	0																6,459
60	3.3	1.2	2.1		0	45	344	3,771	2,654	1,343	768	479	288	175	0															9,867
66	2.8	1.2	1.6		0	34	230	916	7,526	2,410	1,088	605	365	219	133	0														13,524
72	2.6	1.2	1.4		0	26	172	610	1,827	6,834	1,952	857	461	277	167	102	0													13,284
78						22	131	458	1,218	1,659	5,536	1,537	653	350	211	128	77	0												11,980
84							115	349	914	1,106	1,344	4,360	1,171	496	266	162	96	59	0											10,437
90								305	696	830	896	1,058	3,322	891	377	204	122	74	44	0										8,818
96									609	632	672	706	806	2,526	677	289	154	93	56	34	0									7,253
102										553	512	529	538	613	1,920	519	218	118	70	42	26	0								5,658
108											448	403	403	409	466	1,471	390	167	89	53	33	19	0							4,351
114												353	307	307	311	357	1,107	299	126	67	42	24	16	0						3,315
120													269	234	233	238	269	848	226	95	53	30	20	12	0					2,526
126														204	178	179	179	206	640	171	75	38	25	15	8	0				1,918
132															155	136	134	137	155	484	134	54	31	19	11	7	0			1,459
138																119	102	103	104	118	381	98	44	24	13	9	5	0		1,119
144																	90	78	78	78	92	277	79	34	17	11	6	4	0	844
150																		69	59	59	62	67	225	61	24	14	8	5	1	653
156																			52	45	46	45	55	173	43	20	10	6	2	495
162																				39	35	34	36	42	121	37	14	7	2	367
168																					31	26	27	28	29	104	24	10	2	282
174																						22	21	21	20	25	69	18	3	200
180																							18	16	15	17	17	52	6	141
186																								14	11	13	11	13	17	79
192																									10	10	8	8	4	40
198																										8	6	6	3	24
204																											6	5	2	13
210																												4	2	6
216																													1	1

Table 6.8 Area Account Table of Glacier Lakes

Lake No.	1988 (km^2)	1994 (km^2)	1995 (km^2)	1998 (km^2)	Altitude (m)	Distance (km)
1L	0.716	0.764	0.702	0.712	4780	76.2
2L	0.186	0.191	0.176	0.177	4560	68.7
3L	0.257	0.340	0.269	0.283	4640	84.1
4L	0.211	0.186	0.198	0.202	4440	79.7
5L	0.246	0.209	0.230	0.222	4800	88.8
6L	0.224	0.223	0.143	0.158	4720	87.7
7L	0.155	0.159	0.195	0.200	5320	100.1
8L	0.495	0.548	0.548	0.556	5280	99.9
9L	0.641	0.641	0.644	0.655	5080	99.3
10L	0.199	0.188	0.176	0.177	5080	100.3
11L	0.416	0.424	0.154	0.159	4960	99.2
12L	Unite 11L	Unite 11L	0.211	0.217	4960	99.4
13L	0.221	0.224	0.225	0.204	4920	94.3
14L	0.351	0.392	0.384	0.381	4880	97.0
15L	0.413	0.439	0.365	0.413	4640	87.5
16L	0.343	0.482	0.402	0.424	5320	123.9
17L	0.155	0.132	0.183	0.241	5320	121.0
18L	0.928	1.083	0.938	0.938	4560	121.2
19L	1.241	1.244	1.313	1.138	4440	116.7
20L	0.090	0.115	0.182	0.167	4720	107.5
21L	0.233	0.189	0.239	0.215	4360	107.9
22L	0.432	0.371	0.442	0.381	4320	108.2
23L	0.664	0.623	0.617	0.597	5080	96.7
24L	0.713	0.692	0.683	0.667	5000	80.9
25L	0.230	0.190	0.199	0.212	4920	80.7
26L	0.185	0.134	0.182	0.177	4560	73.9
27L	0.336	0.287	0.355	0.317	4520	74.3
28L	0.302	0.251	0.293	0.270	4760	65.0
29L	0.194	0.148	0.204	0.205	4320	67.9
30L	0.214	0.253	0.212	0.231	5160	92.6
31L	0.280	0.308	0.342	0.313	5120	91.6
32L	0.205	0.138	0.218	0.231	4840	91.8
33L	0.225	0.237	0.211	0.210	4800	89.7
34L	0.219	0.238	0.227	0.206	4440	113.5
35L	0.188	Unextracted	0.239	0.267	4280	88.8
Total	12.108	12.042	12.299	12.122		

Table 6.9 Monthly Suspended Sediment at Wangdi Rapids Gauging Station (unit : m^3)

Y/M	JAN	FEB	MAR	APR	MAY	JUN	JUL	AUG	SEP	OCT	NOV	DEC	Total
1992	-	-	-	-	-	-	153,278	190,609	77,187	7,334	2,450	1,301	432,159
1993	3,138	2,608	-	2,314	11,999	32,134	97,067	163,480	46,015	13,797	3,640	2,031	378,223
1994	1,439	814	2,887	3,685	42,880	32,015	153,219	190,926	-	9,325	2,870	1,361	441,421
1995	103,865	158,241	-	-	-	1,358,922	1,045,019	592,909	414,202	19,627	12,039	2,534	3,707,358
1996	2,025	-	2,959	9,265	44,163	277,311	388,473	184,019	187,719	47,989	5,845	2,797	1,152,565
1997	1,794	-	3,303	2,301	10,092	226,888	502,742	273,147	67,512	7,882	-	-	1,095,661
1998	-	-	4,777	-	23,347	310,437	478,999	651,973	-	3,307	1,462	958	1,475,260
1999	1,882	1,328	2,285	1,813	22,881	133,907	337,071	212,110	252,744	108,887	36,553	61,396	1,172,857
MAX	103,865	158,241	4,777	9,265	44,163	1,358,922	1,045,019	651,973	414,202	108,887	36,553	61,396	3,997,263
MIN	1,439	814	2,285	1,813	10,092	32,015	97,067	163,480	46,015	3,307	1,462	958	360,747
AVE	19,024	40,748	3,242	3,876	25,894	338,802	394,484	307,397	174,230	27,269	9,266	10,340	1,354,569

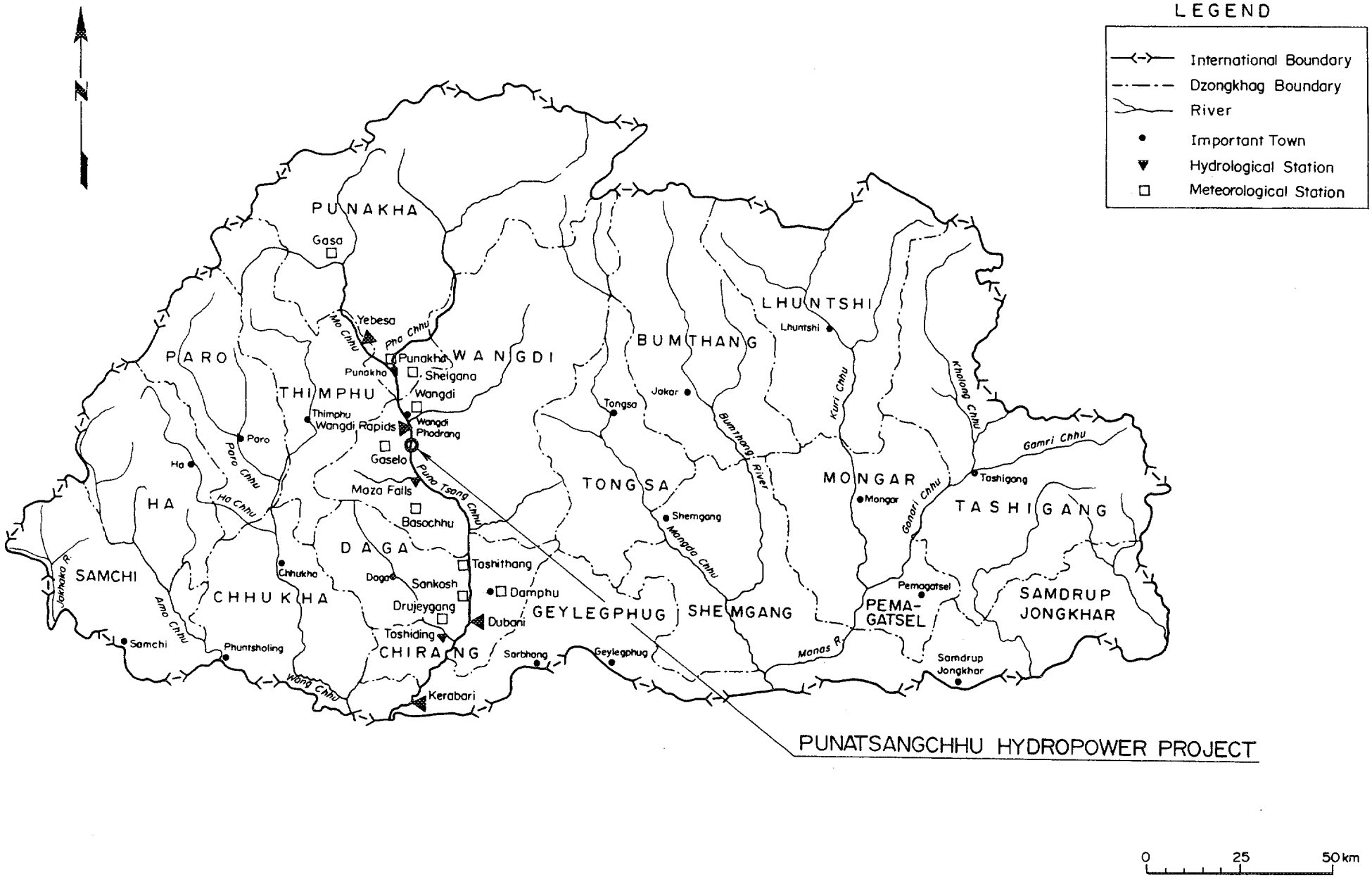

Fig. 6.1 Location Map of Hydrological and Meteorological Stations

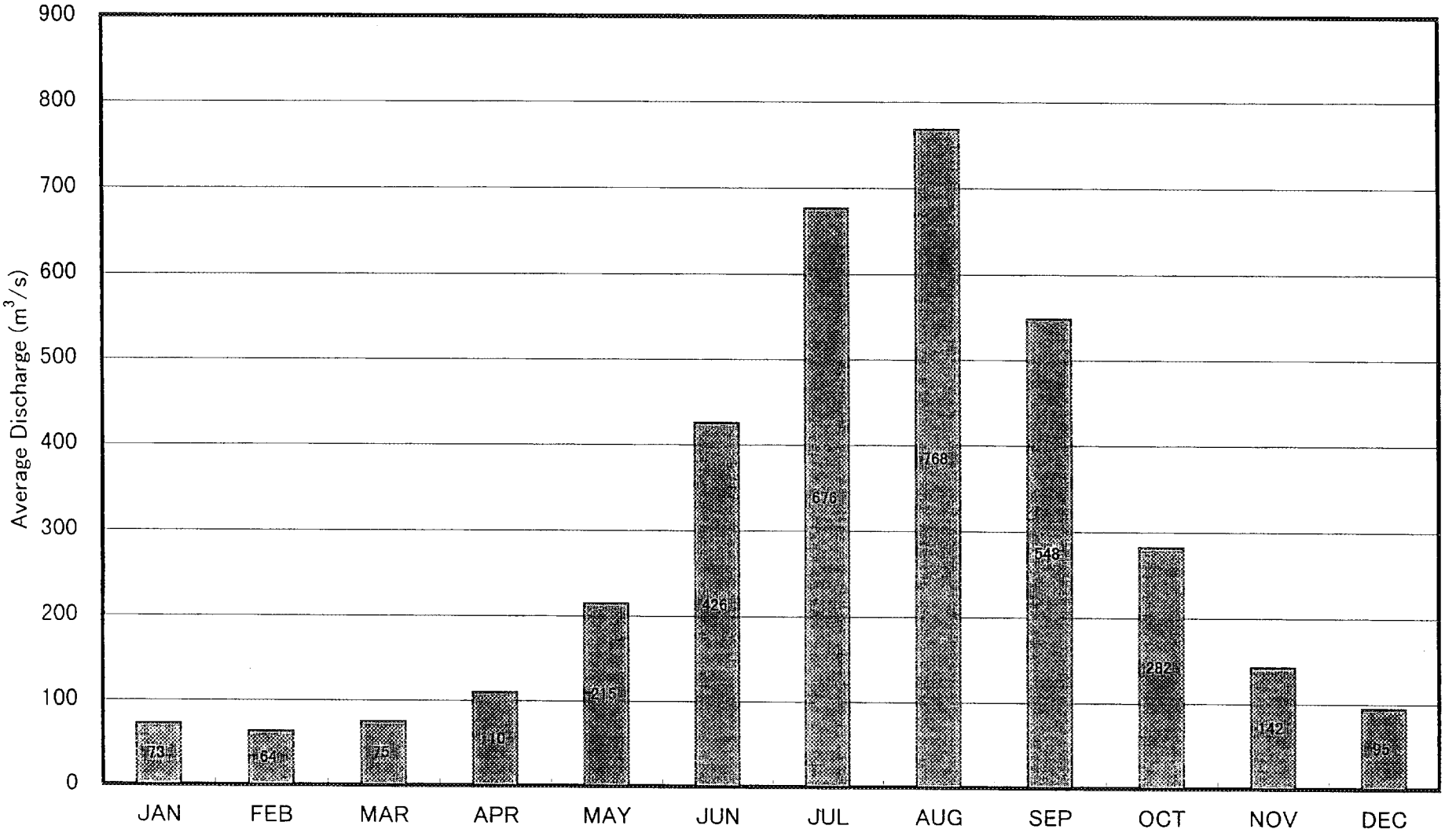

Fig. 6.2 Average Dischrage at Wangdi Rapids Station

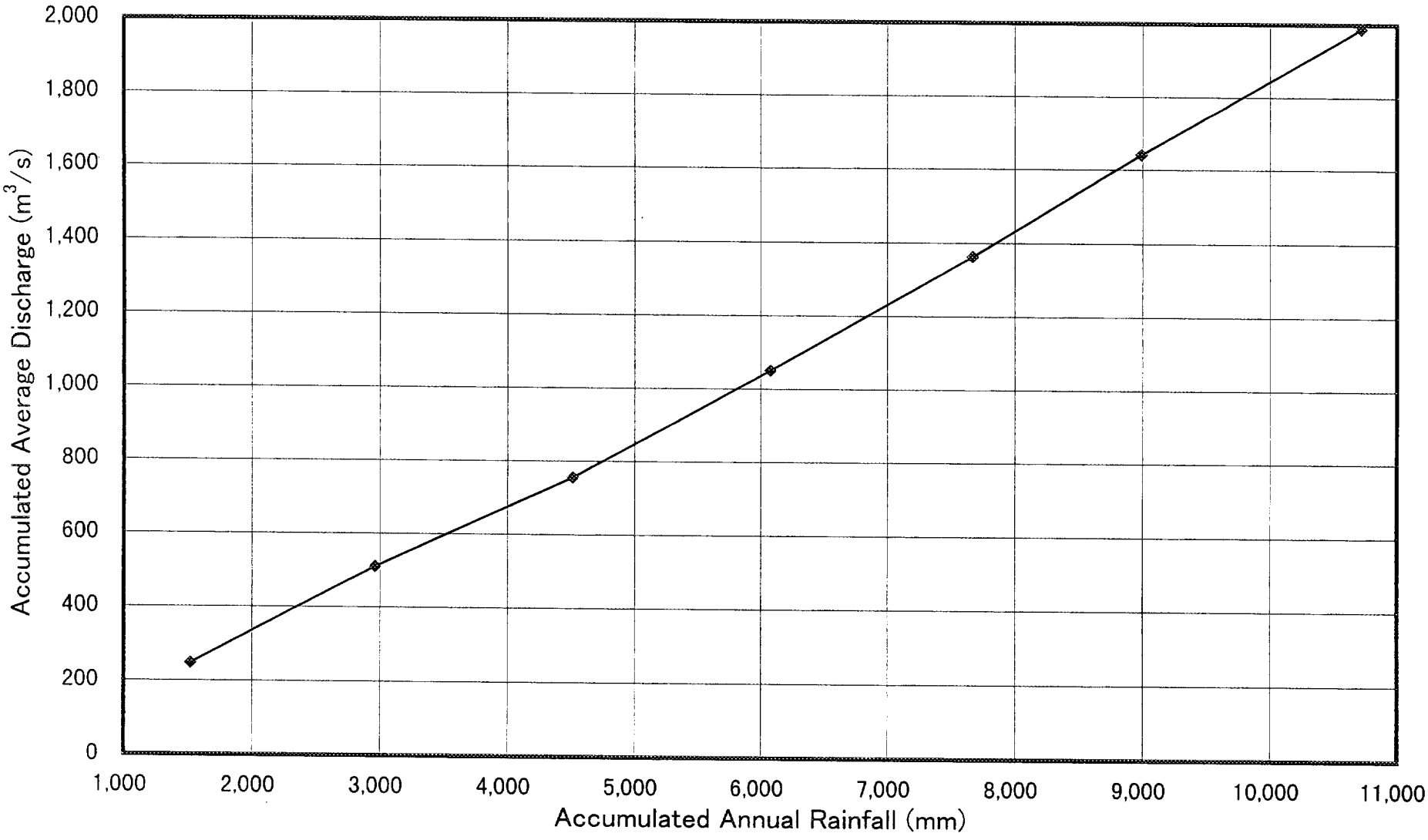

Fig. 6.3 Double Mass Curve

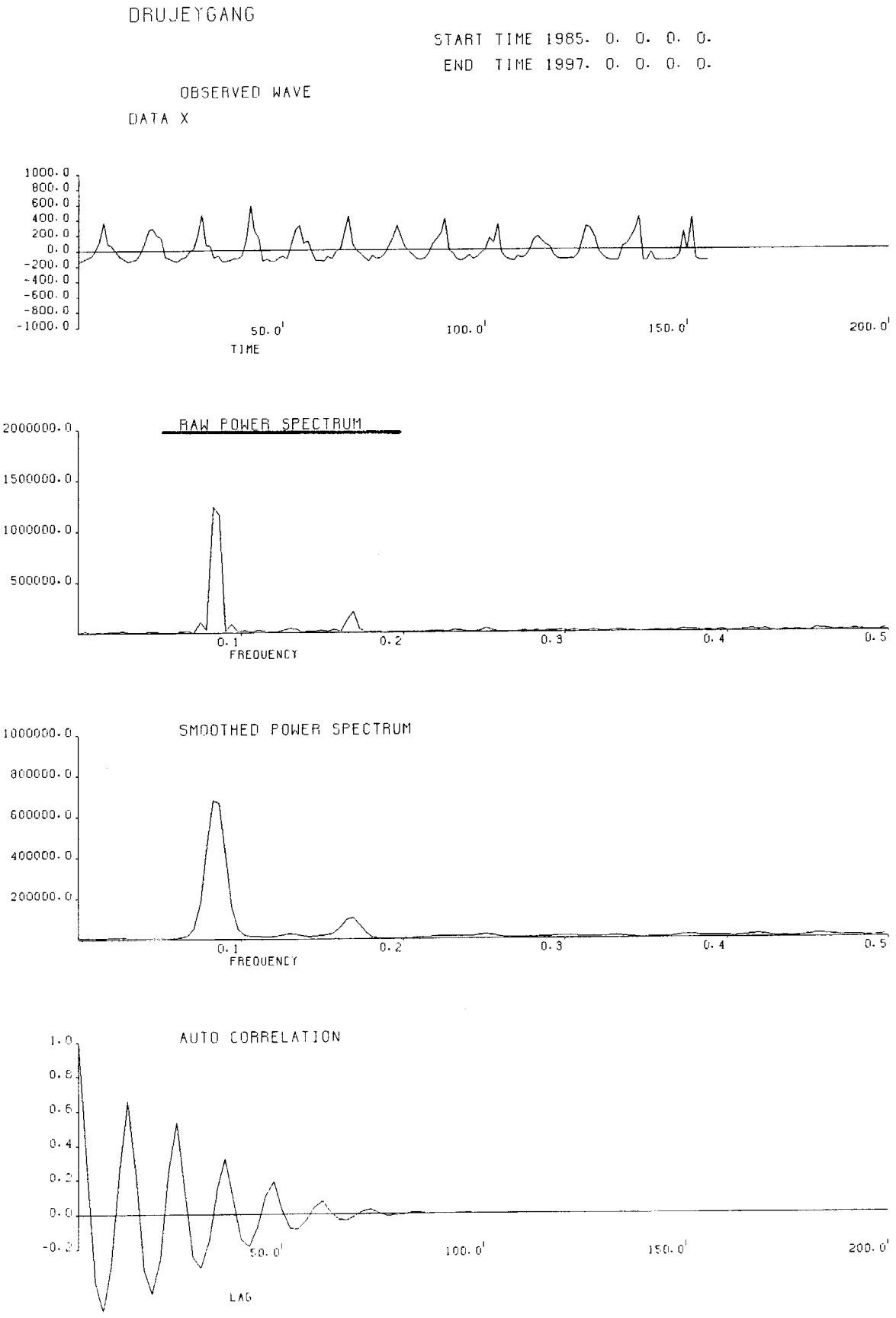

Fig. 6.4 Spectrum Analysis

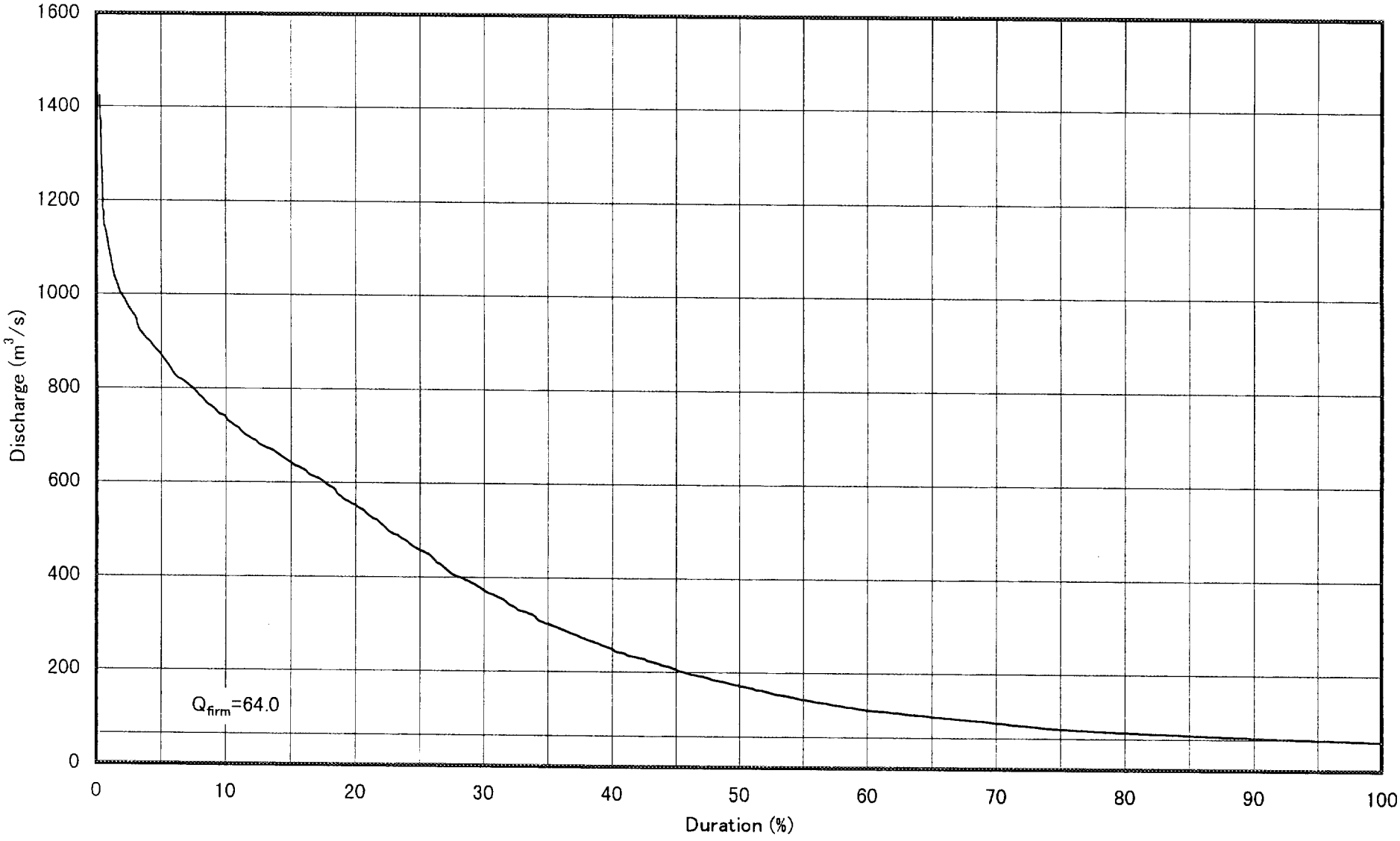

Fig. 6.5 Duration Curve at Dam Site

Distance (km)	Atmospheric Pressure (hPa)	Average Altitude (m)
90	540.2	5,000
80	554.8	4,800
70	577.3	4,500
60	584.9	4,400
50	608.5	4,100
40	666.2	3,400
30	728.3	2,700
20	728.3	2,700
10	756.3	2,400
0	775.4	2,200

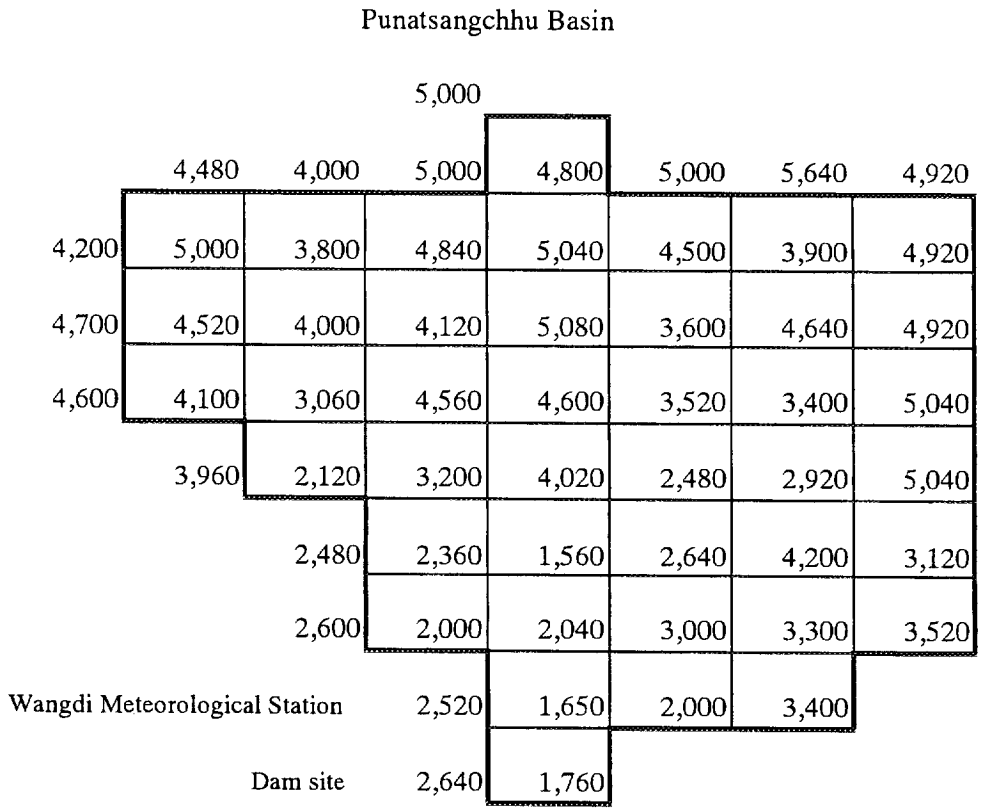

Fig. 6.6 Ground Profile

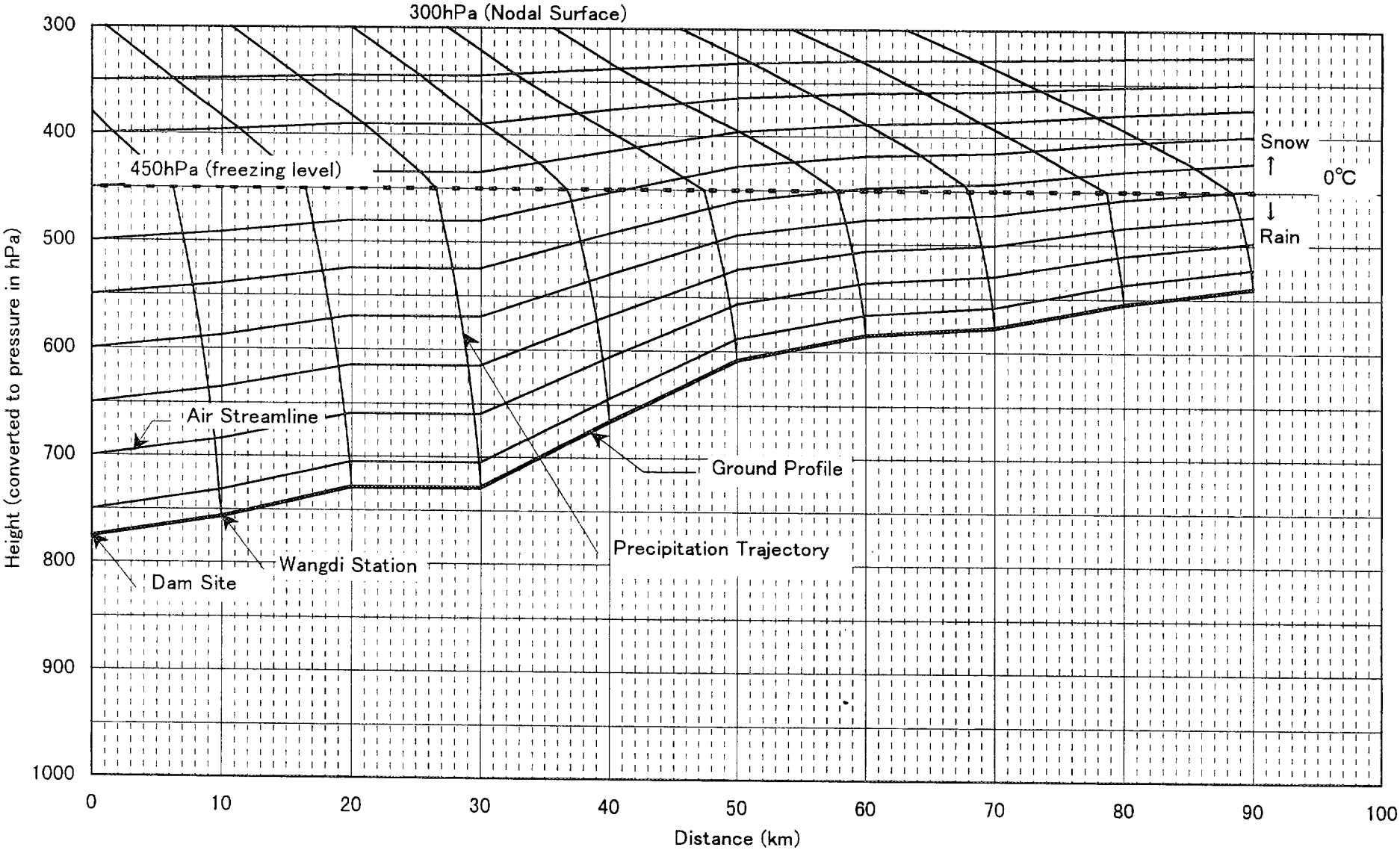

Fig. 6.7 Ground Profile, Air Streamlines and Precipitation Trajectories for PMP Estimation

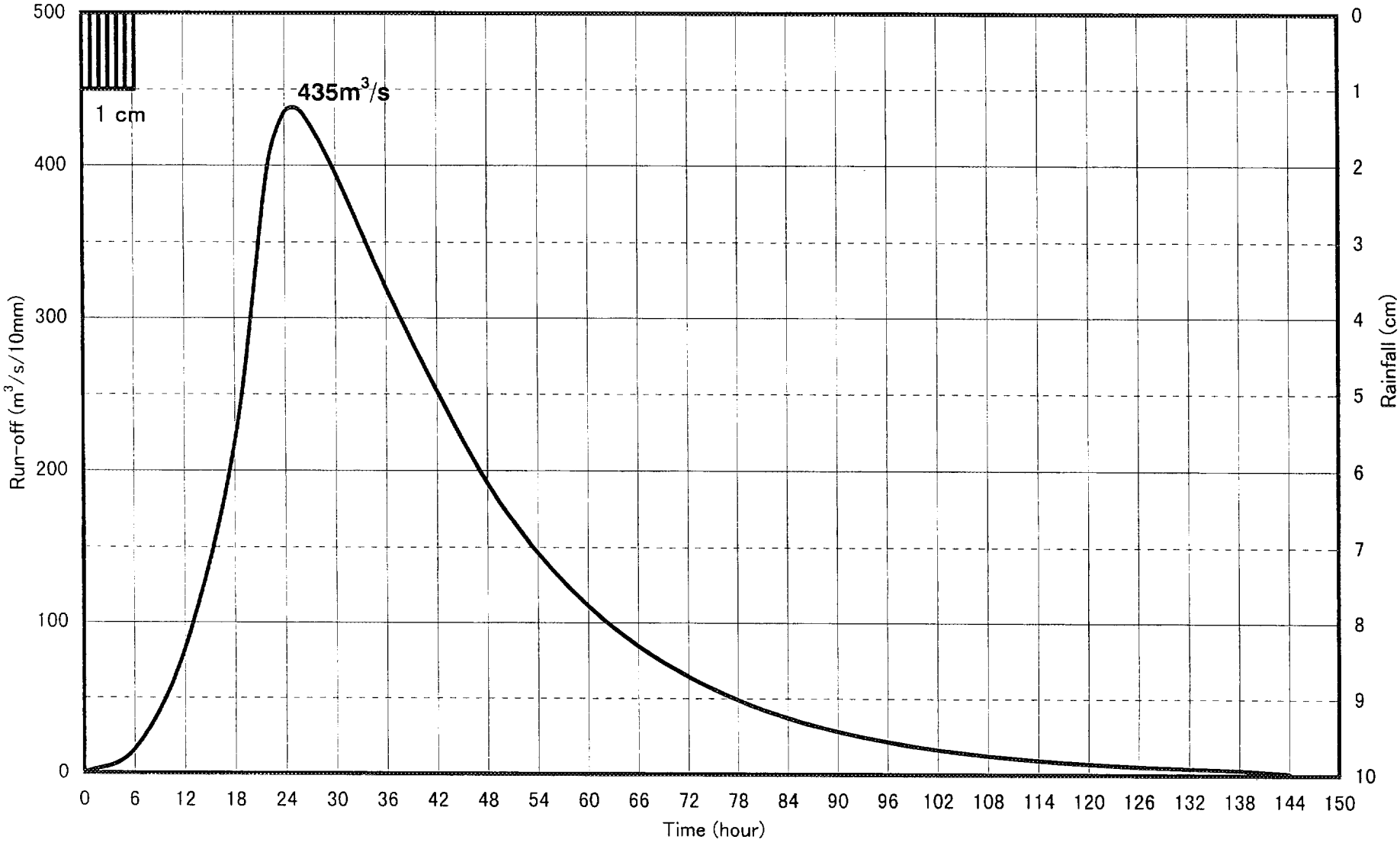

Fig.6.8 Unit Hydrograph at Punatsangchhu Dam Site

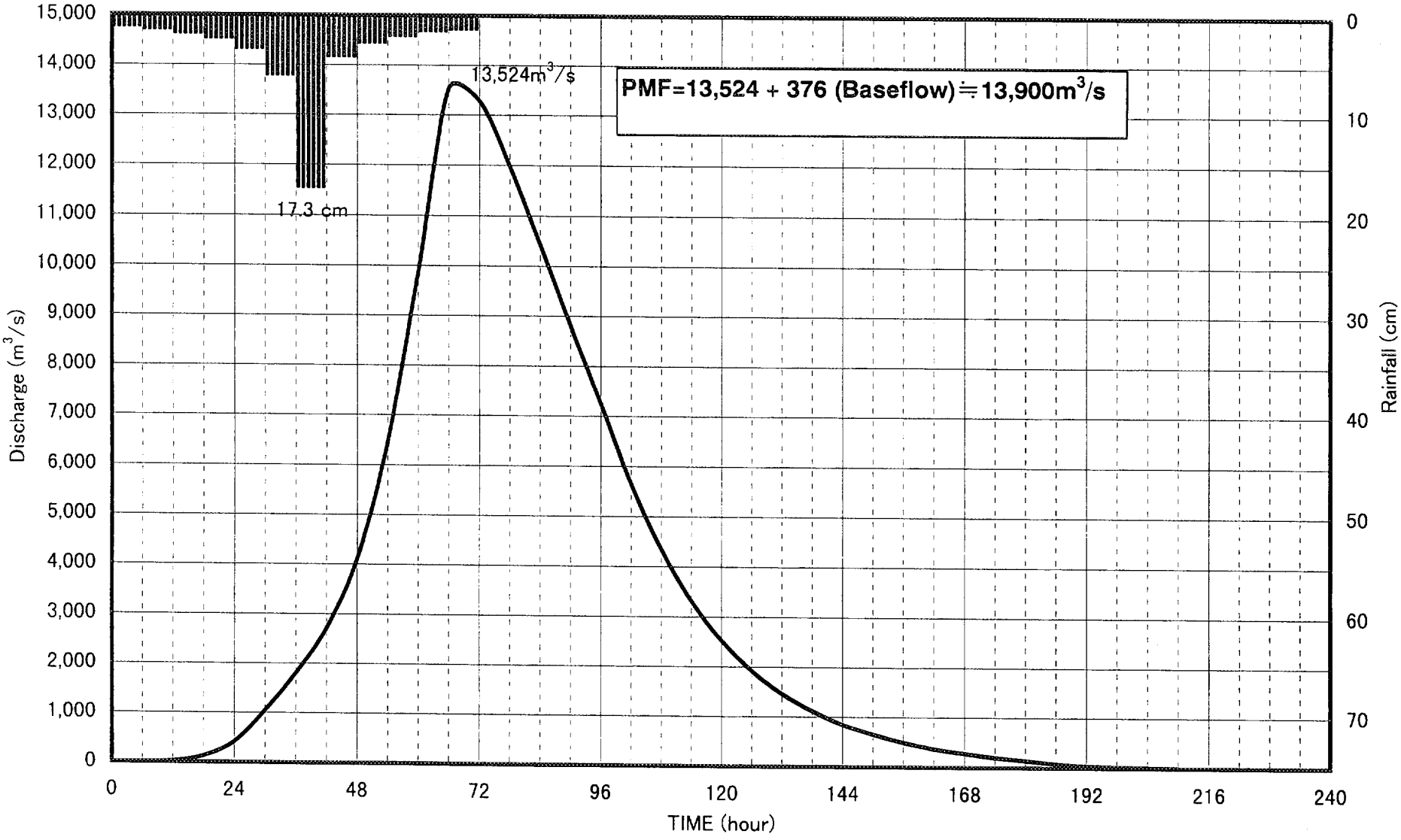

Fig.6.9 Synthesis of Unit Graphs

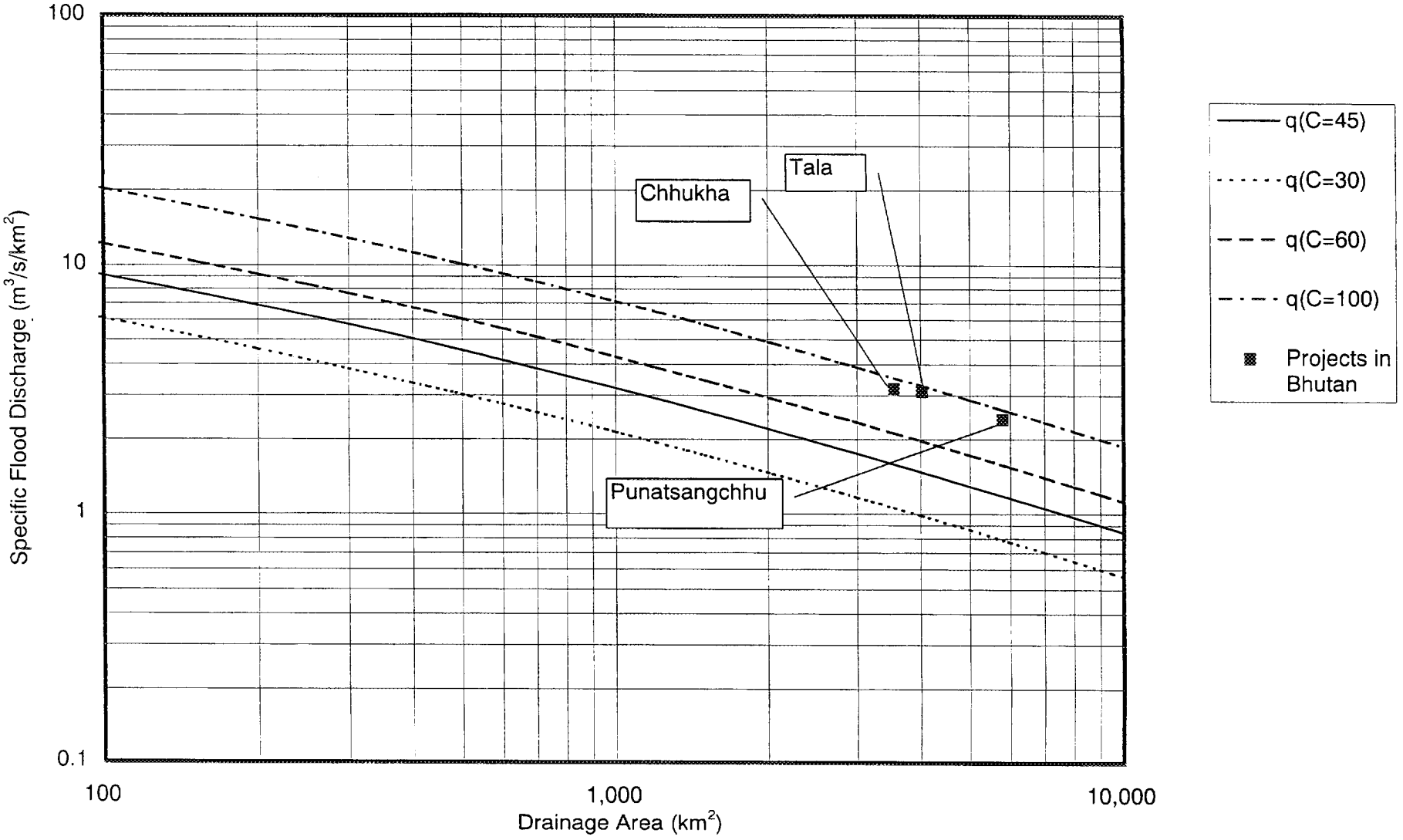

Fig. 6.10 Curves from Creager's Equation

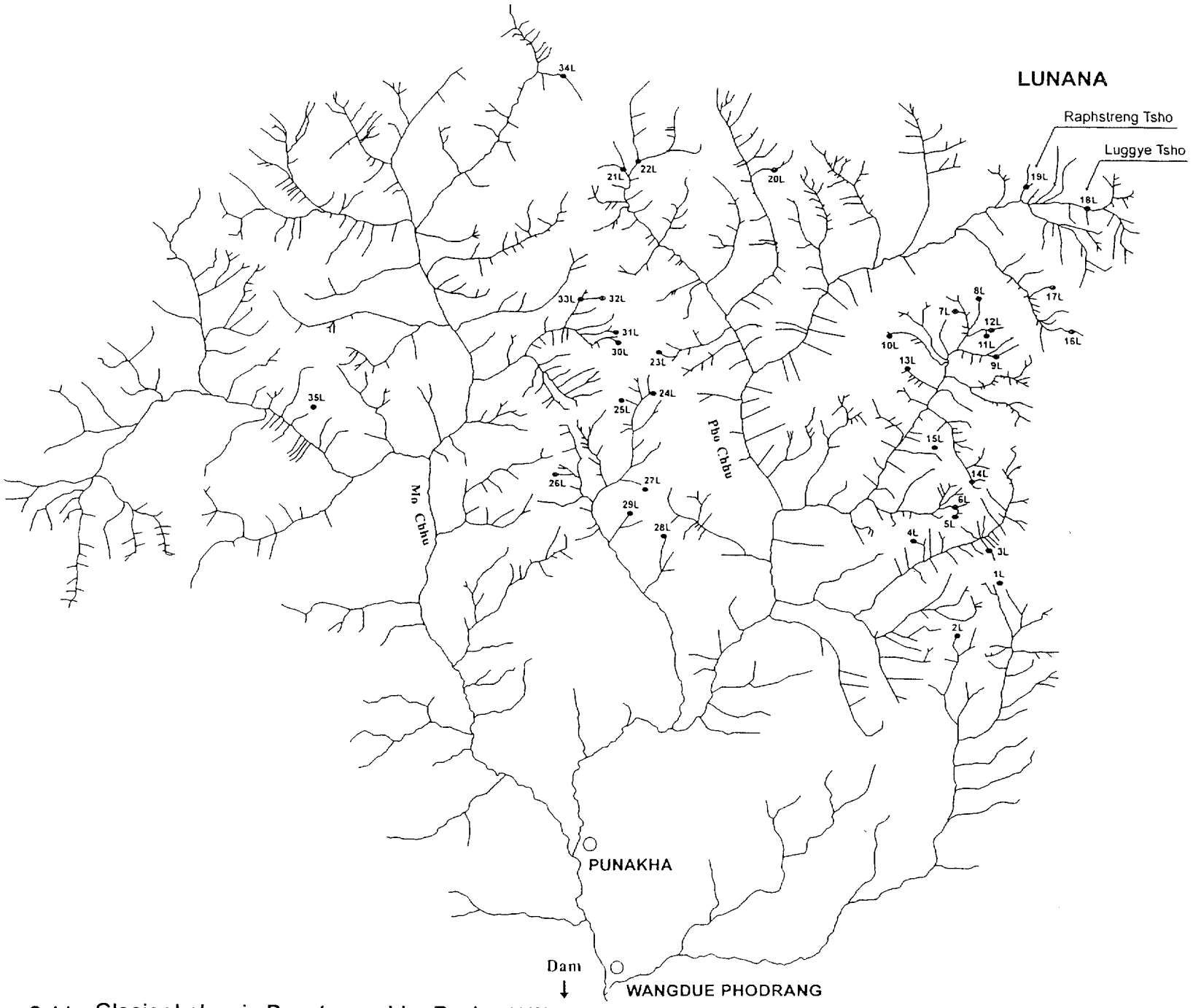

Fig. 6.11 Glacier Lakes in Punatsangchhu Basin (1/3)

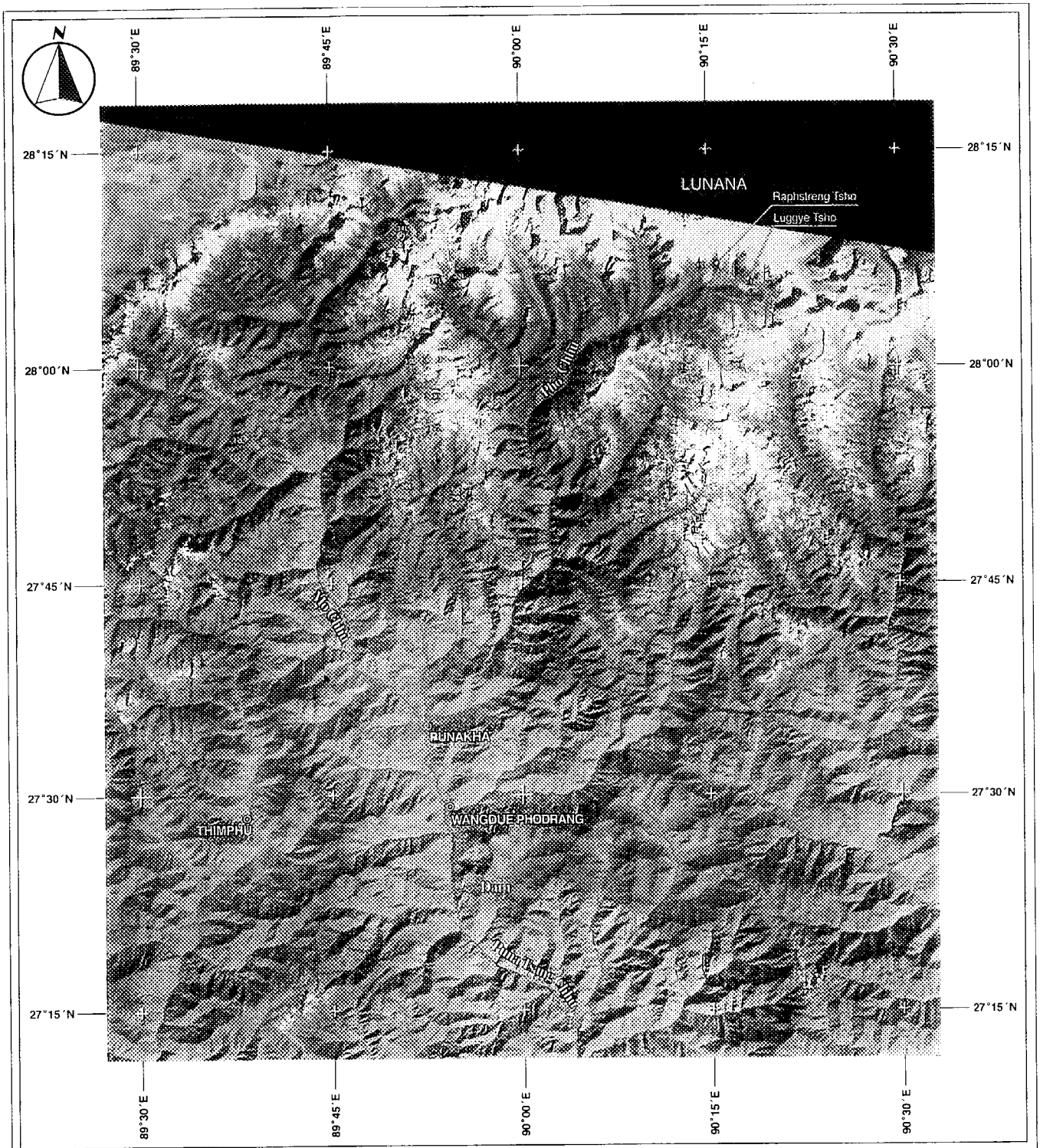

Bhutan Puna Tsang Chhu Satellite Image Analysis

Glacier Lake Distribution Map I

1988 LANDSAT TM data
24-Nov-1988
Path-138 Row-041

1998 RADARSAT SAR Standard Mode
01-Sep-1998

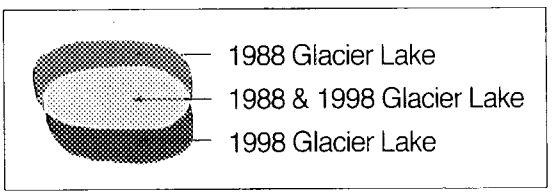

0 30km
1 : 750,000

Fig. 6.11 Glacier Lakes in Punatsangchhu Basin (2/3)

JICA 1999.3

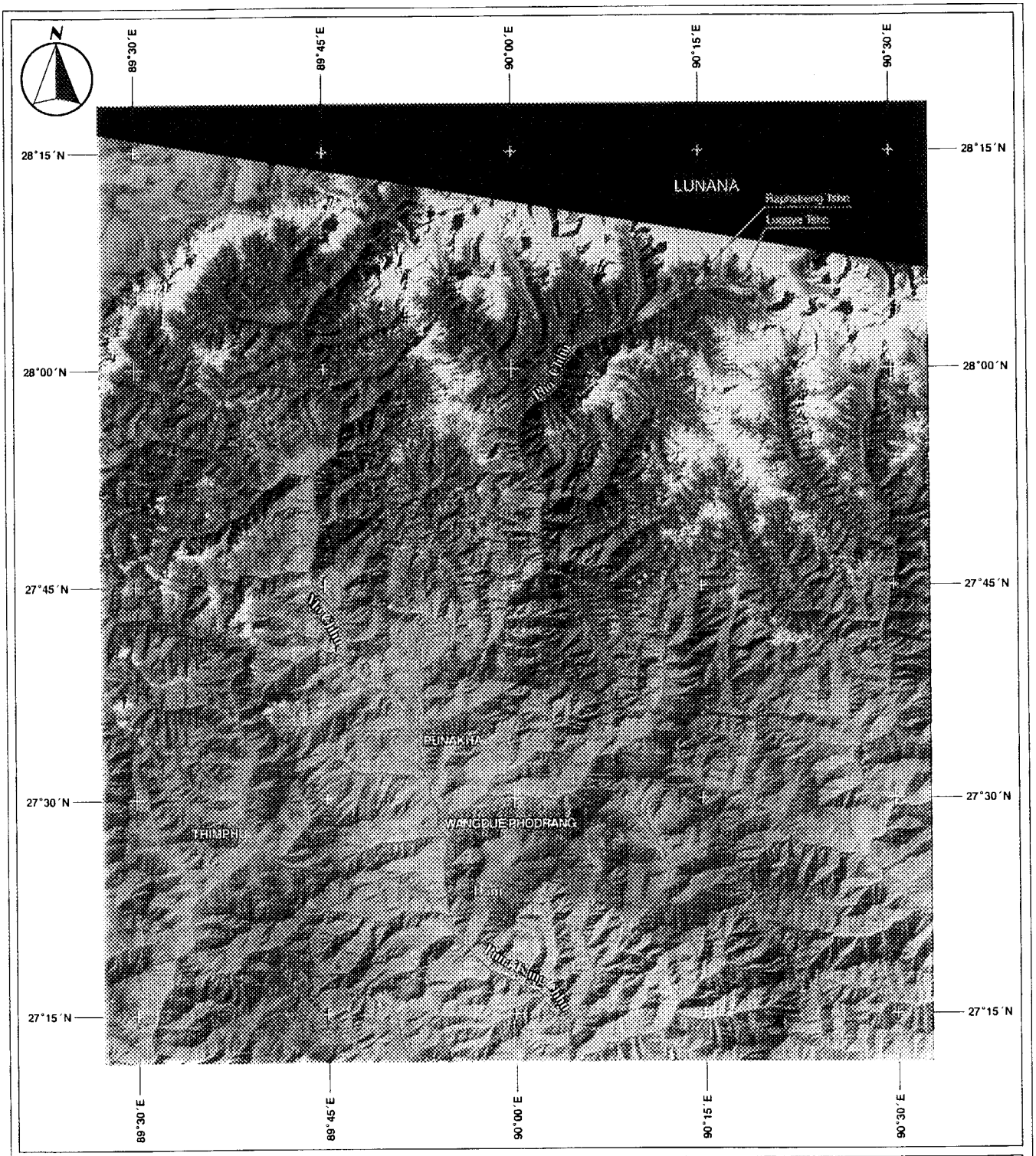

Bhutan Puna Tsang Chhu Satellite Image Analysis

Glacier Lake Distribution Map II

1994 LANDSAT TM data
25-Jan-1994
Path-138 Row-041

1995 LANDSAT TM data
27-Oct-1995
Path-138 Row-041

1994 Glacier Lake
1994 & 1995 Glacier Lake
1995 Glacier Lake

0 30km
1 : 750,000

Fig. 6.11 Glacier Lakes in Punatsangchhu Basin (3/3)

JICA 1999.3

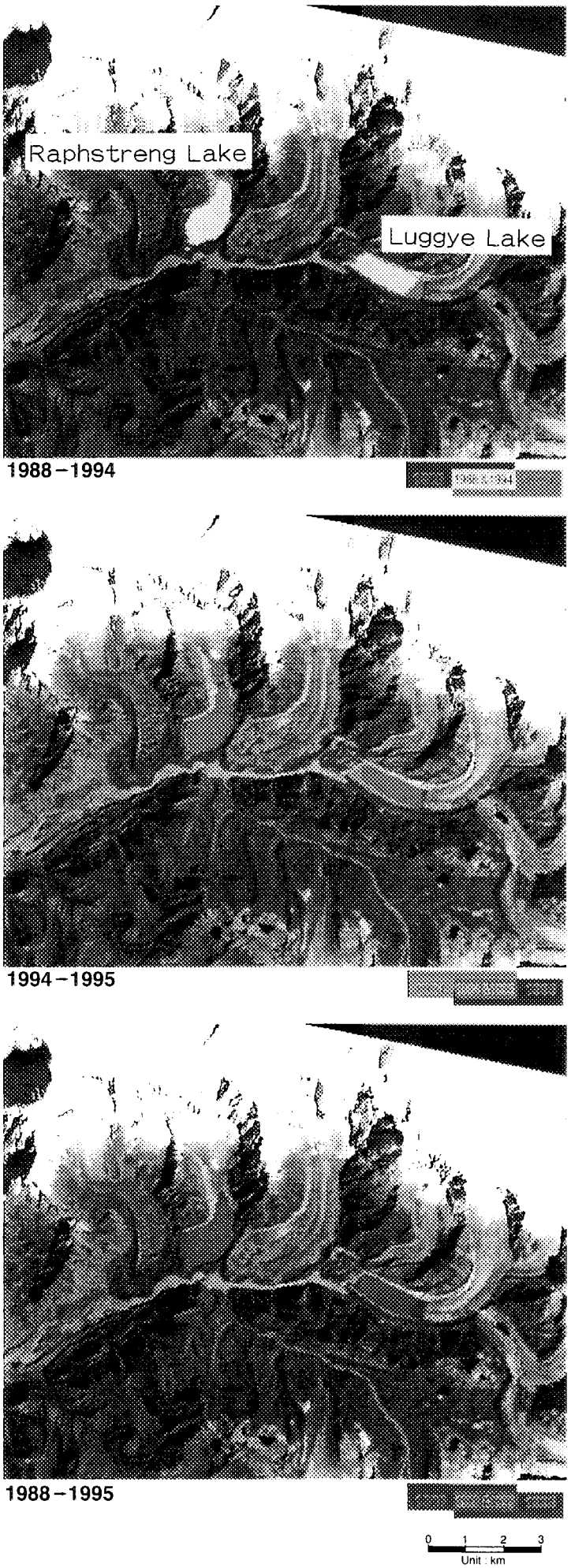

Fig. 6.12 Transition of Luggye and Raphstreng Lake (1994-1995)

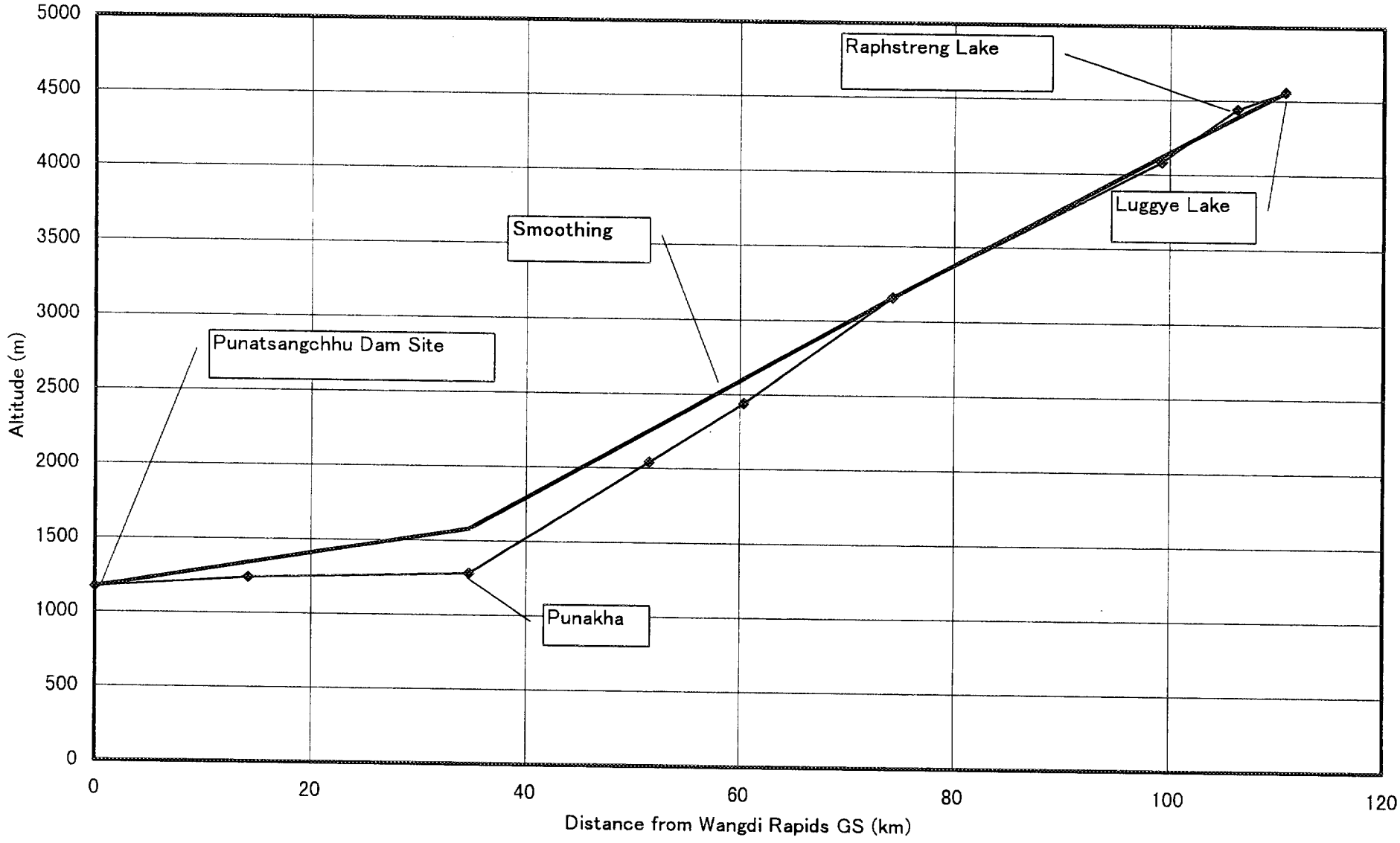

Fig. 6.13 Longitudinal Section of Punatsangchhu

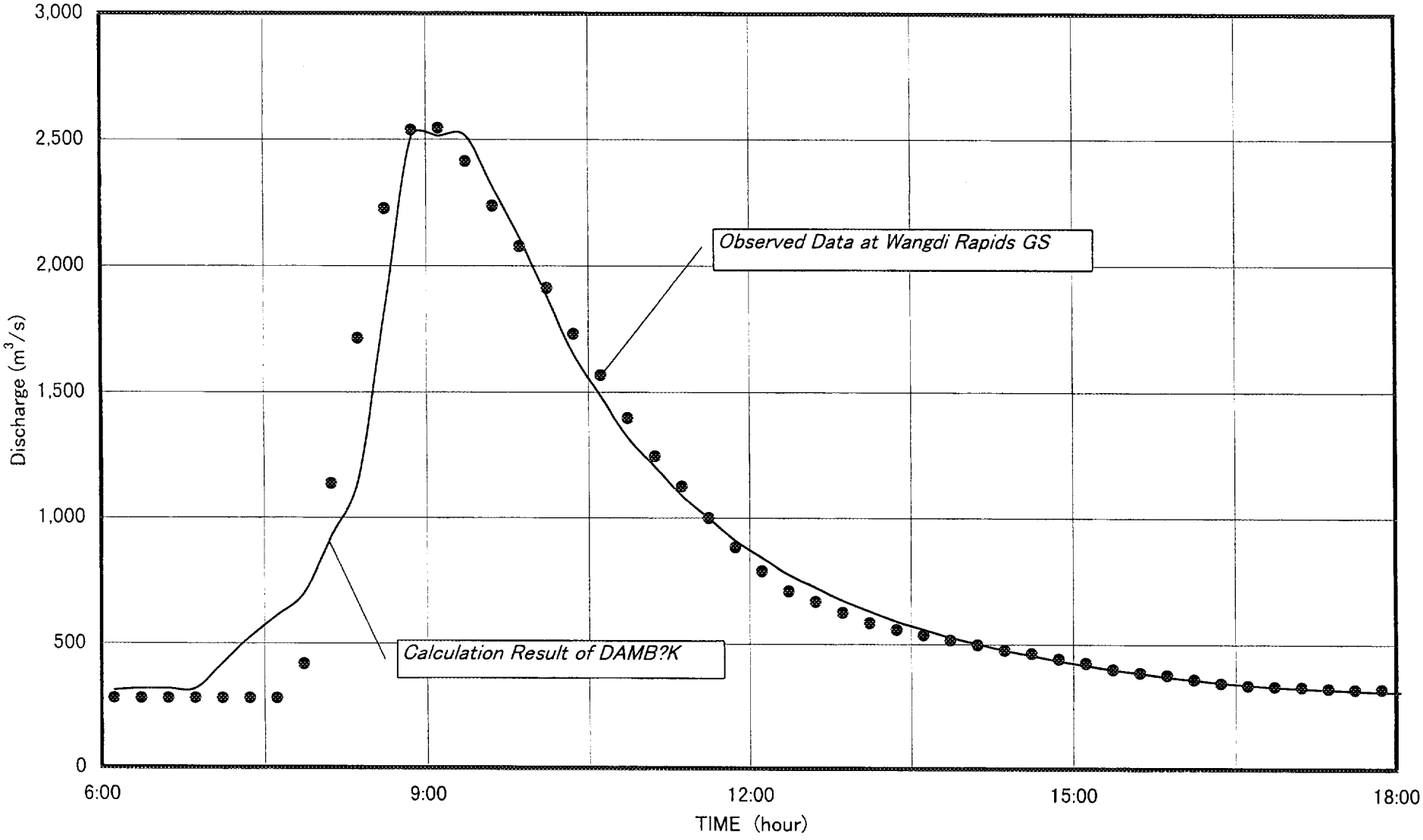

Fig. 6.14 Comparison between Calculation Result and Observed data at Wangdi Rapids GS

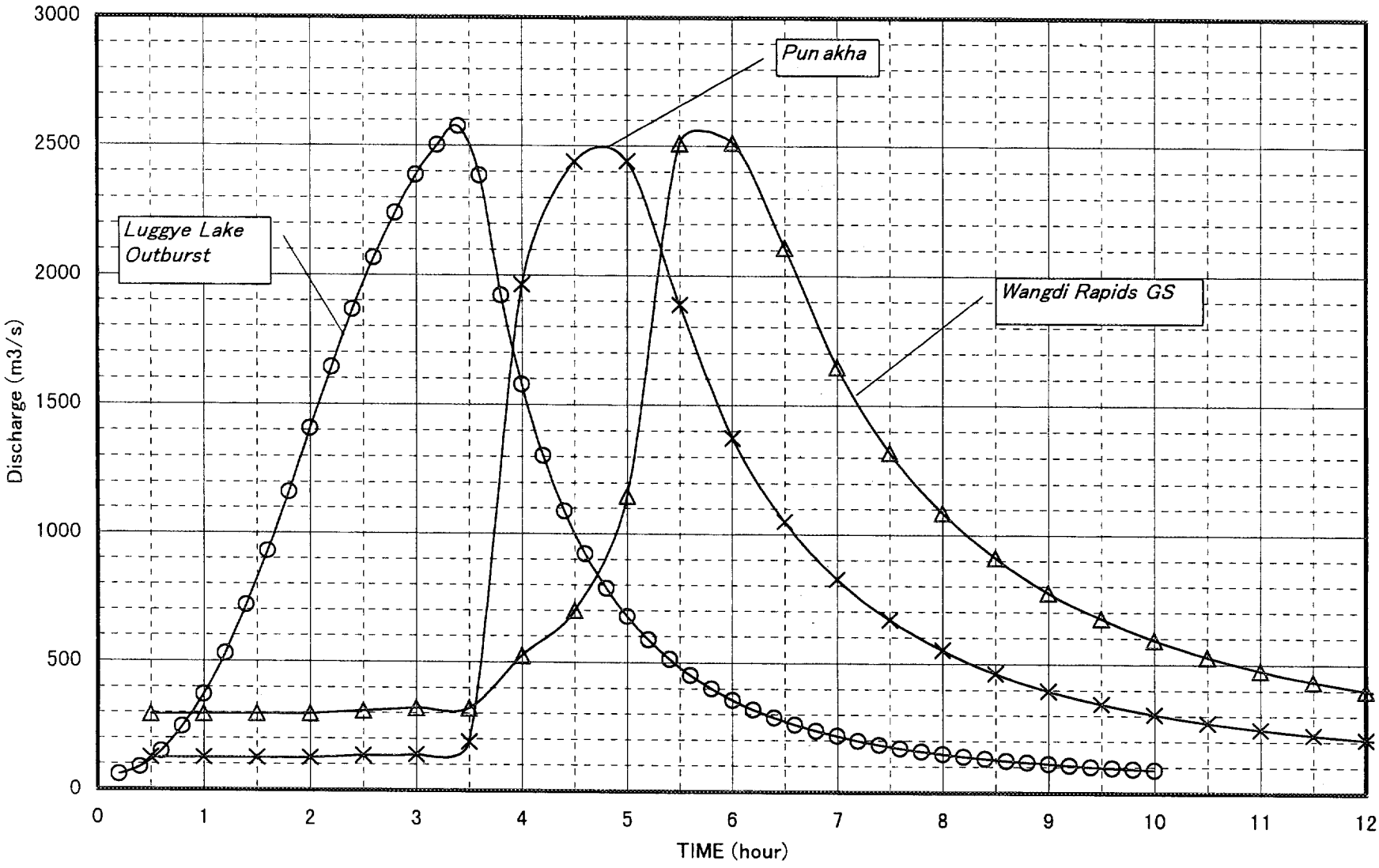

Fig.6.15 Simulation of 1994 GLOF by DAMBRK

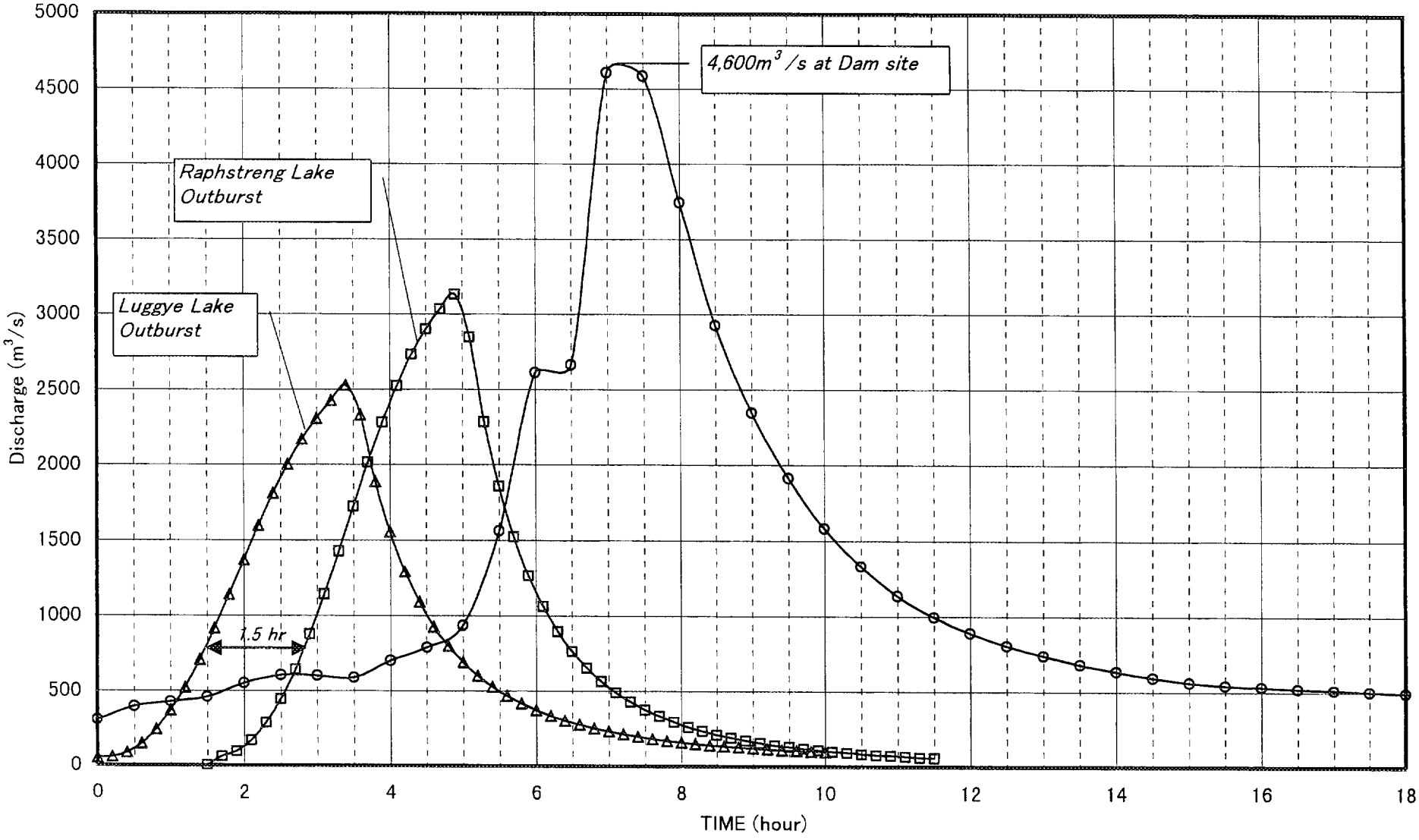

Fig. 6.16 Simulation of GLOF from Luggye and Raphstreng Lake

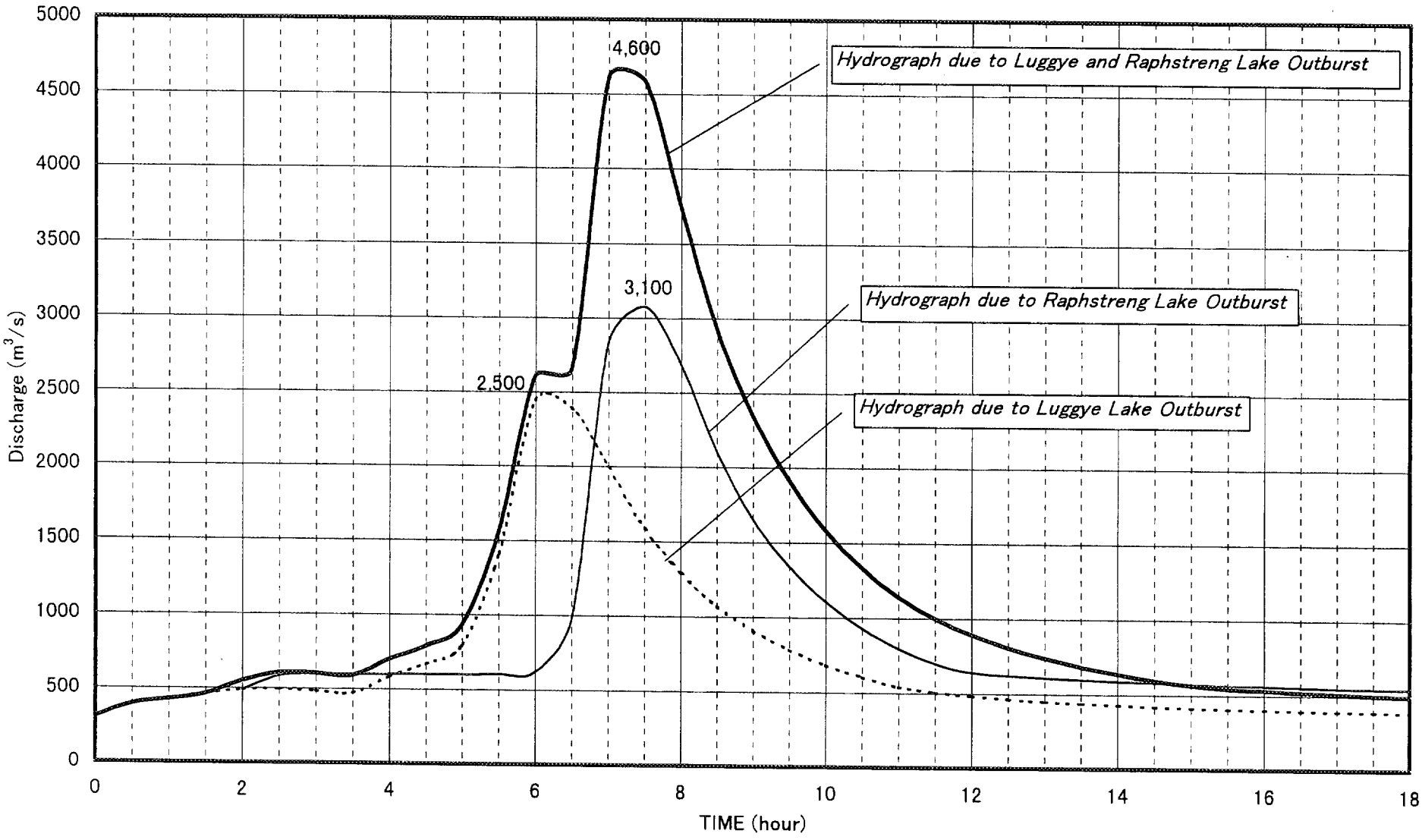

Fig. 6.17 Comparison of Hydrographs at Dam Site

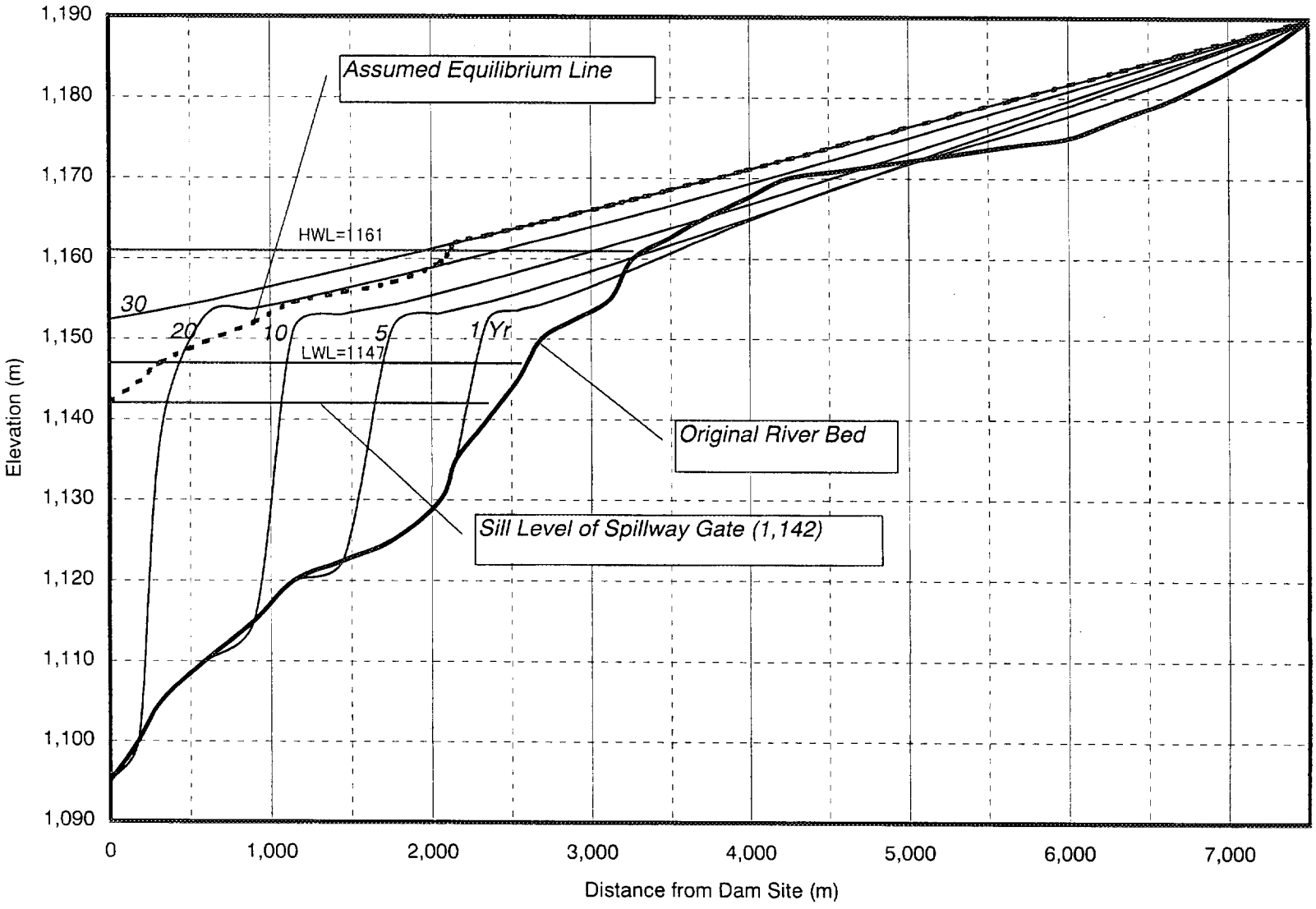

Fig. 6.18 Simulation of Sedimentation

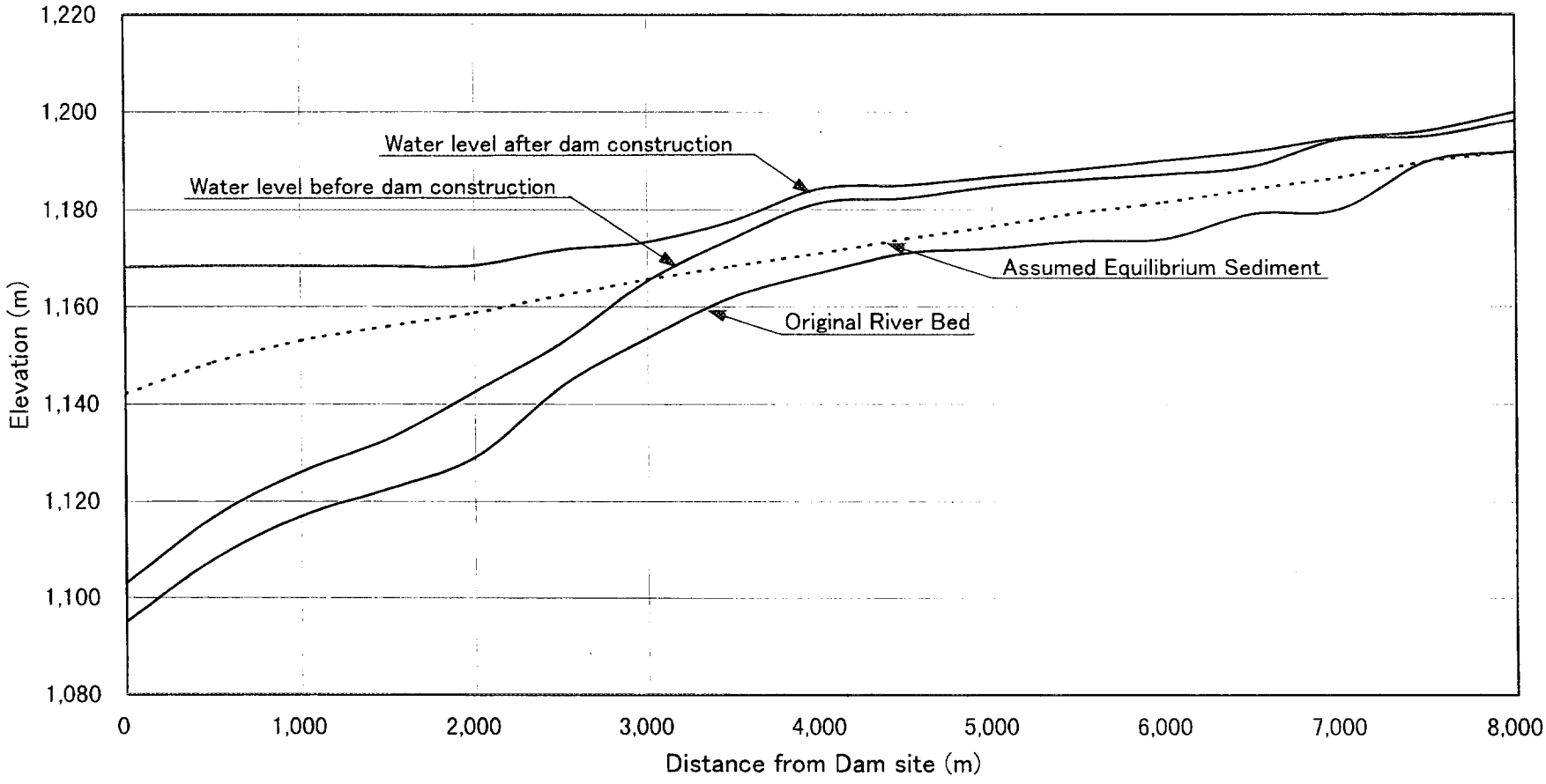

Fig.6.19 Back water curve with a flood discharge(Q_F=4,600 m^3/s)

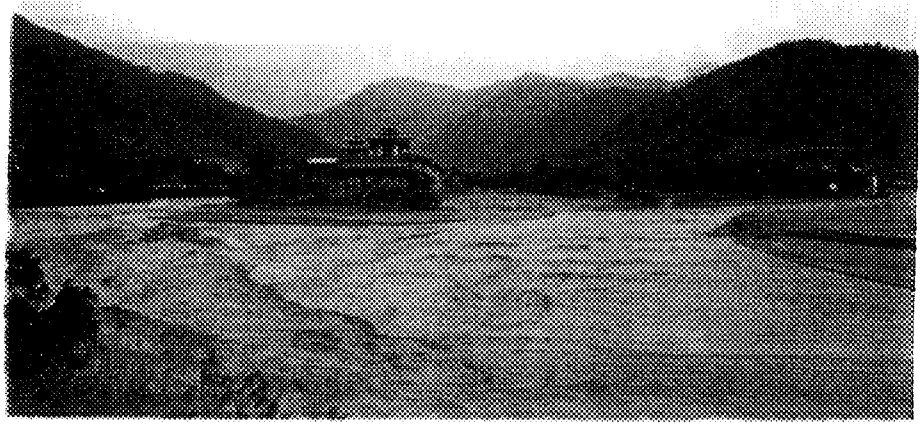

Photo 6.1 1994GLOF (1/4) Punakha (View from Downstream)

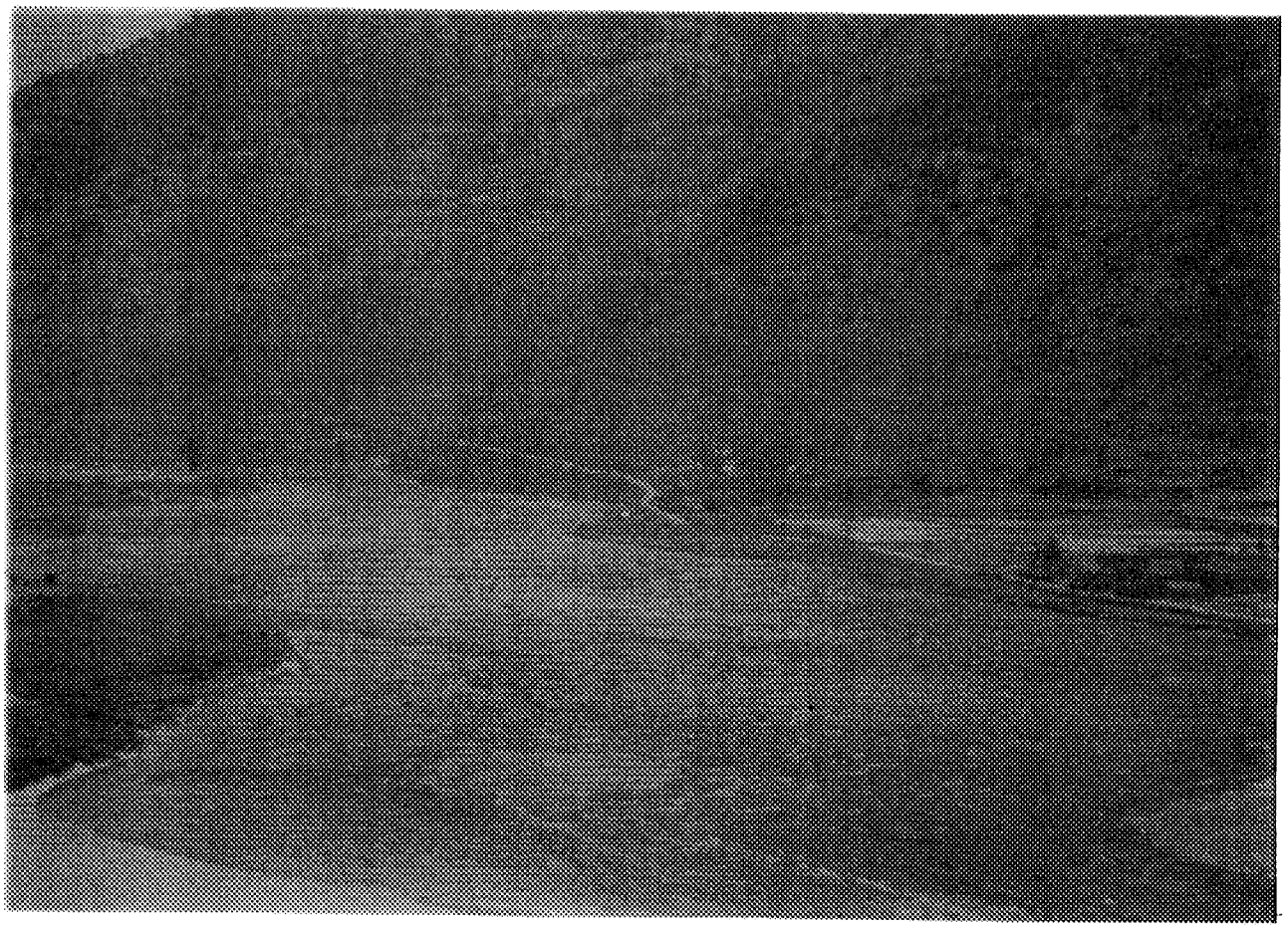

Photo 6.2 1994GLOF (2/4) Punakha – Wangdi (View from Downstream)

Photo 6.3 1994GLOF (3/4) Wangdi (View from Downstream)

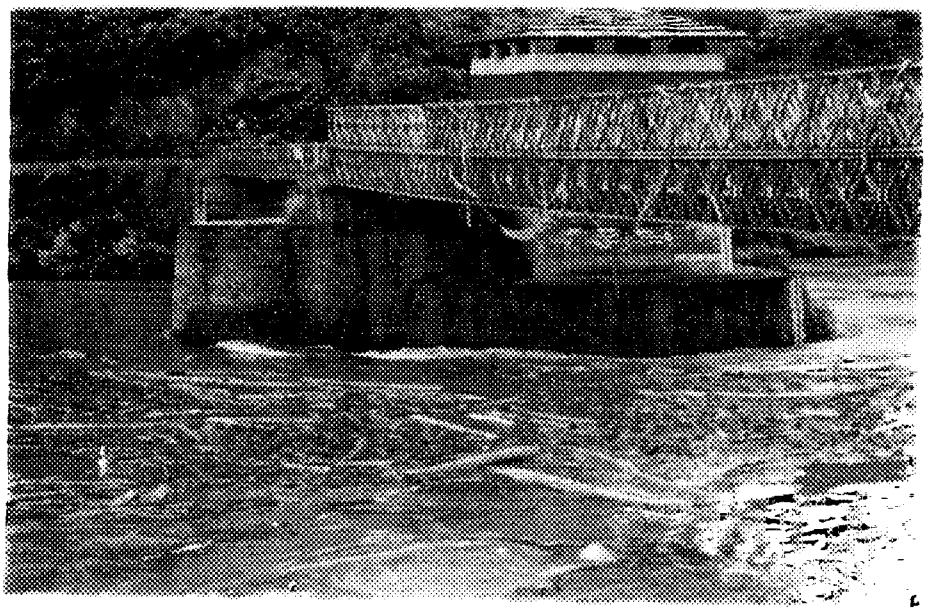

Photo 6.4 1994GLOF (4/4) Wangdi Bridge (View from Right Bank)

CHAPTER 7

GEOLOGY

CONTENTS

7. GEOLOGY

7.1 Existing Information

7.1.1 Existing Information before the Feasibility Study

Existing references published before the feasibility study are listed below. Most of them did not describe details on geology in the project area, therefore, these are utilized for summarizing regional geology of the Punatsangchhu basin.

1) M. Motegi (1998): Physiographic Study on Bhutan, Bhutan Geology, News Letter Sl. No.1, Division of Geology and Mines (Geological Survey of Bhutan), Royal Government of Bhutan

2) M. Motegi (1997): The Spraying of the Main Central Thrust in Nepal and Bhutan Himalayas, Journal of Geology, Vol. 106, No. 3 (952), 320-331p.

3) Department of Power (1993): Bhutan Power System Master Plan, Pre-feasibility Study, Sankosh River – Project 3.120, Final Report

4) United Nations, Economic and Social Commission for Asia and Pacific (1991): Atlas of Mineral Resources of the ESCAP Region, Vol. 8, Bhutan and its Explanatory Brochure

5) A. Gansser (1983): Geology of Bhutan Himalaya, Birkhauser Verlag, 181p.

6) R. Yoshinaka et. al (1988): Rock Mass Classification and its Application, Doboku Kougaku-sha, 231p., (in Japanese)

7.1.2 Geological Investigations during the Feasibility Study

Items and quantities of the geological investigations carried out in the 1999 fiscal year are summarized in Table 7.1, Table 7.2 and Table 7.3. The investigators involved to the investigations are also included in the tables.

(1) Investigations on Bedrock

1) Field Investigation

a) Aerial Photo Interpretation

Aerial photo interpretation was carried out by using about 1/15,000 scale photos taken on 27 October 1999, and total area of the interpretation attained to 10km^2.

The result of the interpretation was complied to the 1/5,000 scale geological maps of the project area.

b) Field Reconnaissance

Geological field reconnaissance was carried out by using the 1/1,250 topographic maps, which were enlarged from the 1/5,000 topographic maps. The reconnaissance covered the whole areas of the structure sites, at where the dam and powerhouse are planned. And in the area along the headrace tunnels, geologic conditions were assumed based on the results of the geological filed reconnaissance along the road passing on the right bank and of the aerial photo interpretation, because the topography of the left bank, on where the headrace tunnels are planned, are so steep to do the reconnaissance.

The results of the reconnaissance were complied to both 1/1,000 and 1/5,000 scale geological maps, combined with the results of the aerial photo interpretation, drilling investigation and seismic prospecting.

c) Core Drilling

All core drilling was carried out at the sites of dam and powerhouse. List of the drill holes is given in Table 7.4, which includes items and quantities of in-situ tests in drill holes.

d) Core Logging

Geologic logging of cores obtained by core drilling was carried out, and its result was summarized in 1/100 scale geologic logs. The obtained cores were taken by digital camera, and the photos of the cores were prepared.

e) Water Level Measurement in Drilled Hole

Twenty four times of the water level measurement was carried out in the drill holes DD-1, DD-4 and DD-6 by March 1999.

f) Permeability Test

Permeability test was carried out in the drill holes DD-1, DD-4 and DD-6 by the single packer method. Water pressure pattern applied in the test is shown in Table 7.5.

The result of the test was presented in the graph of P-Q curve, and the Lugeon values (Lu) were calculated as the volume of water injection per minute per 1m test section at the pressure of 10kgf/cm^2. (l/min m).

g) Seismic Prospecting

Seismic prospecting was carried out for the purposes of assuming the subsurface geologic conditions by means of the character that the seismic wave velocity could be related to physical properties of rock and rock mass. The seismic prospecting was performed at three sites of the dam, powerhouse and the portal of the access tunnel for headrace tunnel. For this project, the seismic refraction method was applied. List of the prospecting lines is given in Table 7.6.

The procedure of the seismic prospecting is provided as follows.

After the identification of both ends of a traverse by surveying, the locations of measuring points at intervals of 5 m by horizontal distance on the traverses were determined and wooden pegs were pounded in. The elevations of the points were calculated by leveling surveys and the topographic profiles were made by those data.

A 24 channel seismograph was used for the prospecting. One spread of this prospecting was 115 m long. 5 to 7 shot points per spread were provided in a traverse, and the signal was initiated at each shot point by explosives set in a blasting hole of a depth approximately 1m.

A block diagram of the field measurement is shown in Fig. 7.1.

Recorded artificial earthquake waveform were read and the travel times were plotted on a time-distance graph. The time-distance curves were analyzed by "Hagiwara's Method" which is suitable for determining the shapes and depths of the irregular boundary planes.

2) Laboratory Test

Cores obtained by drilling were tested in a laboratory. The list of samples, the items and quantities of the test are summarized in Table 7.7 and Table 7.8 respectively.

a) Density

The density test was carried out in conformity to the ISRM suggested method by using the same drilled core samples with those for the uniaxial compression test. In this test, both dry and saturated densities were obtained.

b) Specific Gravity and Absorption

The specific gravity and absorption test were carried out in conformity to ASTM C97 by using the drilled core samples taken from the same places where the uniaxial compression test samples were taken.

c) Water Content

The water content test was carried out in conformity to ASTM D2216 by using the same drilled core samples with those for the uniaxial compression test.

d) Uniaxial Compression Test

The uniaxial compression test was carried out on 20 drilled core samples in conformity to ASTM D3148. The length/diameter ratio of the samples was 2 or more in principal.

e) Petrographic Examination

Petrographic examination under the microscope was carried out on thin sections prepared from 10 drilled core samples, which were obtained from the drill holes DD-1 and DP-1.

(2) Investigations on Concrete Aggregates

1) Field Investigation

a) Pit Excavation

Four pits shown in Table 7.9 were excavated in the river floor located on the right bank about 7km upstream of the dam site, for the purposes of grasping the geologic conditions of alluvium as well as sampling for the laboratory tests on concrete aggregates. Each pit was 1.5 m in depth.

b) Geologic Logging

Excavated pits were logged geologically. The results of logging were complied to 1/20 scale geologic logs.

c) Sampling

Alluvium samples having 60kg in each weight were taken from each excavated pit in conformity to ASTM D75. List of the samples is given in Table 7.10.

The samples taken were transported to the laboratory in Thimphu, and tested by items as described below.

2) Laboratory Test

Laboratory tests on concrete aggregates as shown in Table 7.11 were carried out on the samples taken from the pits, for the purposes of confirming the suitability for concrete aggregate.

(i) Specific Gravity and Absorption

The specific gravity and absorption test was carried out in conformity to ASTM C127 and C128.

(ii) Abrasion Loss

The abrasion loss test was carried out in conformity to ASTM C535 and C131.

(iii) Soundness

The soundness test was carried out in conformity to ASTM C88.

(iv) Sieve Analysis

The sieve analysis was carried out in conformity to ASTM C136.

(v) Finer Material Content

The finer material content test was carried out in conformity to ASTM C117.

(vi) Alkali-aggregate Reactivity

The alkali-aggregate reactivity test was carried out by the chemical method equivalent to ASTM C289.

(vii) Petrographic Examination

The petrographic examination was carried out by the X-ray diffraction method of ASTM C295.

(3) Investigation on Alluvium

Investigations and tests shown in Table 7.12 were carried out on alluvium distributed in the prospective quarry site, for the purposes of grasping characters of alluvium.

(i) Pit Excavation

Pit PQ-1 was excavated in the river floor located on the right bank about 7km upstream of the dam site, for the purposes of grasping the geologic conditions of alluvium as well as sampling for the laboratory tests. The pit was 1.5 m in depth.

(ii) Geologic Logging

Excavated pit was logged geologically. The result of logging was complied to 1/20 scale geologic log.

(iii) Sampling

Alluvium sample having 60kg in weight (sample no. QP-1-01) was taken from excavated pit in conformity to ASTM D75. This sample were transported to the laboratory in Thimphu, and tested by items as described below.

(iv) Sieve Analysis

The sieve analysis was carried out in conformity to ASTM C136.

(v) Petrographic Examination

The petrographic examination was carried out by the X-ray diffraction method of ASTM C295.

7.2 Regional Topography and Geology

7.2.1 Topography

The Kingdom of Bhutan is located in the region of eastern Himalayan Mountains, and the latitude of the country ranges from 26°40'N to 28°20'N, while the longitude ranges from 88°42'E to 92°9'E. The northern boundary borders on China and the other boundary borders on India. The northern boundary is located in the Himalayan Mountain range, which is higher than 5,000 m in elevation, while the southern boundary bordering on India is located in the foot of the southern mountain range, which is about 1,000 m high. Except these northern and southern boundary areas, the most part of the country is called the central mountain range area which consists of the mountains which are about 2,000 to 3,000m high and the basins surrounded by the mountains.

Punatsangchhu, where this hydropower project is proposed, originates from Tibetan Plateau, runs southward in parallel with the longitude 90°E and its total length attains to about 320km.

The main tributaries in the catchment area of Punatsangchhu Project are listed in the following table.

Side	Name	Location
Right Bank	Mhochhu	Join at Punakha
	Tabayrongchhu	About 5km downstream from Punakha
	Basochhu	About 13km downstream from Wangdue Phodrang
	Rurichhu	About 2.5km downstream from Basochhu
Left Bank	Phochhu	Join at Punakha
	Dangwechhu	Join at Wangdue Phodrang
	Pazachhu	About 18km downstream from Wangdue Phodrang

The dam site of the Punatsangchhu Project is planned about 10 km downstream of Wangdue Phodrang and the powerhouse is planned about 8km downstream of the dam site.

The topography of Punatsangchhu Project area is summarized as follows;

(1) The area about 22 km long from Punakha to the dam site via Wangdue Phodrang

The river topography of this area shows the one of the old stage characterized by the gentle river gradient (1/368) and by the thick alluvium (about 35 m thick at the Wangdue Phodrang Bridge).

Accordingly, the topography on both banks of the river forms gentle slopes while there are some variations. Especially, at the right bank area from Tabayrong Chhu to about 5 km downstream of Wangdue Phodrang, the gentle slopes, which are formed by thick colluvium and the landslide material slid along the gneissosity of bedrock, are distributed widely and utilized for cultivation.

Moreover, on the left bank in this area, because the gneissosity of the bedrock dip towards the mountain, the topography of the banks is stable and gentle as a whole.

(2) The river about 8 km from the dam site to the powerhouse site

The river in this area shows the topography of the maturity stage characterized by the steep river gradient (1/8~1/78) and many rapids.

Accordingly, the topography on the left banks where the gneissosity dip against the mountain slopes form many cliffs having the dipping of more than 45° and many gorges are found. However, at the right banks where gneissosity dips along the slopes of the river bank, the colluvium containing many large to huge boulders are found in many places.

(3) Terrace

The terrace deposits are found in various places of the project area, however the remarkable terrace topography can be seen at the left bank of the Wangdue Phodrang Bridge. The thickness of sand and gravel here is 40 to 50 m and the strata are horizontal. On the other hand, the terraces on the right bank (the opposite bank) can be seen, but they are disturbed. Probably, they are disturbed by the landslide movement after the upheaval.

7.2.2 Geology

The geologic units in the catchment area are mainly Thimphu Formation and Tirkhola Formation as shown in Fig.7.2. According to the reference, Thimphu Formation consists of migmatite, biotite-granite gneiss and mica schist, with subordinate amounts of limestone and amphibolite dyke.

Thimphu Formation distributed in the Punatsangchhu Project area consists mainly of gneiss containing subordinate amounts of granite and migmatite. The gneiss in this area, judging from geotechnical viewpoints, can be called as "biotite gneiss" (hereinafter referred to as "gneiss").

As mentioned above, according to the reference, Thimphu Formation contains limestone, which is not found in the project area. It is distributed in the area near Punakha.

On the other hand, Tirkhola Formation consists of bedded quartzite and phyllitic quartzite. Near the project area, this formation can be seen at the upstream areas of Basochhu and Rurichhu, especially, at the sites of the intake and dam of Basochhu Project.

The bedrock distributed in the project area (reservoir, dam, headrace tunnel and powerhouse areas) consists mainly of gneiss with subordinate amounts of granite and migmatite, which can be found near the Basochhu gorge and the junction point of the main river and Rurichhu. Moreover, black schist is distributed in the area near the backwater of the reservoir. Gneissosity of bedrock in the project area trends N30°E to N50°E and dips 30 to 40°SE, however, dips and strikes of gneissosity near granite intrusions change locally and their general orientation show N70°E to EW/10 to 20°SE.

Such tendency of gneissosity was confirmed at both banks of the project area and also the gneissosity of bedrock along the road to Basochhu at about EL.1, 770 m was confirmed to be N30°E/30°SE. Moreover, schistosity of black schist at the outcrops along the road were also NS to N25°E/15 to 30°SE.

Judging from such tendency of gneissosity at the project area, the bedrock of the project area seems to be located at the eastern wing of the large scale anticlinal structure.

Concerning the fault, it cannot be found on outcrops along the road, however, according to the reference the boundary between gneiss and schist near the proposed reservoir end may be one of MCT (Main Central Thrust). But the width of the sheared zone is reported to be less than 1m.

Because of the steep topography and scarce access to the left bank, geological field reconnaissance at the left bank was restricted. Therefore, the left bank area was investigated by the aerial photo interpretation and the assumption from the geological field reconnaissance on the right bank. Based on such reconnaissance, many cliffs at the left bank have the possibility to be landslide scarp caused by unstable topography. The typical samples of these landslide scarps are the opposite bank of the junction point of the main river and Ruri Chhu, the back field of the proposed switchyard site and the northern colonized area from the proposed surge tank site. These areas are now completely stable.

7.3 Site Geology

7.3.1 Geology of Reservoir

(1) Topography

The proposed reservoir has a high water level of 1,161 m in elevation, and its back-water reaches about 3.2 km upstream of the dam site. The width of the reservoir is 300 m or less, and becomes widest near the place where a tributary discharges from right bank side at about 600 m upstream of the dam site. There are two tributaries, which discharge into the proposed reservoir. Both are running on the right bank, and flow water along the tributaries is recognized even in dry season. One of the tributaries discharges into Puna Tsang Chhu at the place about 600m upstream of the dam site, and the other (Layalum Chhu) at about 1,200 m upstream of the dam site. The topography between the above tributaries forms gentle slopes (inclination about 10 degrees), and used for cultivation areas. Gradient of Punatsangchhu within the reservoir area is as gentle as 1/50 in average.

Most of the proposed reservoir and its surrounding areas are occupied by gentle slopes of 30□ or less in inclination. On the left bank, upper ends of the gentle slopes are connected to steep cliffs be exposed by rocks. On the right bank, the gentle slopes continue to higher elevation and the upper ends of the slopes reach to an elevation of more than 1,300 m.

No large landslide was found in the proposed reservoir nor its surrounding areas. Surface collapses along the rim of the proposed reservoir were observed at the places listed below.

1) Right bank about 100 m upstream of the dam site;

   width 20 to 40 m, height 35 to 60 m, composed of colluvium

2) Left bank about 2.3km upstream of the dam site;

width 230m, height 45m, composed of colluvium

Mountain bodies of both banks are thick, and there is no deep valley, which may become a cause of leakage from the reservoir.

(2) Geology

Geology of the reservoir was described based on the results of the geological field reconnaissance and the aerial photo interpretation.

1) Surface Deposits

The right bank of the reservoir is covered by thick and wide colluvium, which is considered to be accumulated by downward sliding of the bedrock along gneissosity. The thickness of colluvium is 20m in minimum assumed from the result of the geological field reconnaissance and the drill holes DD-6, DD7 and DD-8 located on the right bank of the dam site. Boulders of 15 m diameter are observed in colluvium in outcrops on the roadside.

The left bank is also covered by colluvium, which is derived from upper slopes, and its distribution is 50 to 300 m wide and 600 to 800 m long. Boulders of gneiss are also included in colluvium. On the left bank, wide distribution of colluvium is observed at the following 2 locations.

a) Left bank about 300 m upstream of the dam site;

width 150 m, length 550 m

b) Left bank about 1.3 km upstream of the dam site;

width 400 m, height 950 m

2) Bedrock

Bedrock in the reservoir and its surrounding areas is mainly composed of gneiss. Towards the upstream, this gneiss becomes weakly metamorphosed and shifts into schist.

Geologic structures in the reservoir area is difficult to clarify precisely, because the area along the road provides less outcrops. Assuming from outcrops on the left bank and the structural topography interpreted on the aerial photos, the gneissosity trends N10°E to N30°E and dips 10 to 30°SE. Therefore, the right bank has so called "a dipping to slopes" structure resulting in forming gentle slopes in parallel with gneissosity. On the other hand, the right bank has "a dipping against slopes" resulting in forming stable slopes or cliffs.

No outcrop of fault could be found in the geological field reconnaissance. According to the reference (ii) (Motegi, 1997), gneiss is in a gentle dipping fault contact with schist at about 2.5 km upstream of the dam site. This fault is reported as one of the MCT (Main Central Thrust). In this reference, the width of the sheared zone is reported less than 1m.

(3) Geotechnical Evaluation

1) Slope Stability

- No large landslide active at present was found in the reservoir nor its surrounding areas, and the slopes around the reservoir are gentle. Therefore, there is low possibility to occur large landslide, which may hinder the functions of the reservoir.

- However, colluvium is distributed widely along the rim of the reservoir. Therefore, the possibility still remains that the surface collapse may occur accompanied with impoundment. Especially thick colluvium is assumed in the left bank area 300m and 1,300m upstream of the dam site, where there is a possibility to occur surface collapse during the operation of the reservoir.

2) Water Tightness

No soluble rock such as limestone is distributed in the reservoir area. Furthermore, the mountain bodies of both banks are thick. Therefore, no leakage from the reservoir to the neighboring basin is predicted. As mentioned above, the water-tightness of the reservoir is evaluated to be sufficient from geotechnical viewpoints.

7.3.2 Geology at Dam Site

(1) Topography

Dam site is planned at the place about 10km downstream of Wangdue Phodrang. The area upstream of the dam site shows old age topography having the width of the river floor more than 60 m. And the both banks form gentle slopes of 10 to 30° in inclination. In the area downstream of the dam site, the width of the river floor becomes narrower to 50 m, and slope on both banks become steeper. The river gradient also becomes steeper towards the downstream of the dam site. The river gradient is about 1/50 where upstream of the dam site, and about 1/20 where downstream of the dam site.

The topography at the dam site is quite different between right and left banks. The left bank, which has "dipping against slopes" structure, shows steep slopes of more than 40° in inclination or cliffs be exposed by rocks. However, the right bank is mostly occupied by slopes of about 40° in inclination, except scattered distributions of rock outcrops (height 9 to 36 m). Collapse of the bedrock along

gneissosity is remarkable on the right bank, resulting in accumulating widely distributed colluvium, which frequently includes boulders of several meters in diameter.

Furthermore, the slopes on the right bank above the dam crest (elevation 1,150 m or higher) show topographic characteristics that the slopes having about 40° inclination occur mutually with the cliffs having about 70□ inclination. The relationship between the elevation and the slope inclination is summarized in the following table.

Elevation (m)	Slope Inclination (degree)	Geology	Remarks
1,110~1,155	70	Bedrock (gneiss)	River floor to dam crest
1,155~1,230	40	Colluvium	Dam crest to the road and above
1,230~1,240	75	Bedrock (gneiss)	Cliff, about 10m in height
1,240~1,300	38	Colluvium	
1,300=1,310		Bedrock (gneiss)	Cliff, about 9m in height
Above 1,310		Colluvium	

Such step-like topography indicates the existence of a kind of discontinuity in the rock mass. This step-like topography is observed at the elevations of about 1,230 m and 1,300 m, and extends in parallel with the river direction. As described in the next clause (2) Geology 2) Bedrock, the discontinuity is inferred to be sub-vertical and to be formed by the downward movement of rock mass along gneissosity.

(2) Geology

1) Surface Deposits

Surface deposits distributed in the dam area can be divided into two.

One is thick alluvium distributed along the river, and its thickness is assumed 70 m in maximum based on the result of drilling DD-3, DD-4 and DD-5. Boulders of 6 m in diameter are included in alluvium, and the rock type of boulders is mostly gneiss. The width of alluvium distribution is about 125m along the dam axis. According to the result of the seismic prospecting along the dam axis SD-2, the velocity layer of more than 2.0 km/sec exists in alluvium deeper than 20 m below the ground surface. The seismic velocity in this part is considered to be provided by the conditions that alluvium is compact and includes many boulders.

The other surface deposit is colluvium derived from upper slopes of both banks.

On the right bank, colluvium about 5m thick is distributed in the place at the elevation about 1,110 m, that is just below the cliff. Thick colluvium is distributed in the places at the elevation from 1,155 to 1,230 m, that is above the right abutment of the dam, and attains to 28.9 m in thickness based on the results of geologic logging of DD-7 and DD-8. Further to the downstream of the dam axis, i.e. right side downstream toe of the dam, thick colluvium is distributed, and its thickness attains to more than 20m in the drill hole DD-6.

On the left bank, colluvium about 5m thick is distributed in the place at the elevation about 1,110 m, that is just below the cliff. And colluvium derived from upper cliffs is distributed at elevations between 1,135 and 1,165 m, corresponding to the elevation of the dam crest. The thickness of colluvium there is about 7m based on the result of drilling DD-1 and DD-2. The geological field reconnaissance revealed that colluvium includes boulders about 5m in diameter.

2) Bedrock

The bedrock at the dam site is composed of gneiss. Gneiss shows clear foliation and includes garnet crystals. Gneiss intercalates pegmatite layer of less than 1m thick, and contains minor amount of migmatite. Gneiss is fresh and hard below the bedrock surface. Its uniaxial compressive strength is 322 kgf/cm^2 in average and ranges from 217 to 577 kgf/cm^2. The result of laboratory tests on drilled cores are summarized in Table 7.13.

3) Weathering

The weathering of bedrock is generally weak, based on the results of drilling DD-1, DD-2, DD-4, DD-5 and DD-6 located at the dam site. Weathering conditions below the bedrock surface can be classified based on the rock mass classification criteria as follows.

Depth below Bedrock Surface (m)	Weathering Grade
0～6	3～2
More than 6	2～1

(Scale of Weathering)

Scale	Description
1	Very fresh. No weathering mineral component.
2	Fresh. Some minerals are weathered slightly. Usually no brown crack.
3	Fairly fresh. Some minerals are weathered. Cracks are stained and with weathered material.
4	Weathered. Fresh portions still remain partially.
5	Strongly weathered. Most minerals are weathered and altered to second minerals.

In drill hole DD-1 and DD-2, moderately weathered rock classified into 2 to 3 weathering grade reaches 2.6 to 5.4m deep below the bedrock surface, and corresponds to the velocity layer of 1.2 km/sec or less. The bedrock becomes fresh below this moderately weathered rock. Within fresh rock, there are some brown colored weathered zones along gneissosity or joints, but they are less than 2m thick. Such brown colored weathered zones may not influence to the rock mass stability of dam foundation.

Fresh rock classified into weathering grade 2 is observed below the bedrock surface in drill hole DD-4, located on the right side river floor. In DD-4, there is weakly weathered zone at a depth from 26.4 to 35.4 m, and classified into 2 to 3 weathering grade. Depth of this zone is more than 15 m below the bedrock surface, therefore, this weakly weathered part may not influence to the stability of dam foundation. In drill hole DD-5, the rock of 2 to 3 weathering grade continues more than 9 m below the bedrock surface, but this weathering is judged due to that the drill hole penetrated bedrock close to the bedrock surface as shown in geologic section of the dam.

Fresh rock was recognized below the bedrock surface in drill hole DD-7 and DD-8, located at the elevation near the dam crest (1,170 m). The depths to the bedrock are 18.9 m in DD-7 and 28.4 m in DD-8 respectively.

4) Discontinuity

(i) Gneissosity

Trend of gneissosity at the dam site can be clarified by the measurement of gneissosity attitudes in the geological filed reconnaissance. There is not much difference on orientation of gneissosity between left and right banks. The gneissosity trends N20°E to N40°E and dips 30 to 40°SE. Attitude of gneissosity N22□E/32□SE is applied as a representative trend of gneissosity at the dam site in

the geologic section of the dam. A phenomena of rock apart along gneissosity is observed on cliffs above the elevation 1,165m on the left bank. That phenomena may be induced by stress relief and weathering.

(ii) Joint

No highly jointed rock was found on outcrops. Only two orientations of joint were recognized, they were N78°E/52°N and N2°E/36°E. Dipping of joints on drilled cores ranges from 30 to 70°.

(iii) Fault

No lineament indicating major fault was interpreted on the aerial photos. A sheared zone of 0.5 m wide was found on a outcrop, located on a creek running on the left bank about 250 m downstream of the dam site. The attitude of this fault is N46°W/84°N.

A pale bluish gray clay was found on core of drill hole DB-1 at a depth between 37.85 and 38.6 m, and was judged to be a minor fault. The dipping of this fault is 80° and actual width of the sheared zone is 2 cm.

As described above, no fault having a sheared zone of more than 1m thick was found. However, as mentioned in a clause of topography, there are two probable discontinuityies indicated by the step-like topography on the right bank slopes above the dam at elevations about 1,230 m and 1,300 m, extending in parallel with the river direction.

These step-like topographies are considered to be formed by the sub-vertical discontinuities in the bedrock resulted from the downward movement of rocks along gneissosity, from the basis below.

- A cliff (height about 10 m) at an elevation of 1,230 m extends more than 150 m along the right bank.
- The gneissosity of bedrock shows "dipping to slopes" structure on the right bank.
- Loosening of rocks induced by the movement along gneissosity was observed on a roadside outcrop about 80m upstream of the dam site.
- Cracks dipping 70 to 80° were observed on drilled cores of DD-7 at the depths of 61 to 65 m and 86.5 to 87.0 m.

- Most of cores were lost at the section from 41.55 to 48.7 m in drill hole DD-7.

The closest discontinuity in rock mass is considered to pass on the right bank about 70m towards the mountain from the right end of the dam.

5) Rock Mass Classification

(i) Classification System

The rock mass classification system of CRIEPI (Central Research Institute of Electric Power Industry, Japan) is employed for this feasibility study as a geotechnical rock mass classification. In this system, the rock mass is classified into 6 classes. The criteria of the classification is shown in Table 7.14. Drilled cores obtained at the sites of dam and powerhouse were classified according to this system, and the result of the classification is described in the geologic logs.

(ii) Rock Mass Classification of Bedrock

The result of rock mass classification of the dam foundation can be summarized as follows based on the geologic logging of drill hole DD-1, DD-2, DD-4, DD-5 and DD-6.

- Most of the drilled cores obtained within the area of dam foundation are classified into CM Class.

- The bedrock below the prospective excavation line is composed of CM and CH Classes, and CH Class is dominant.

6) Water Tightness of Bedrock and Groundwater Level

Permeability test in drill holes was carried out in DD-1, DD-4 and DD-6. The details of the test result are shown in the geologic logs, and the characteristics of bedrock at the dam site can be described in terms of water tightness as follows.

- The bedrock of the left dam abutment shows mostly less than 10 Lu.

- The bedrock deeper than 14.4m below the bedrock surface shows less than 10 Lu at the lower elevations of the right bank.

- Permeability of bedrock in the right abutment is assumed as follows based on the seismic velocity and RQD of drilled cores, although no permeability test was carried out in drill hole DD-7 and DD-8 located at the right bank.

  • The bedrock showing its seismic velocity 1.8 to 2.2 km/sec has an average RQD of 55% (from 18.9 to 47 m in DD-7), such part may be relatively permeable.

- The bedrock showing its seismic velocity more than 4.0 km/sec has an average RQD of 72% (deeper than 47 m in DD-7), such part may be impermeable.

Groundwater level could not be detected in the whole section of DD-7 and DD-8, located on the right bank, according to the driller's information. Furthermore, no water flow along the creeks was observed on the right bank, where the drill hole DD-7 is located. Therefore, there is possibility that the groundwater level within the bedrock becomes lower towards the river in the right bank induced by the probable discontinuities as described in the clause "Fault" as well as the loosening of the bedrock induced by the movement along gneissosity.

The final water level in drill hole DD-1 on the left bank was 51.0m below the ground surface, and this water level is almost equal to the river water level. However, the groundwater level is considered to become higher from DD-1 towards the mountain side based on the reasons described below.

- Flow water was observed even in dry season along the small creek on the left bank about 250m downstream of the dam site.
- On the left bank, there is no deep valley, which may become a cause of lowering the groundwater level.

(3) Geotechnical Assessment

1) General Geology

- The bedrock is composed of gneiss
- Gneissosity trends N20°E to N40°E and dips 30 to 40°SE
- Most of slopes on the right bank are covered by thick colluvium, except the cliff at lower elevations on the dam axis.
- No sheared zone of more than 1m wide was detected on neither outcrops nor drilled cores. However, two discontinuities can be assumed in the bedrock on the right bank based on the topographic characteristics etc. And the closest discontinuity is assumed to pass a place 70 m from the right end of the dam crest. The discontinuity seems to extend in parallel with the river direction, and to dip 70 to 80° based on the result of geologic logging of drilled cores.

2) Surface Deposits

- Thick alluvium is distributed in the river floor, and its maximum thickness is assumed to be about 70 m.

- The thickness of colluvium on the right bank is assumed to be about 28m in maximum, and the slope instability may be induced by the excavation of the dam foundation.

- Thick colluvium is distributed in the area near the right side toe of the dam, therefore, careful attention is necessary to pay for the distribution of colluvium in considering the foundation excavation. The thickness of colluvium in drill hole DD-6 is more than 20m.

- Colluvium distributed in the area of the left bank is relatively thin in thickness (about 7m in maximum), and has relatively narrow distributions. Therefore, the colluvium may not become a cause of serious problem in excavation of the dam foundation.

3) Rock and Rock Mass Properties

Properties of fresh rock are obtained by the laboratory tests using drilled cores. They are;

- Dry Density: 2.72 to 2.89 gf/cm^3

- Saturated Density: 2.74 to 2.90 gf/cm^3

- Water Content: 0.14 to 0.61%

- Uniaxial Compressive Strength: 217 to 577 kgf/cm^2

Furthermore, shear strength of the bedrock by each rock class can be summarized, according to the existing references, as shown in Table 7.15.

4) Foundation Treatment

- Permeability of the bedrock on the left bank is less than 10 Lu, therefore, improvement by grouting is considered to be highly possible.

- At the lower elevations on the right bank (drill hole DD-4), permeability of the bedrock is 10 to 13 Lu from the bedrock surface to the depth of 14.4 m, and less than 10Lu in deeper section. Therefore, improvement by grouting is considered to be highly possible.

- On the right abutment, careful attention is necessary to pay for the foundation improvement of the bedrock within the section showing the seismic velocity 1.8 to 2.2 km/sec (18.9 to 47 m below the ground surface). The bedrock 47 m below the ground surface or deeper shows the seismic velocity of more than 4.0 km/sec, then the bedrock is considered to be compact and relatively impermeable.

- Groundwater level in the right bank may become lower towards the river, because of the existence of probable discontinuity, therefore, it is necessary to take care of the groundwater level in considering the foundation treatment.

- In general, it is evaluated that the permeability of the bedrock at the dam site is highly possible to be improved.

5) Excavation of Dam Foundation

Based on the results of geologic logging of the drilled cores, assumption on the depth of foundation excavation at the dam site is summarized in Table 7.16 from geotechnical viewpoints by each drill hole.

Good rock occurs below the bedrock surface in the area covered by alluvium at the lower elevation of the dam. Therefore, dam foundation excavation below the elevation 1,100m is considered to be the removal of alluvium and the trimming of rock surface. However, it is noted that the thickness of alluvium is inferred to be about 70m, and the alluvium includes boulders of 6m in diameter. Furthermore, primary wave velocity in the part deeper than 8m below the ground surface shows more than 1.8km/sec, and this fact indicates that alluvium there is compact.

On the abutment of the left bank, the foundation excavation is considered to be the removal of alluvium and the trimming of rock surface. The depth of foundation excavation below the ground surface is inferred to range from 9.8 to 12.6 m at the place near drill hole DD-1 and DD-2.

Slope instability of the right bank above the dam abutment may occur during the foundation excavation, because the slopes there are covered by thick colluvium (28.3m in DD-8) and shallower part of the bedrock is loosened by movement along gneissosity.

7.3.3 Geology at Settling Basin Site

(1) Topography

The topography around the settling basin is composed of steep slopes of more than 40□ or cliffs, as mentioned in the clause of "Geology of Dam".

Settling basin is planned in underground about 80 to 180 m from the left side end of the dam, and the depth below the ground surface is about 150 to 200 m. The settling basin consists of two underground caverns, and their longitudinal axes are almost parallel to the left side slopes of Puna Tsang Chhu. Each cavern has a length of 320m and a width of 25 m.

(2) Geology

1) Surface Deposits

In and around the settling basin area, there is no distribution of thick colluvium, that may become a cause of underground cavern instability. Topography around the settling basin site forms cliffs of more than 50 m high, and the most of the ground surface expose the rocks.

2) Bedrock

The bedrock in and around the settling basin area is composed of gneiss, and is considered to be fresh and hard in general. In the seismic prospecting line SD-4, the seismic velocity at the depth more than 30 m below the ground surface ranges from 4.0 to 4.2 km/sec. Furthermore, fresh and hard bedrock can be expected at the depth deeper than 12.6 m, based on the geologic conditions of cores in DD-1, which is about 200 m apart from the settling basin site. The laboratory test results using the cores of DD-1 include the uniaxial compressive strength of fresh gneiss, which is 322 kgf/cm^2 in average and ranges from 217 to 577 kgf/cm^2.

3) Weathering

The fresh bedrock was encountered in drill hole DD-1 and DD-2 at the depths of 9.8 and 12.6 m respectively (weathering grade 2 or less). The thickness of the overburden at the settling basin site is more than 150 m, therefore, the bedrock surrounding the settling basin is expected to be fresh. However, the possibility remains that brown colored weathered part along gneissosity or joint may appear partially.

4) Discontinuity

(i) Gneissosity

The trend of gneissosity is considered to be similar with that at the dam site. Attitude of gneissosity measured in the geological field reconnaissance ranges from N30°E to N60°E and dips 24 to 58°E.

(ii) Joint

No highly jointed bedrock was recognized on the ground surface, but the measured attitudes of joints are listed as follows.

- N78°E/52°N
- N2°E/36°E

(iii) Fault

Aerial photo interpretation detected no lineament indicating a major fault. On outcrops, a sheared zone of 0.5 m wide was found in the creek about 250 m downstream of the dam site, and its attitude is N46°W/84°N. This sheared zone is composed of pale bluish gray colored clay. The possibility remains that this fault extends to the site of the settling basin.

5) Groundwater

Flow water was observed along the small creek about 250 m downstream of the dam site even in dry season. The settling basin is located about 50 m towards mountain side from this creek, therefore, the underground cavern may be below the groundwater level.

(3) Geotechnical Assessment

Geologic conditions at the settling basin site can be summarized geotechnically as follows.

The bedrock is composed of gneiss.

- Gneissosity trends N30°E to N60°E and dips 24 to 58°SE. Strike of gneissosity is almost perpendicular to the longitudinal axis of the underground cavern, but dipping is relatively gentle. Therefore, it is necessary to take care of the stability of cavern roof.
- The possibility remains that the water flow into the cavern occurs in underground excavation, but its quantity may not become so much problem which will make the construction be difficult.
- Existence of major fault is not assumed based on the results of the aerial photo interpretation and the geological field reconnaissance. However, the possibility of minor fault still remains, because the sheared zone of 0.5 m wide was found on the ground surface.

7.3.4 Geology along Headrace Tunnel

(1) Topography

The proposed headrace tunnel extends approximately 7 km from the intake to the surge tank, passing through the mountain body on the left side of Punatsangchhu nearly in parallel with the river direction. The left bank slopes, where the headrace tunnels are planned, is "dipping against slopes" in terms of structural geology, and form steep cliffs in many places.

The ground surface elevation along the headrace tunnels ranges from 1,150 to 1,800 m, and the tunnels are planned between elevations of 1,130 m and 1,150 m. The thickness of the overburden is 60 to 660 m, except the area near the intake. Along the headrace tunnel route, the thickness of the

overburden reaches more than 300 m in the section between the place 1,450m downstream of the intake and the place 800 m upstream of the surge tank. The thickness of the overburden becomes in maximum at the place 1,600 m upstream of the surge tank, and reaches to about 660 m. On the other hand, it becomes in minimum at the place connecting to the surge tank, and is about 60 m.

The thick surface deposits along the headrace tunnel route is inferred to be distributed in the area about 1 to 1.5 km downstream of the intake. This surface deposits may not influence to the tunnels, because the thickness of the overburden is more than 300m there.

The river running within the area of the headrace tunnel shows maturity stage river topography characterized by a steep river gradient (1/20 to 1/30) accompanied with many rapids. And the topography on the left bank, that the proposed headrace tunnel passes, forms steep slopes and cliffs of more than 45° inclination in many places. This topography results from the orientation of gneissosity, i.e. "a dipping against slopes", as already stated.

(2) Geology

It was very hard to do the geological field reconnaissance in the areas on the left bank where the proposed headrace tunnel passes, because the slopes are very steep. Therefore, the descriptions on geology along the headrace tunnel is based on the results of the aerial photo interpretation and the geological field reconnaissance along the road on the right bank.

1) Bedrock

The bedrock distributed along the headrace tunnel is composed mainly of gneiss with subordinate amount of granite intrusions.

2) Weathering

Most of the headrace tunnel route passes more than 60 m below the ground surface. Therefore, it hardly seems possible that the weathering becomes a cause of tunnel instability.

3) Discontinuity

(i) Gneissosity

Gneissosity trends N20□E to N70□E and dips southwestward at 15 to 40°. Towards the downstream from the intake to the surge tank, strikes of gneissosity gradually changes from NNE-SSW to ENE-WSW. Furthermore, the gneissosity are disturbed by small intrusions of granite in the areas between Basochhu and Rurichhu.

(ii) Joint

There was no outcrop showing highly jointed rock, but the recorded joints show the strike of N78°E to N75°W and the dip of 50 to 80°SE.

(iii) Fault

As mentioned precisely in the clause "Geology at Surge Tank, Penstock and Powerhouse", the bedrock is inferred to include many sheared places resulted from movement along gneissosity within the section between the surge tank and the place 800 m upstream of the surge tank.

Sheared rock was observed on an outcrop located on the road passing near the proposed site of the access tunnel for headrace tunnel. This sheared rock has a width of about 20 m along the road, but the direction was unclear. Therefore, this probable fault is not drawn on geological map "Geology, Project Area, Plan". In case that this sheared rock has E-W trend and continuity, there is a possibility that the sheared rock appears in the headrace tunnel excavation.

(3) Geotechnical Assessment

1) Rock Property

The bedrock distributed along the headrace tunnel was not tested in a laboratory, therefore, properties of rock are assumed based on the results of laboratory tests on drilled cores of the dam and powerhouse sites. The uniaxial compressive strength is predicted to range from 250 to 600 kgf/cm^2.

2) Groundwater and Water Inflow

Most of the tunnel sections is inferred to be under the groundwater level, from the reasons below.

- The thickness of the overburden along the tunnel route is mostly 60 m or more.
- Some creeks on the left bank of Punatsangchhu show flow water.

Water flow into the tunnel may occur mainly within the sections below.

- 1,450 m section from the intake, where the thickness of the overburden becomes thinner
- 800 m section from the surge tank

3) Tunnel Support

It is necessary to take care of tunnel support design for the place near the intake, because the bedrock is inferred to be loosened at some degree due to the stress relief.

Furthermore, there is a high possibility that the bedrock is sheared by the movement along gneissosity within the section 800 m upstream of the surge tank. Therefore, careful attention shall be paid for the civil design of the tunnel support within the above section.

7.3.5 Geology at Surge Tank, Penstock and Powerhouse Sites

(1) Topography

The surge tank, penstock and powerhouse are planned at the ridge of 1m upstream from the confluence point of the main river and Pazachhu.

The slopes of this ridge, where the surge tank, penstock and powerhouse are located, are 25 to 30° in inclination.

The surge tank is located near the top of the ridge. The bottom elevation is 1,12 8 m while the top elevation is about 1,200 m. The penstock is vertical shaft style. The top elevation of the penstock is 1,128 m, while the bottom elevation of the penstock is 842 m. The powerhouse is planned as underground cavern. The elevation of the arch roof of the powerhouse is 86 1m. The ground surface elevation above the powerhouse is around 1,100 m. Therefore, the thickness between the ground surface and the arch of the powerhouse is about 230 m. The longitudinal axis of the powerhouse is perpendicular to the ridge direction. The width of the ridge at elevation 1,000 m is about 150 m where the upstream side, and about 300 m where the downstream side. The thickness between the surface and the arch of the powerhouse is enough for stability of the powerhouse arch whose elevation is 861 m.

The topographic features near the powerhouse site are two landslide scarps.

One is observed near the switchyard site, which is planned just upstream of the ridge. The switchyard site is planned within the colluvium distribution, which is about 500 m long along the river and 100 to 150 m wide. This colluvium is derived from the landslide area behind the switchyard site. This landslide seems to be formed by the huge mass movement towards the river, which was induced by the weak structure of the bedrock.

The other one is observed north of the surge tank ridge and accompanied with the gentle slope extending in parallel with the tributary Pazachhu. The width of the gentle slope is about 500m (east-west) and the length about 400 m long (north-south). Several farmers now utilize this slope for cultivation. This landslide also seems to be formed by the huge mass movement, which was induced by the weak structure of the bedrock like the switchyard site. The feature of this area is a huge quantity of accumulation consisting of weathered materials and boulders, which were transported by this landslide movement to the downstream area (Right Bank of Pazachhu and the downstream of the powerhouse ridge).

(2) Geology

1) Surface Deposits

At this site, one drill hole (length 180 m) and the seismic prospecting (four lines, totaling 2,400 m) were conducted adding to the geological field reconnaissance. On the basis of the investigation results, the thick distribution of colluvium is clearly defined to the areas of the right bank slope of Pazachhu and of the junction of Pazachhu and the main river, as mentioned in the clause "Topography". The thickness of colluvium seems to attain to 20 m or more. At the ridge of the powerhouse site, the thickness of surface deposits is as thin as 3 to 5 m in general, judged from the results of the drilling and seismic prospecting.

As mentioned in the clause "Topography", representative colluvium is distributed in the area in and around the switchyard site, which is located upstream of the powerhouse site.

2) Bedrock

The bedrock at the surge tank, penstock and powerhouse sites is mainly composed of gneiss with occasional intercalations of pegmatite. Gneiss is generally fresh and hard except the near surface part of bedrock. However, as mentioned later, many core loss parts were recognized even in deeper part of the drill hole. Table 7.17 shows the laboratory test results on fresh rock cores taken at the depth of 20 m or more, such as uniaxial compressive strength and pulse velocity.

3) Weathering

As shown in the geologic log of drill hole DP-1, the weathering grade of the bedrock at the powerhouse site is generally weak, and can be classified as follows by means of the rock mass classification criteria.

Depth below Bedrock Surface (m)	Weathering Grade
0～6	3~2
More than 6	2~1

(Scale of Weathering)

Scale	Description
1	Very fresh. No weathering mineral component.
2	Fresh. Some minerals are weathered slightly. Usually no brown crack.
3	Fairly fresh. Some minerals are weathered. Cracks are stained and with weathered material.
4	Weathered. Fresh portions still remain partially.
5	Strongly weathered. Most minerals are weathered and altered to second minerals.

The above classification is applied only for the recovered core, however, there are many core loss parts as shown in the geologic log. Furthermore, the low to medium seismic velocity layer (1 to 2 km/sec) is as thick as 100 m based on the results of the seismic prospecting. The comprehensive discussions are made in the following clauses on the subject that the investigation results is susceptible to what factor of the bedrock, such as discontinuity and groundwater level.

4) Discontinuity

(i) Gneissosity

The bedrock is poorly exposed at the ridge of the powerhouse site, therefore, it is very difficult to collect the attitudes of gneissosity. Measured gneissosity on outcrops exposed around the powerhouse site and the right bank trends N40°E to N70°E and dips 15 to 30°SE. The gneissosity is tight and stiff on outcrops, which expose on the riverbed accompanied with flow water and forms round shape. On the other hand at the cliff, which has open side, the rocks disperse along gneiss at an interval from several 10 cm to several meters, and form outcrops seemed to be composed of bedded rock.

(ii) Joint

The joints observed in outcrops are not so many. The trends of the major joint sets are N70°W to N75°W/50 to 80°SW and N60°E to N80°E/80 to 90°SE. The joints observed in drilling cores dip 45 to 65°.

(iii) Fault

No fault was found in the geological field reconnaissance. Two faults are inferred to exist on drilled cores as follows.

- Fault F-1: depth 108.4 to 116.6 m
- Fault F-2: depth 128.0 to 136.0 m

In addition, four sheared zones are identified on drilled cores as follows.

- FRZ-1: depth 86.0~108.4m
- FRZ-2: depth 116.6~119.75m
- FRZ-3: depth 123.8~128.0m
- FRZ-4: depth 136.0~142.8m

Above faults and sheared zones show that FRZ-1 is positioned on the upper side of F-1 and FRZ-2 on the lower side, and that FRZ-3 is positioned on the upper side of F-2 and FRZ-4 on the lower side. The reason, why these two faults (F-1 and F-2) are assumed as faults, is that F-1 has about 10 cm thick fault gouge at depth of 115 m and fault F-2 has core sample which is judged as slime of fault zone at the depth of 133.15 ~136.0 m in addition to the core sample with many slickensided surfaces at the bottom of the slime. These two zones where there have lots of core loss are determined by the reason mentioned above, therefore, the crushed core or very poor core recovery zones which are located above and below F-1 and F-2 are judged as the sheared zones which are related to the fault hanging side and foot wall.

On the other hand, the upper zone above F-1 fault including sheared zone (depth from 14 to 86.0 m) has 12 core loss places in total. These 12 core loss places might be faults or sheared zones by the following reasons judged by reviewing the drilling cores.

- Almost all of the core loss places are accompanied with crushed cores.
- Black material like graphite sticks on gneissosity of crushed cores or coin-shape cores.
- Some of the cracks have clear slickensided surface.
- According to the driller's information, he could not find any condition that the drilling rods dropped rapidly at the depth of core loss places.

Finally, the deep underground faults at this site is estimated to have the almost same strike and dip as the gneissic structure by the reason that slip plane is almost along the gneissosity by the core inspection even if the accurate strike and dip of these deep ground faults cannot be measured in situ.

5) Groundwater

Surface flowing water around the powerhouse ridge was found at the small valleys of about 600m upstream and 200 m downstream from the ridge. On the other hand, the mountain body which is located at the back of the powerhouse ridge is big in size and has topographically enough volume which can supply the ground water to the powerhouse ridge.

The drill hole DP-1 at the powerhouse site could not have its strainer pipe for water level measurement. Therefore, the current water level can not be measured. The water level measurement data up to now are as follows.

Date	Bottom of Hole	Ground Water Level	Remarks
1999/12/4 7:30AM	93.50 m	84.90 m	Before daily work
1999/12/20 8:00AM	145.70 m	125.10 m	Before daily work
1999/12/31 9:00AM	175.55 m	157.80 m	Before daily work

Core inspection data shows that the brown colored weathering (oxidation phenomenon) decreases rapidly from the depth of around 50 m and finally it vanishes at the depth of 100 m and more.

According to these data, groundwater level at the powerhouse site is estimated as follows.

- There seems to be no water table up to the depth of 50 m (elevation about 1,000 m).
- The water table might be between the depth of 80 m (elevation about 980 m) and 100 m (elevation about 960 m). However, it is dry up there in the dry season.
- The water level on December 31 (elevation 903 m) was measured accurately, however, the water level might be a little low compared to the river water level (elevation 850 m). And the core weathering conditions show that the water level might be higher than the measured level. Therefore, the constant water level is judged to be at the depth of around 100 m (elevation 960 m). The water level measured on December 31 showed the instantly lowered water lever, which might be recovered to the constant water level.

6) valuation of the Drilling and Seismic Prospecting Results

As shown in the geologic log of drilling hole, DP-1, which was drilled near the powerhouse, total length of 36.4 m (about 20% of 180 m) at 21 places are core loss. The 21 places are divided into 15 places (22.5 m long) between the depth of 0 and 100 m and

6 places (13.9 m long) between the depth of 100 and 180 m. On the other hand, the seismic prospecting result shows that there is the velocity boundary at the depth of 110 m of drilling site or 120 m of the surge tank site from the surface between the layers of 1.8 to 2.2 km/sec and of 4.0 to 4.2 km/sec.

As mentioned at the discontinuity section, if the core loss places are about the same fault or sheared zones, the shallower part above the depth of 100m has 2.5 times number of faults as the deeper part below there and thicker sheared zone by 9 m. This is one of the reasons why there is velocity boundary between the layers of 1.8 to 2.2 km/sec and of 4.0 to 4.2 km/sec near the depth of 100 m. On the other hand, the constant water level seems to be located at the depth of 100 m near the drill hole DP-1. The seismic velocity increases by the water saturation in bedrock. So, the above velocity boundary might show the water table. However, the water level measurement data are very few. Therefore, it is very difficult to discuss this matter more precisely.

Overall, the field investigations results are evaluated as good as expected because the results of the seismic prospecting and the drilling are compared very well. The geology and the proposed structure are described at the following section, geotechnical evaluation.

(3) Geotechnical Evaluation

1) General Geology

The bedrock at the surge tank, penstock and powerhouse sites are summarized geotechnically as follows.

- The bedrock is composed of gneiss. The fresh part of the bedrock is stiff enough for the structures. The compressive strength ranges from 264 to 589 kgf/cm^2 as shown in Table 7.17.

- The gneissosity of the bedrock trends N40°E to N70°E and dips 15 to 30°SE. At this section, N70°E/30°SE is adopted for the geotechnical evaluation.

- The many faults seems to exist inside of the powerhouse ridge. According to the core inspection of the drill hole, DP-1, there are 21 faults and sheared zones which are small or big. The most remarkable ones are fault F-1 (depth 108.4 to 116.6 m) and fault F-2 (depth 128.0 to 136.0 m) which have fault gouge or strongly sheared zones. F-1 has about 22 m thick sheared zone on the hanging side and 3 m thick one on the foot wall side while F-2 has about 4 m thick sheared zone on the hanging side and 6 m thick one on the foot wall side. Therefore, the total width of faults and sheared zone is quite big.

- The accurate strike and dip of these deep underground faults cannot be measured in situ because there is no outcrop for the measurement. According to the core inspection, most of crushed cores or coin-type cores are cracked along the gneissosity structural plane. So, the deep underground faults at this site is estimated to have the almost same strike and dip as the gneissic structure.

- The landslide scarps which are located at the upstream (western side) and northern side might be induced by the activity of F-1 and F-2.

2) Powerhouse

The bedrock at the powerhouse site is evaluated as follows from the engineering geological point of view.

- The apparent dip of the gneissosity at the powerhouse site is 20° and inclined to the main river. However, this apparent dip is calculated by the assumption that the strike is N70°E. Therefore, this dip might be a little steeper than the real apparent dip. This apparent dip depends on the strike.

- There are F-1, F-2 and their sheared zones at the powerhouse site. The deepest part of F-2 sheared zone is 142.80m deep from the surface (elevation 918.2 m). The drilling core which was caught deeper than 143 m is fresh but has so many cracks along the gneissosity till the depth of 155 m (RQD between depth of 142.8m and 155m is 0%.). And average RQD between depth of 155 m and the bottom of the hole (depth of 180 m, elevation 881m) is only about 50%. The reason of this poor RQD is estimated because of the influence of F-1 and F-2. The bedrock between the bottom of the hole (elevation 881 m) and the arch of the powerhouse (elevation 861m) might be very fresh and compact without fail. However, the dip of gneissosity is comparatively gentle and the bedrock near the site often has intercalation of biotite and typical gneissic structure. Therefore, these geologic conditions must be carefully taken account of for the civil design of the powerhouse.

- There is some possibility that water may spring at the time of excavation. However, it is thought that so much water that will make the excavation very difficult may not spring.

3) Surge Tank

The bedrock at surge tank site is evaluated as follows from geotechnical viewpoints.

- The bedrock here is gneiss. The apparent dip of the gneissosity here is about 20° and inclined to the main river like at the powerhouse site.

- There might be the extended part of F-1, F-2 and their sheared zones at the surge tank site because the size of these zones are quite big. The F-1 and its sheared zone is estimated to be located at the depth of between 100~120 m from the surface (elevation 1,080 to 1,060 m).

- The sheared zone along the gneissic structure is predicted to be distributed at the some part of the surge tank excavation. However, the apparent dip of the gneissosity here is about 20° and gentle. Therefore, this geologic structure will not interfere with the excavation of the vertical shaft.

- Near the surface, the bedrock is estimated to be exfoliated along the gneissosity and joints and be like huge boulders.

- The vertical shaft is located above the water level. Therefore, it is estimated almost impossible that water may spring at the time of excavation.

4) Penstock

The bedrock at penstock site is evaluated as follows from geotechnical viewpoints.

- At the section between about 50 m and 200 m from the upstream end of the penstock, the bedrock is predicted to be very bad, because the section might be crossed by F-1, F-2 and their sheared zones.

- It is impossible to tell the quantity of water spring during the excavation. It is thought to be highly possible that water may spring constantly at the time of excavation.

7.3.6 Geology of Miscellaneous Structure Sites

(1) Intake

Two intake structures are planned on the left bank at the places about 15 to 65 m upstream of the dam site. Bedrock crops out near the intake site, and the thickness of the surface deposits is inferred to be relatively thin.

(2) Access Tunnel to Headrace Tunnel

The portal of the access tunnel for headrace tunnel is located at the place higher than the distribution of the thick colluvium. According to the results of seismic prospecting SA-1 and SA-2 carried out within the distributions of colluvium, the boundary of the velocity layer between 2.0 to 2.2 km/sec and 4.0 to 4.2 km/sec exists 40 to 5 0m below the ground surface.

(3) Switchyard

The switchyard site is covered by colluvium, which is derived from upper landslide. This landslide seems to be quite stable at the present.

7.4 Concrete Aggregate

The alluvium distributed in the river floor at the prospective quarry site is composed of round gravels, cobbles and boulders less than 70cm in diameter together with medium to fine grained sand. Gneiss and metasedimentary rock is the rock type of gravel, cobbles and boulders containing in alluvium.

(1) Site Selection

Alluvium is most favorable material for the concrete aggregates, because it is easy to take. Furthermore, it is favorable that the prospective quarry is located on the right bank, where the access to the existing road is easy.

Considering the above conditions, the wide river floor located about 7 km upstream of the dam site was selected as a most prospective quarry for the concrete aggregates.

(2) Investigation on Quantity

The thickness of alluvium distributed in the prospective quarry site is confirmed to be more than 10 m based on the results of drilling DQ-1, DQ-2, DQ-3 and DQ-4.

(3) Investigation on Quality

The laboratory tests, such as sieve analysis and abrasion loss, were carried out on samples taken from the pits which were excavated at four locations (test pit QP-2, QP-3, QP-4 and QP-5) on the river floor, for the purposes of investigating the suitability of alluvium as the concrete aggregates. The results of the laboratory tests are summarized in Table 7.18. The result of the sieve analysis is shown in Fig. 7.8.

7.5 Investigation on Alluvium

Investigations on alluvium were carried out at the prospective quarry site, for the purposes of confirming the characteristics of materials deposited on the river floor. Items of the investigation were pit excavation, geologic logging, sampling, sieve analysis and petrographic examination. The results of the investigation are shown in Table 7.19 and Fig. 7.9.

Table 7.1 Summary of Geological Investigations for Foundation Rocks

1) Field Investigation

Item	Unit	Quantity	Investigator	Remarks
Aerial Photo Interpretation	km^2	10	JICA Study Team	
Site Reconnaissance	km^2	10	JICA Study Team	
Drilling	hole	13	Geological Survey of Bhutan	
	m	760.0		
Geotechnical Logging	hole	13	JICA Study Team	
	m	760.0		
Long Term Water Level Measurement	hole	3	Division of Power	
	time	24		
Permeability Test	hole	3	Geological Survey of Bhutan	
	time	41		
Seismic Prospecting	line	10	Kelwang Consultancy	
	m	4,000		

2) Laboratory Test

Item	Unit	Quantity	Investigator	Remarks
Density	Sample	20	Division of Roads	
Specific Gravity and Water Absorption	Sample	20	Division of Roads	
Water Content	Sample	20	Division of Roads	
Uniaxial Compression Test	Sample	20	Division of Roads	
Petrographic Examination (thin section)	Sample	10	JICA Study Team	

Table 7.2 Summary of Geological Investigations for Concrete Aggregates

1) Field Investigation

Item	Unit	Quantity	Investigator	Remarks
Pit Excavation	pit	4	Division of Roads	
	m	6.0		
Pit Logging	pit	4	JICA Study Team	
	m	6.0		
Sampling	pit	4	Division of Roads	
	sample	4		

2) Laboratory Test

Item	Unit	Quantity	Investigator	Remarks
Specific Gravity and Water Absorption	sample	4	Division of Roads	
Abrasion Loss	sample	4	Division of Roads	
Soundness	sample	4	Division of Roads	
Sieve Analysis	sample	4	Division of Roads	
Fineness Modulus	sample	4	Division of Roads	
Alkali-aggregate Reactivity	sample	4	JICA Study Team	
Petrographic Examination (X-ray diffraction method)	sample	4	JICA Study Team	

Table 7.3 Summary of Geological Investigations for River Deposits

Item	Unit	Quantity	Investigator	Remarks
Pit Excavation	pit	1	Division of Roads	
	m	1.5		
Pit Logging	pit	1	JICA Study Team	
	m	1.5		
Sampling	pit	1	Division of Roads	
	sample	1		
Sieve Analysis	sample	1	Division of Roads	
Petrographic Examination (X-ray diffraction method)	sample	1	JICA Study Team	

Table 7.4 Details of Drilling Investigation

Hole No.	Length (m)	Inclination and Direction	Elevation (m)	Coordinates		Permeability Test	Remarks
				Northing (X)	Easting (Y)		
DD-01	60.00	90°	1,145.873	1,073,183.854	2,734,299.387	9	
DD-02	30.15	60°, N60°E	1,145.873	1,073,183.854	2,734,299.387	None	
DD-03	60.00	90°	1,106.602	1,073,158.971	2,734,256.509	None	
DD-04	50.00	90°	1,101.393	1,073,118.698	2,734,187.112	17	
DD-05	60.00	60°, N60°E	1,101.393	1,073,118.698	2,734,187.112	None	
DD-06	80.00	90°	1,129.499	1,073,037.539	2,734,204.415	15	
DD-07	100.00	90°	1,187.070	1,073,072.552	2,734,128.125	None	
DD-08	50.20	60°, S70°W	1,187.070	1,073,072.552	2,734,128.125	None	
DB-01	50.05	60°, N60°E	1,147.473	1,073,270.738	2,734,251.427	None	
DP-01	180.10	90°	1,070.575	1,066,305.563	2,737,235.033	None	
DQ-01	10.00	90°	-	-	-	None	
DQ-02	10.00	90°	-	-	-	None	
DQ-03	10.00	90°	-	-	-	None	
DQ-04	10.00	90°	-	-	-	None	
14holes	**760.0M**						**41 tests**

Table 7.5 Water Pressure Pattern for Permeability Test in Drill Holes

Depth from rock surface to the center of the testing section	Water Pressure (kgf/cm^2)
Less than 5m	1-2-3-2-1
5 to 10m	1-3-5-3-1
More than 10m	1-5-10-5-1

Table 7.6 List of Seismic Prospecting Lines

Location	Line No.	Length (m)	Remarks
Dam	SD-1, SD-2	285.0	
	SD-3	300.0	
	SD-4	300.0	
Intake	SD-5	115.0	
Powerhouse	SP-1	1,000.0	
	SP-2	500.0	
	SP-3	500.0	
	SP-4	400.0	
Adit	SA-1	300.0	
	SA-2	300.0	
total10 lines		**4,000.0m**	

Table 7.7 List of Core Samples

Location	Sample No.	Hole No.	Sampling Depth (m)		Rock Type
			from	To	
Dam	DD-1-01	DD-1	16.40	16.60	Gneiss
	DD-1-02	DD-1	16.60	16.85	Gneiss
	DD-1-03	DD-1	18.50	18.80	Pegmatite
	DD-1-04	DD-1	32.20	32.50	Gneiss
	DD-1-05	DD-1	50.10	50.50	Gneiss
	DD-5-01	DD-5	16.05	16.35	Gneiss
	DD-5-02	DD-5	21.00	21.30	Gneiss
	DD-5-03	DD-5	21.30	21.70	Gneiss
	DD-5-04	DD-5	21.70	22.00	Gneiss
	DD-5-05	DD-5	36.00	36.30	Gneiss
Powerhouse	DP-1-01	DP-1	39.60	39.90	Gneiss
	DP-1-02	DP-1	44.25	44.50	Pegmatite
	DP-1-03	DP-1	55.20	55.50	Pegmatite
	DP-1-04	DP-1	62.30	62.50	Pegmatite
	DP-1-05	DP-1	68.40	68.70	Migmatite
	DP-1-06	DP-1	74.70	74.90	Migmatite
	DP-1-07	DP-1	77.50	77.80	Gneiss
	DP-1-08	DP-1	96.40	96.60	Gneiss
	DP-1-09	DP-1	118.30	118.50	Gneiss
	DP-1-10	DP-1	154.70	155.00	Gneiss
	DP-1-11	DP-1	158.50	158.80	Gneiss
	DP-1-12	DP-1	168.60	168.85	Gneiss
total 22 samples					

Table 7.8 List of Laboratory Tests on Core Samples

Item	Quantity (sample)			Testing Standard	Remarks
	Dam	Powerhouse	Total		
Density	9	12	20	ISRM	
Specific Gravity and Absorption	9	12	20	ASTM C97	
Water Content	9	12	20	ASTM D2216	
Compression Strength	9	12	20	ASTM D3148	
Petrographic Examination (thin section)	5	5	10	ASTM C295	

Table 7.9 List of Pit

Location	Pit No.	Depth (m)	Remarks
Quarry	QP-2	1.5	
	QP-3	1.5	
	QP-4	1.5	
	QP-5	1.5	
			total 4pits 6.0m

Table 7.10 List of Samples for Concrete Aggregate Tests

Location	Sample No.	Pit No.	Depth of Sampling (m)		Remarks
			From	To	
Quarry	QP-2-01	QP-2	0.5	1.5	
	QP-3-01	QP-3	0.5	1.5	
	QP-4-01	QP-4	0.5	1.5	
	QP-5-01	QP-5	0.5	1.5	
					total 4samples

Table 7.11 List of Laboratory Tests on Concrete Aggregates

Item	Quantity (sample)	Testing Standard	Remarks
Specific Gravity and Water Absorption	4	ASTM C127, C128	
Abrasion Loss	4	ASTM C535, C131	
Soundness	4	ASTM C88	
Sieve Analysis	4	ASTM C136	
Finess Modulus	4	ASTM C117	
Alkali-aggregate Reactivity	4	Equivalent of ASTM C289	
Petrographic Examination (X-ray diffraction method)	4	ASTM C295	

Table 7.12 Item and Quantities of Investigations for River Deposits

Item	Unit	Quantity	Remarks
Pit Excavation	Pit	1	
	M	1.5	
Sampling	Sample	1	
Sieve Analysis	Sample	1	
Petrographic Examination (X-ray diffraction method)	Sample	1	

Table 7.13 Summary of Laboratory Test Results on Rock Cores (Dam)

	Location	Dam	
	Rock Type	Gneiss	Pegmatite
Dry Density (g/cm^3)	Average	2.80	2.74
	Minimum	2.72	-
	Maximum	2.89	-
	Number of Data	8	1
Saturated Density (g/cm^3)	Average	2.81	2.74
	Minimum	2.74	-
	Maximum	2.90	-
	Number of Data	8	1
Specific Gravity	Average	2.67	2.51
	Minimum	2.58	-
	Maximum	2.75	-
	Number of Data	8	1
Water Absorption (%)	Average	1.56	2.64
	Minimum	1.00	-
	Maximum	2.22	-
	Number of Data	8	1
Water Content (%)	Average	0.43	0.27
	Minimum	0.14	-
	Maximum	0.61	-
	Number of Data	8	1
Compressive Strength (kgf/cm^2)	Average	322	351
	Minimum	217	-
	Maximum	577	-
	Number of Data	8	1

Table 7.14 Rock Mass Classification by CRIEPI

Rock Class	Description
A	The rock mass is very fresh, and the rock forming minerals and grains undergo neither weathering nor alteration. Joints are extremely tight and their surfaces have no visible sign of weathering. Sound by hammer blow is clear.
B	The rock mass is solid. There is no opening joint and crack (even of 1mm). But rock forming minerals and grains undergo a little weathering and alteration in partly. Sound by hammer blow is clear.
CH	The rock mass is relatively solid. The rock forming minerals and grains undergo weathering except for quartz. The rock is contaminated by limonite, etc. The cohesion of joints and cracks is slightly decreased and rock blocks are separated by firm hammer blow along the joints. Clay minerals remain on the separation surface. Sound by hammer blow is a little dim.
CM	The rock mass is somewhat soft. The rock forming minerals and grains are somewhat softened by weathering, except for quartz. The cohesion of joints and cracks is somewhat decreased and rock blocks are separated by ordinary hammer blow along the joints. Clay minerals remain on the separation surface. Sound by hammer blow is somewhat dim.
CL	The rock mass is soft. The rock forming minerals and grains are softened by weathering. The cohesion of joints and cracks is decreased and rock blocks are separated by soft hammer blow along joints. Clay minerals remain on the separation surface. Sound by hammer blow is dim.
D	The rock mass is remarkably soft. The rock forming minerals and grains are softened by weathering. The cohesion of joints and cracks is almost absent. The rock mass collapses by light hammer blow. Clay minerals remain on the separation surface. Sound by hammer blow is remarkably dim.

Table 7.15 Shear Strength by Rock Class

Rock Class	Cohesion (kgf/cm^2)	Internal Friction Angle (degree)
CH	20～40	40～55
CM	10～20	30～45
CL	less than 10	15～38

Table 7.16 Estimated Depth of Foundation Excavation at Dam Site

Hole No.	Estimated Depth of Foundation Excavation [judging from drilled cores] (m)	Remarks
DD-1	12.6	
DD-2	9.8	
DD-3	unknown	Alluvium
DD-4	12.0	
DD-5	51.6	
DD-6	34.0	
DD-7	19.0	
DD-8	29.0	

Table 7.17 Summary of Laboratory Test Results on Rock Cores (Powerhouse)

	Location	Powerhouse		
	Rock Type	Gneiss	Pegmatite	Migmatite
Dry Density (g/cm^3)	Average	2.70	2.53	2.64
	Minimum	2.58	2.29	2.62
	Maximum	2.82	2.70	2.65
	Number of Data	7	3	2
Saturated Density (g/cm^3)	Average	2.73	2.54	2.66
	Minimum	2.62	2.30	2.64
	Maximum	2.87	2.70	2.67
	Number of Data	7	3	2
Specific Gravity	Average	2.47	2.61	2.75
	Minimum	1.90	2.55	2.70
	Maximum	2.70	2.71	2.79
	Number of Data	7	3	2
Water Absorption (%)	Average	1.37	1.68	0.90
	Minimum	0.60	1.61	0.80
	Maximum	2.21	1.81	1.00
	Number of Data	7	3	2
Water Content (%)	Average	1.06	0.33	0.67
	Minimum	0.13	0.11	0.56
	Maximum	1.82	0.76	0.77
	Number of Data	7	3	2
Compressive Strength (kgf/cm^2)	Average	411	914	1,080
	Minimum	264	686	1,008
	Maximum	589	1,239	1,152
	Number of Data	6	3	2
Pulse Velocity (km/sec)	Primary Wave (Vp)	2.92～4.49	-	-
	Secondary Wave (Vs)	1.89	-	-

Table 7.18 Summary of Laboratory Test Results on Concrete Aggregate

Item		Result	Remarks
Specific Gravity (coarse aggregate)	Average	2.45	
	Minimum	2.01	
	Maximum	2.64	
	Number of Data	4	
Specific Gravity (fine aggregate)	Average	2.54	
	Minimum	2.47	
	Maximum	2.61	
	Number of Data	5	
Water Absorption (%)	Average	1.5	
	Minimum	1.4	
	Maximum	1.6	
	Number of Data	4	
Abrasion Loss (%)	Average	36.5	
	Minimum	33.0	
	Maximum	41.0	
	Number of Data	4	
Soundness (%)	Average	2.0	
	Minimum	1.4	
	Maximum	3.0	
	Number of Data	4	
Fineness Modulus	Average	3.73	
	Minimum	2.80	
	Maximum	4.16	
	Number of Data	4	
Alkali-aggregate Reactivity	Result	Innocuous	
	Number of Data	4	

Table 7.19 Result of Investigations on River Deposits

Item		Result	Remarks
Fineness Modulus	Result	4.04	
	Number of Data	1	

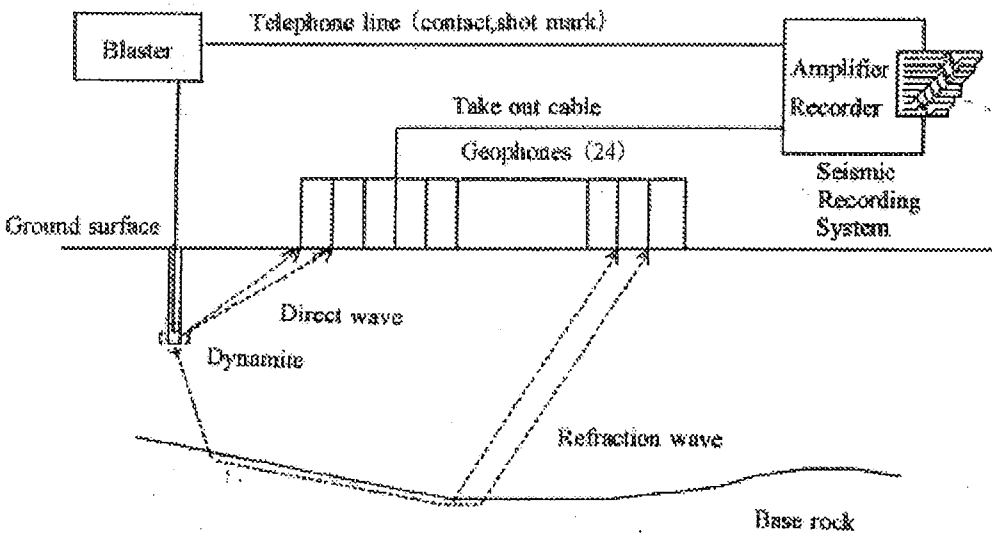

Fig. 7.1 Block Diagram of Seismic Prospecting

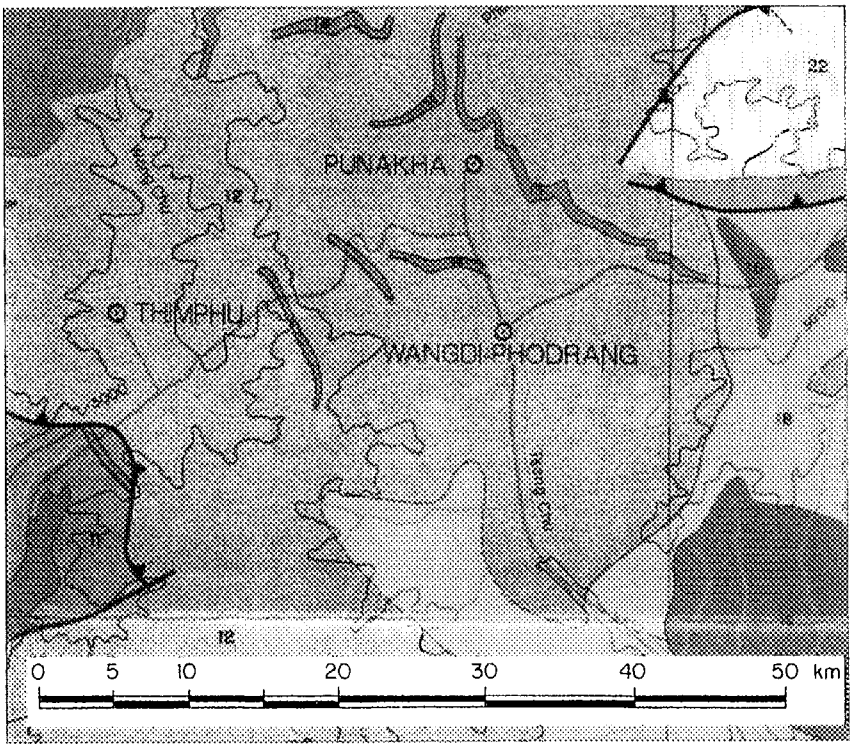

Legend

12:Thimphu Formation	migmatite and biotite-granite gneisses with thin beds of quartzite, mica schist, calc-silicate rocks and marbles
13:Thimphu Formation	individual limestone beds
14:Thimphu Formation	amphibolite dykes/sills
18:Tirkhola Formation	bedded quartzites and phyllitic quartzites, locally limestone

Fig. 7.2 Regional Geological Map of the Project Area

(after ESCAP (1991): Atlas of Mineral Resources of the ESCAP Region, Vol.8 Bhutan)

LEGEND

- Al — Alluvium
- Co — Colluvium
- Te — Terrace Deposit
- Gn — Gneiss
- Geologic Boundary
- Landslide Scarp
- Attitude of Bedding Plane (54)
- Attitude of Joint (84)
- Attitude of Fault and Width of Sheared Zone (62, alt=250)

PLAN

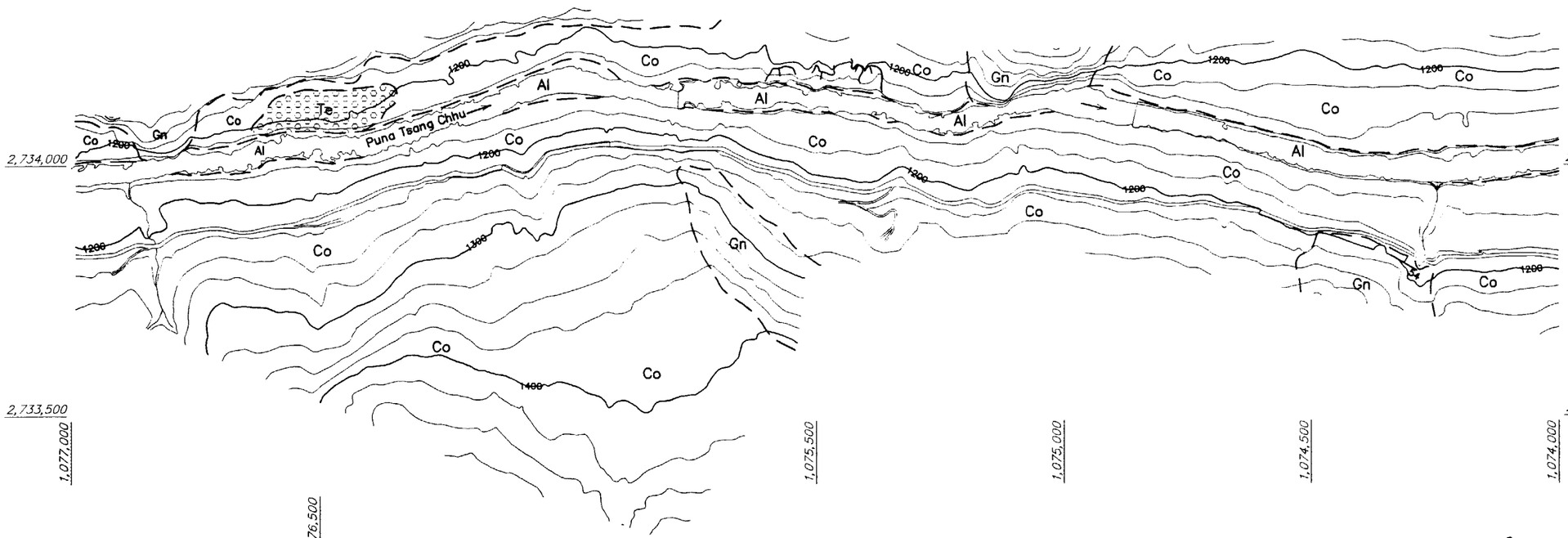

PUNA TSANG CHHU HYDROPOWER PROJECT

GEOLOGY
PROJECT AREA
PLAN (1–4)

Fig.7.3

LOCATION	DATE	DESCRIPTION	BY
REVISION			

SHEET NO. OF

LEGEND

- Al — Alluvium
- Co — Colluvium
- Terrace Deposit
- Gn — Gneiss
- Geologic Boundary
- Landslide Scarp
- Attitude of Bedding Plane
- Attitude of Joint
- Attitude of Fault and Width of Sheared Zone

*) For the location of the investigations, see "Geology, Dam, Plan"

PLAN

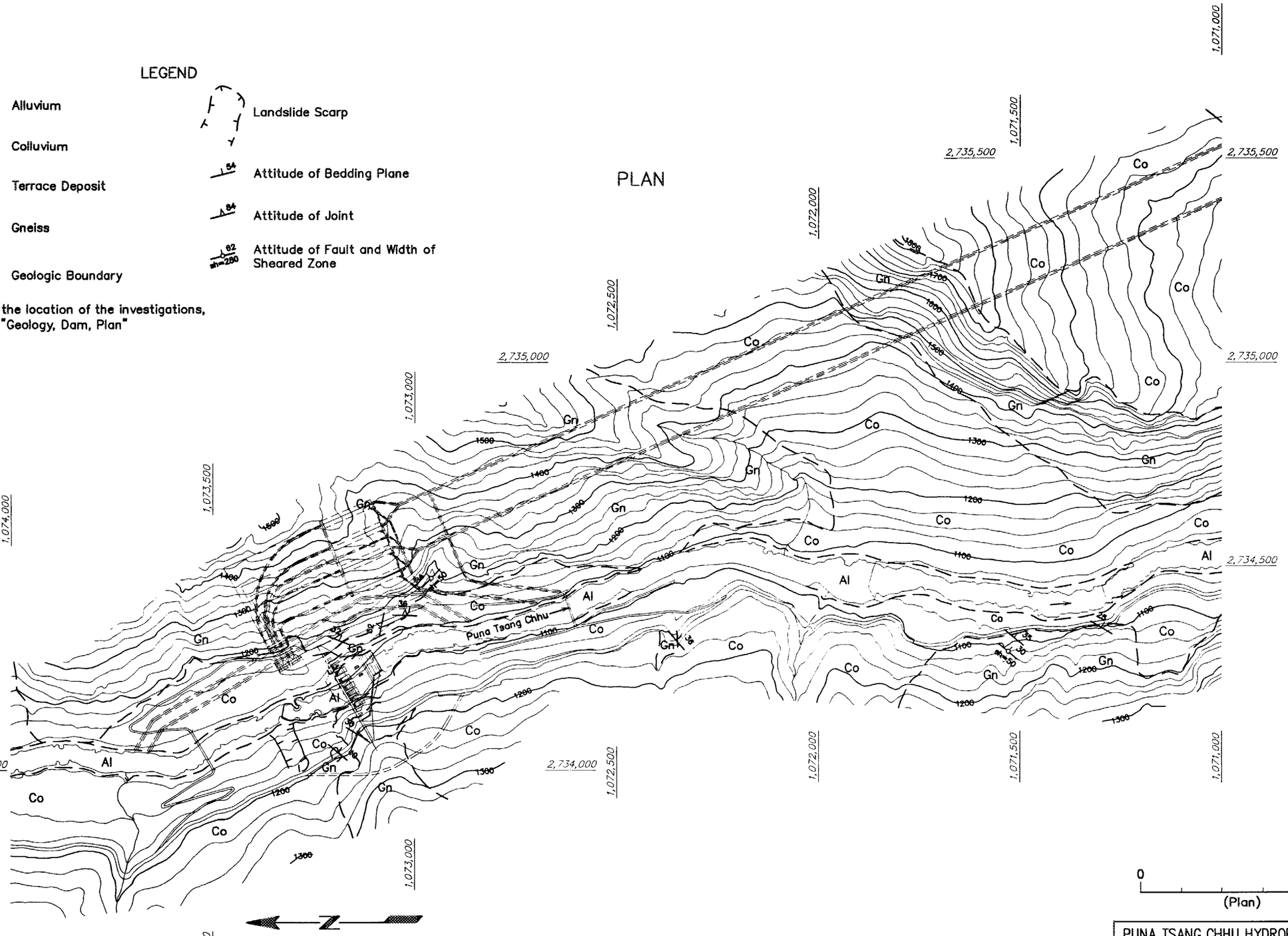

0 500 m
(Plan)

PUNA TSANG CHHU HYDROPOWER PROJECT

GEOLOGY
PROJECT AREA
PLAN (2-4)

Fig.7.3

LOCATION	DATE	DESCRIPTION	BY
		REVISION	

SHEET NO. OF

LEGEND

- Al — Alluvium
- Co — Colluvium
- Te — Terrace Deposit
- Gn — Gneiss
- Geologic Boundary
- Seismic Prospecting Line
- SA–1, L: 300.0 — Name and Length (m)
- Landslide Scarp
- 54 — Attitude of Bedding Plane
- 84 — Attitude of Joint
- 82 / sh=280 — Attitude of Fault and Width of Sheared Zone

PLAN

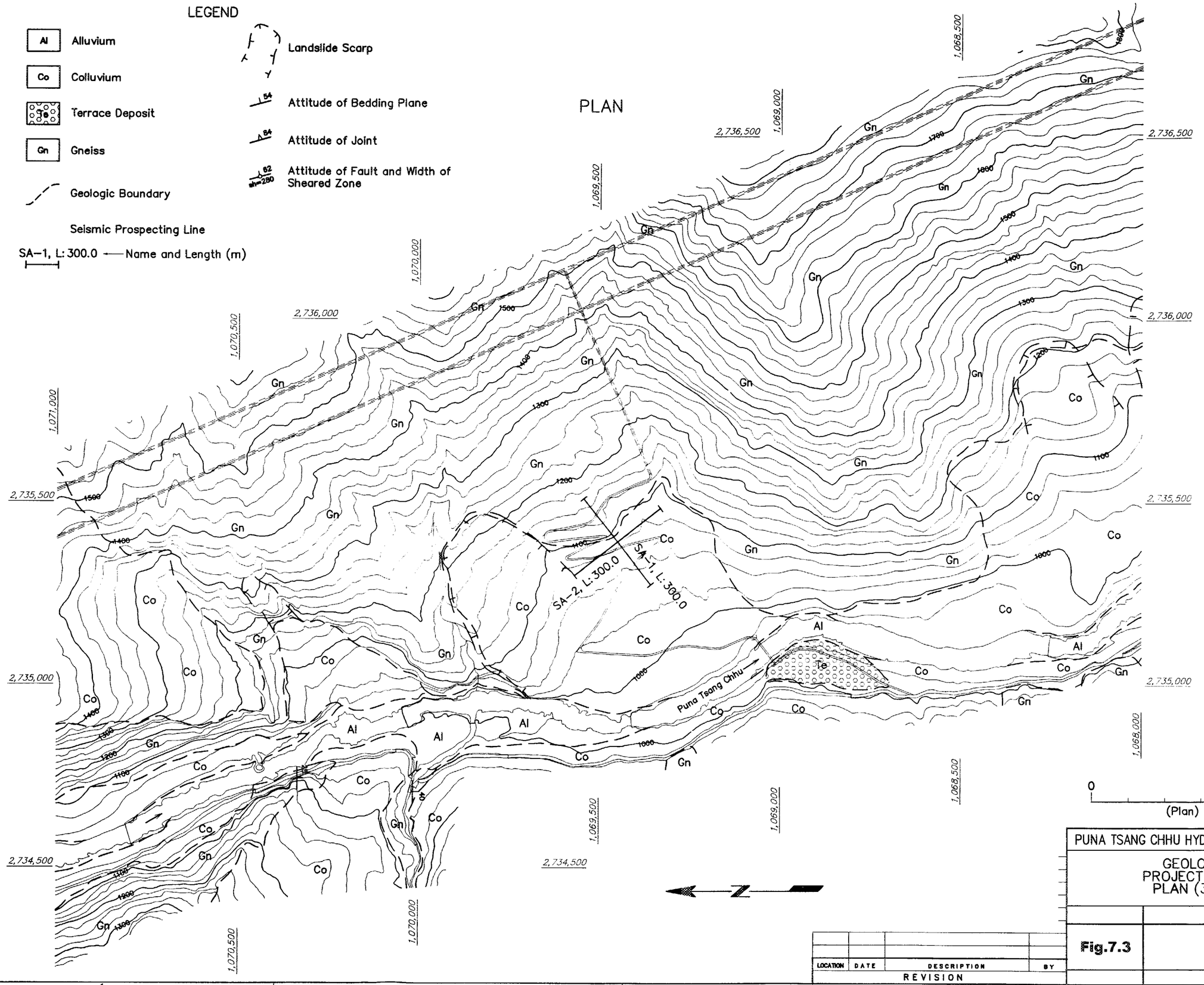

LOCATION	DATE	DESCRIPTION	BY

REVISION

PUNA TSANG CHHU HYDROPOWER PROJECT

GEOLOGY
PROJECT AREA
PLAN (3–4)

Fig.7.3

SHEET NO. OF

PLAN

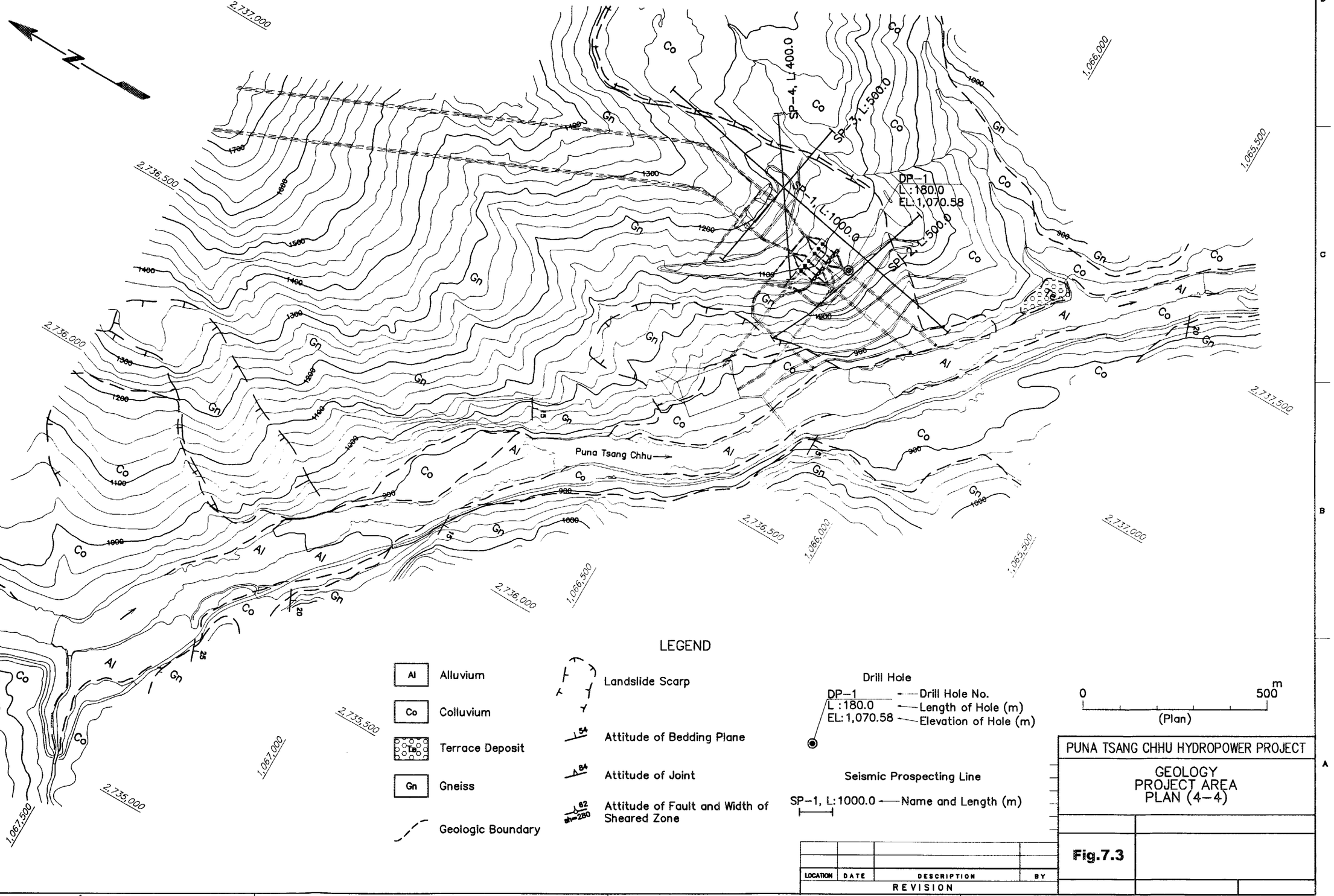

LEGEND

Al	Alluvium
Co	Colluvium
Te	Terrace Deposit
Gn	Gneiss
	Geologic Boundary
	Landslide Scarp
54	Attitude of Bedding Plane
84	Attitude of Joint
62 shr 220	Attitude of Fault and Width of Sheared Zone

Drill Hole
DP-1 — Drill Hole No.
L:180.0 — Length of Hole (m)
EL:1,070.58 — Elevation of Hole (m)

Seismic Prospecting Line
SP-1, L:1000.0 — Name and Length (m)

0 500 m
(Plan)

PUNA TSANG CHHU HYDROPOWER PROJECT

GEOLOGY
PROJECT AREA
PLAN (4-4)

Fig.7.3

LOCATION	DATE	DESCRIPTION	BY
REVISION			

SHEET NO. OF

PLAN

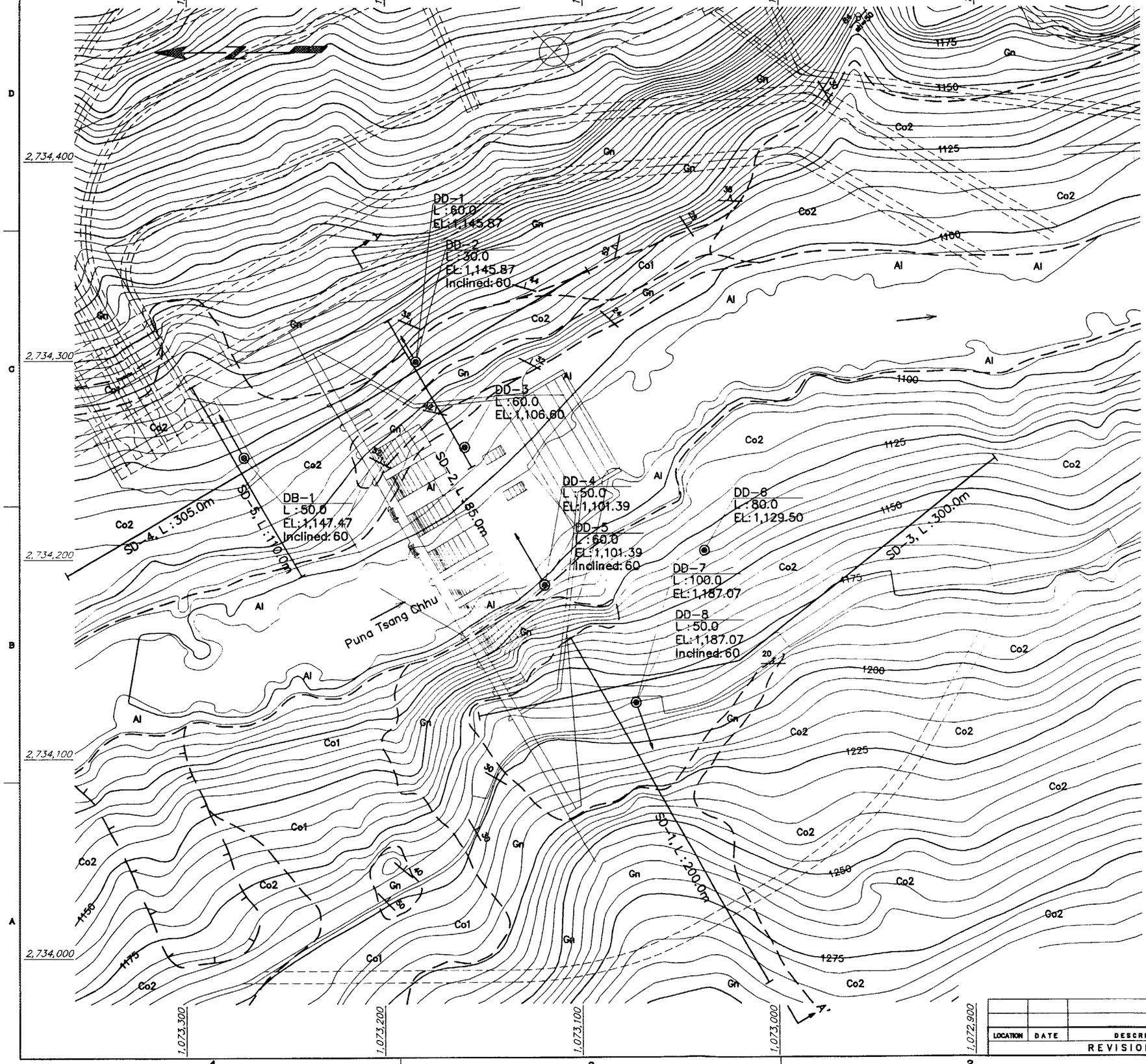

LEGEND

- Al — Alluvium
- Co1 — Colluvium (less than 3m thick)
- Co2 — Colluvium (3m thick or more)
- Gn — Gneiss (intercalated with pegmatite)
- Geologic Boundary
- Fault
- Attitude of Gneissosity
- Attitude of Joint
- Attitude of Fault and Width of Sheared Zone (in cm)

Drill Hole

DD-2 — Drill Hole No.
L : 30.0 — Length of Hole (m)
EL: 1,145.87 — Elevation of Hole (m)
inclined: 60 — Inclination of Hole (degree)

Seismic Prospecting Line

SD-1, L: 200.0 — Name and Length (m)

A A' — Location of Section

Collapse

0 50 100 m
(Plan)

PUNA TSANG CHHU HYDROPOWER PROJECT

GEOLOGY
DAM
PLAN

Fig.7.4

LOCATION	DATE	DESCRIPTION	BY
REVISION			

SHEET NO. OF

SECTION (A–A')

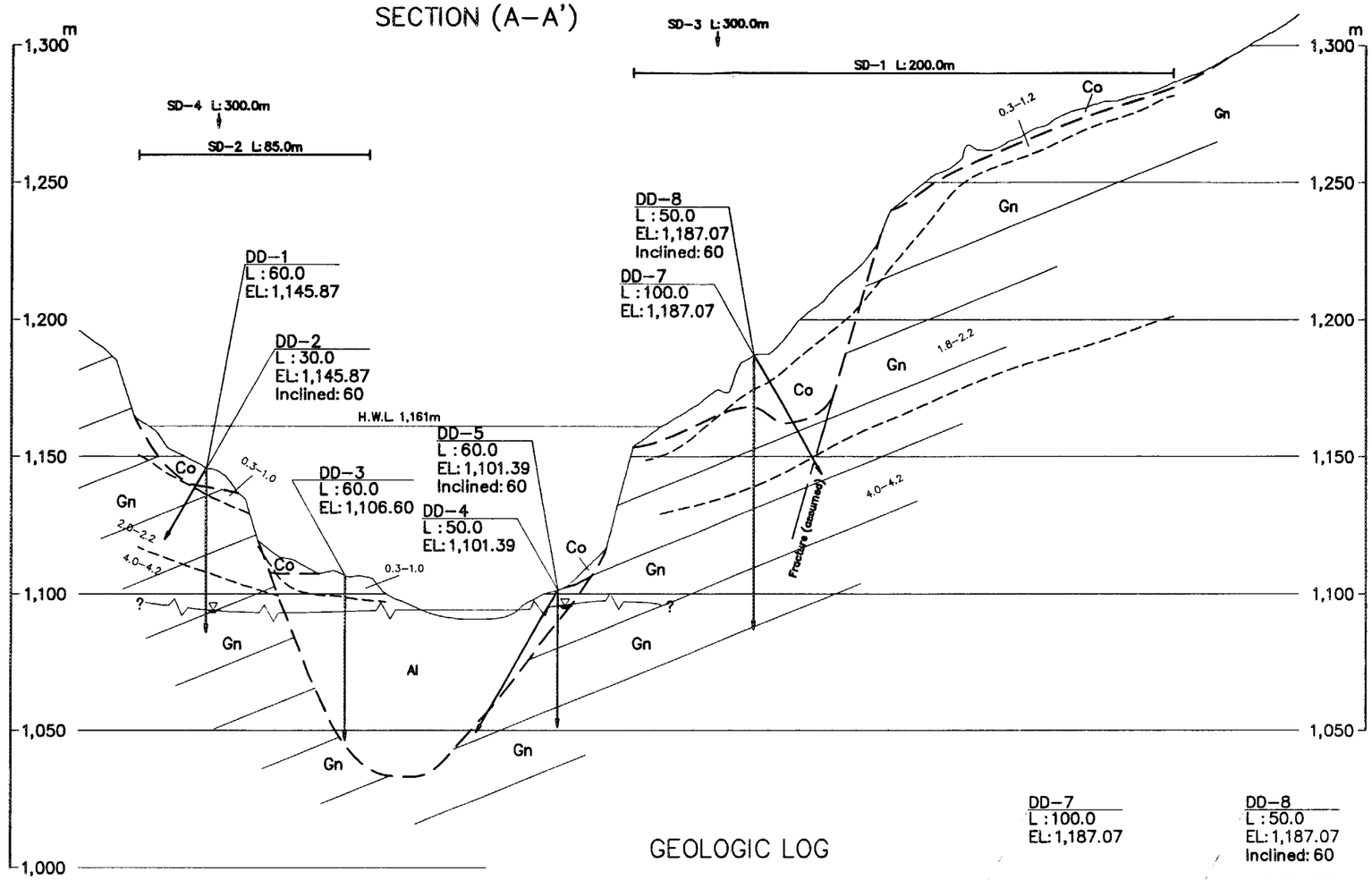

LEGEND

- Al — Alluvium
- Co — Colluvium
- Gn — Gneiss (intecalated with Pegmatite)
- Pg — Pegmatite
- Gn/Pg — Banding of Gneiss and Pegmatite

for geologic log

- Geologic Boundary
- Fault
- Structural Trend
- Ground Water Level
- Boundary of Seismic Velocity Layer and Seismic Velocity (km/sec)
- Location of Seismic Prospecting

Drill Hole

DD–2
L : 30.0
EL: 1,145.87
Inclined: 60

- Drill Hole No.
- Length of Hole (m)
- Elevation of Hole (m)
- Inclination of Hole (degree)

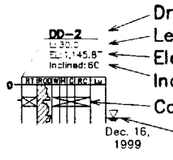

- Drill Hole No.
- Length of Hole (m)
- Elevation of Hole (m)
- Inclination of Hole (degree)
- Core Loss
- Ground Water Level and Date of Measurement

RT: Rock Type(see the Legend above)
RQD: Rock Quality Designation
W: Weathering *1)
H: Hardness *2)
C: Crack Spacing *3)
RC: Rock Class
Lu: Lugeon Value

*1) Weathering

1	Fresh
2	Slightly Weathered
3	Moderately Weathered
4	Highly Weathered
5	Completely Weathered

*2) Hardness

1	Very Hard
2	Hard
3	Medium Hard
4	Soft
5	Very Soft

*3) Crack Spacing

1	More than 30cm
2	10–30cm
3	3–10cm
4	1–3cm
5	Less than 1cm

GEOLOGIC LOG

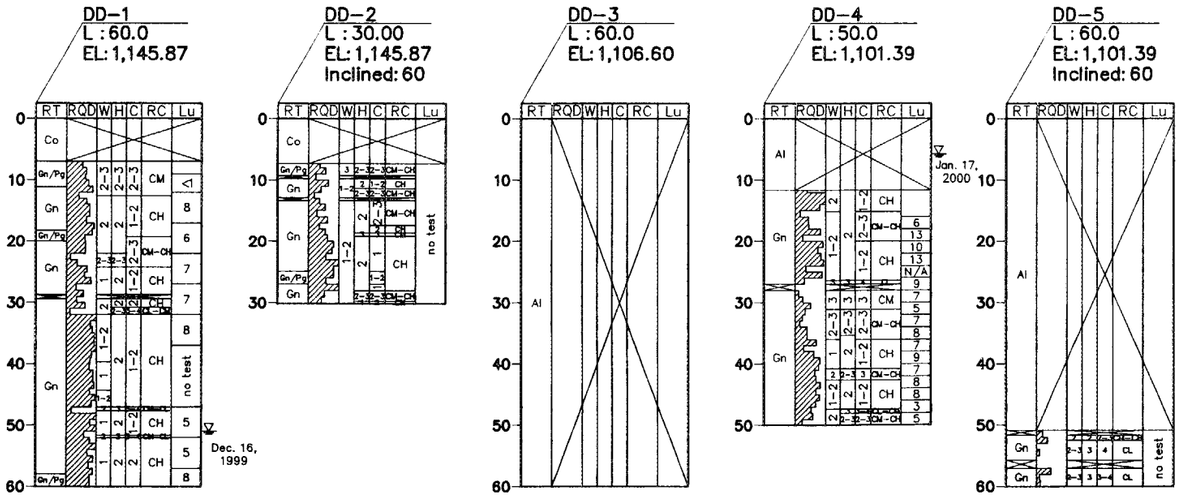

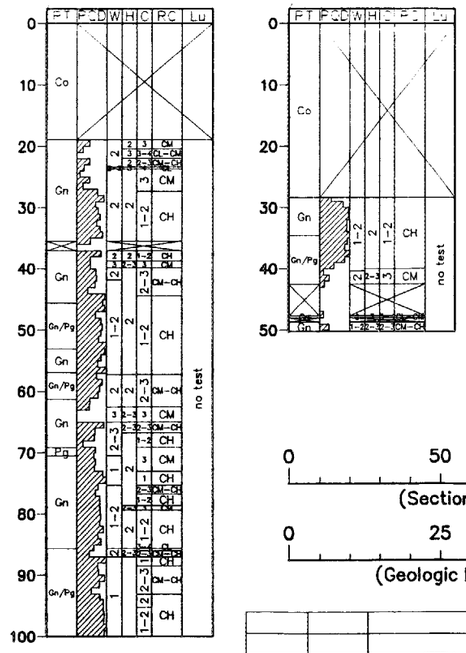

0 50 100 m (Section)

0 25 50 m (Geologic Log)

PUNA TSANG CHHU HYDROPOWER PROJECT

GEOLOGY
DAM
SECTION

Fig.7.5

LOCATION	DATE	DESCRIPTION	BY

REVISION

SHEET NO. OF

PLAN

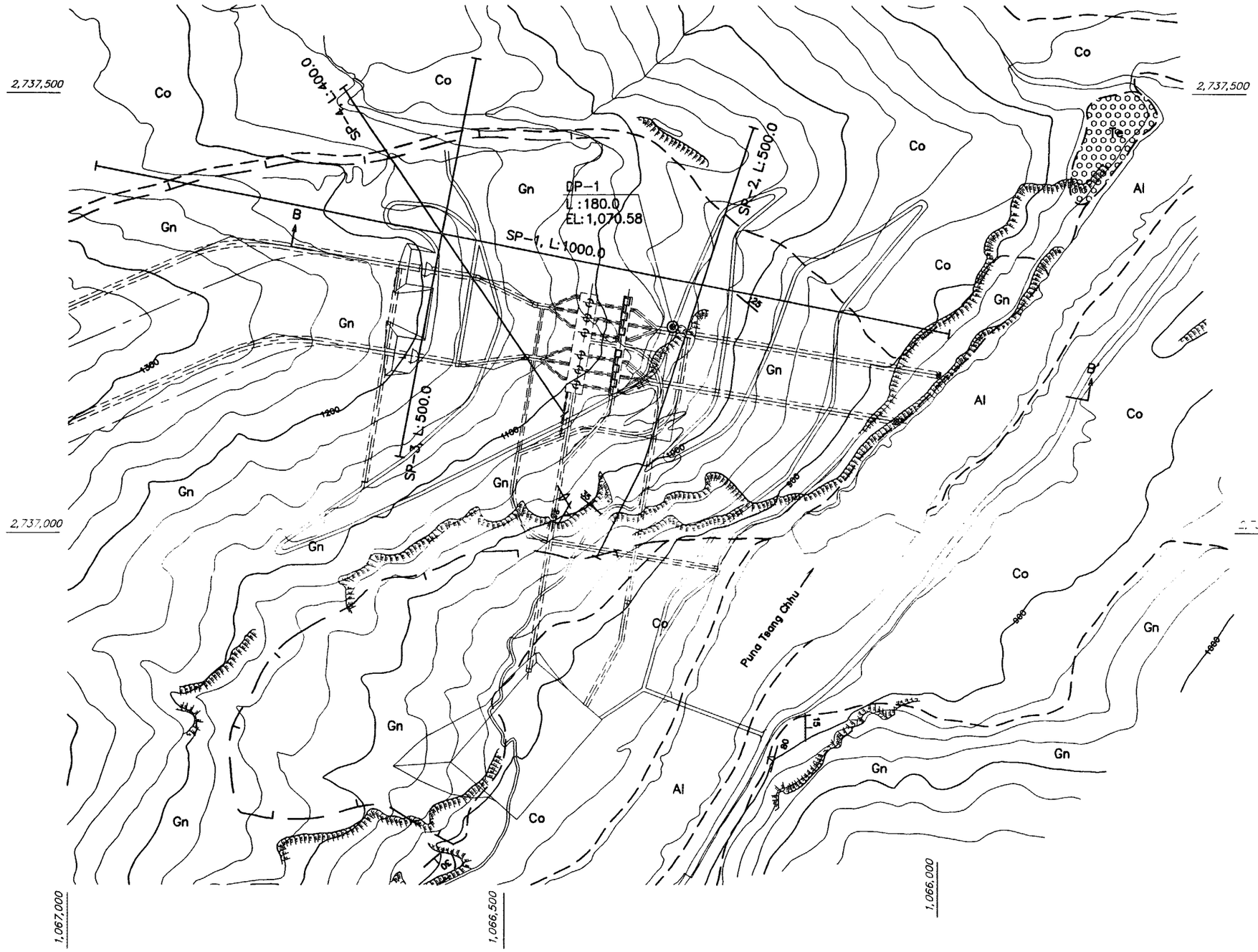

LEGEND

- Al — Alluvium
- Co — Colluvium
- Terrace Deposit
- Gn — Gneiss
- Geologic Boundary
- Landslide Scarp
- 54 — Attitude of Bedding Plane
- 84 — Attitude of Joint
- 62 / sh=280 — Attitude of Fault and Width of Sheared Zone

Drill Hole

DP-1 — Drill Hole No.
L:180.0 — Length of Hole (m)
EL:1,070.58 — Elevation of Hole (m)

Seismic Prospecting Line

SP-1, L:1000.0 — Name and Length (m)

B B' — Location of Section

0 — 250 m

(Plan)

PUNA TSANG CHHU HYDROPOWER PROJECT

GEOLOGY
POWERHOUSE
PLAN

Fig.7.6

LOCATION	DATE	DESCRIPTION	BY
		REVISION	

SHEET NO. OF

PROFILE (B–B')

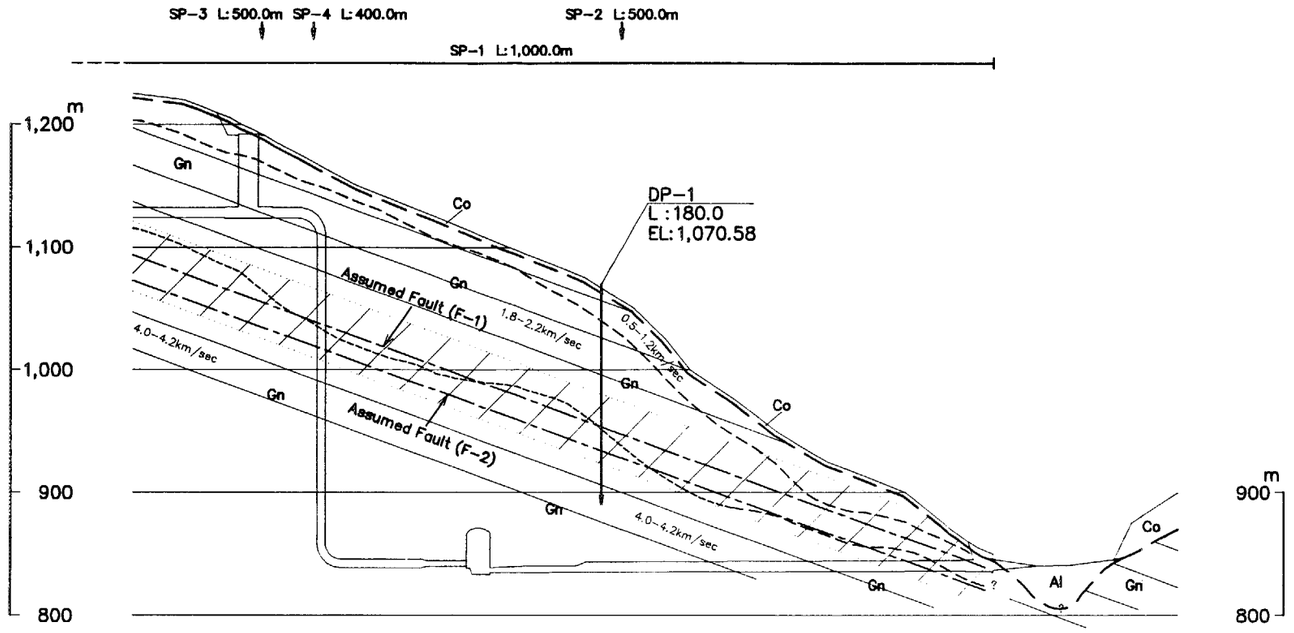

LEGEND FOR PROFILE

- Al — Alluvium
- Co — Colluvium
- Gn — Gneiss (intecalated with Pegmatite)
- Sheared Zone
- Geologic Boundary
- Fault
- Structural Trend

Drill Hole

DP–1 — Drill Hole No.
L :180.0 — Length of Hole (m)
EL:1,070.58 — Elevation of Hole (m)

Seismic Prospecting

SP–3 L:500.0m — Location of Seismic Prospecting and Line No.

2.3–2.2 / 2.0–2.2 / 4.0–4.2 — Boundary of Seismic Velocity Layer and Seismic Velocity (km/sec)

GEOLOGIC LOG

DP–1
L :180.0
EL:1,070.58

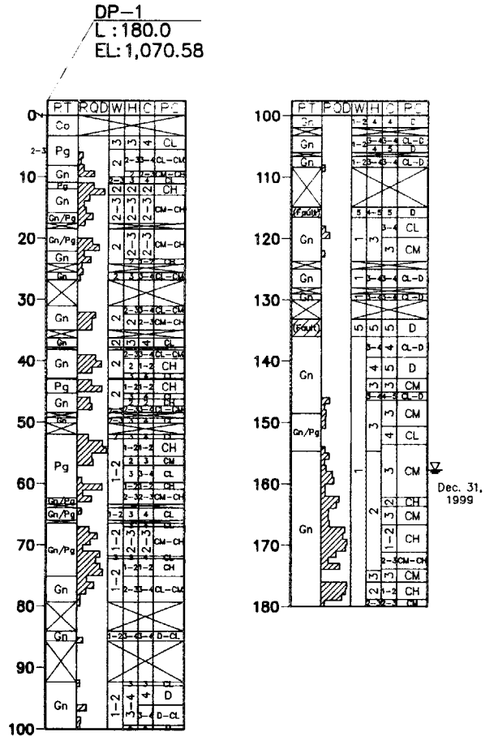

LEGEND FOR GEOLOGIC LOG

- Co — Colluvium
- Gn — Gneiss
- Pg — Pegmatite
- Gn/Pg — Banding of Gneiss and Pegmatite
- (Fault) — Fault

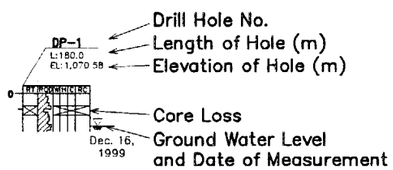

RT: Rock Type(see the Legend above)
RQD: Rock Quality Designation
W: Weathering *1)
H: Hardness *2)
C: Crack Spacing *3)
RC: Rock Class

***1) Weathering**

1	Fresh
2	Slightly Weathered
3	Moderately Weathered
4	Highly Weathered
5	Completely Weathered

***2) Hardness**

1	Very Hard
2	Hard
3	Medium Hard
4	Soft
5	Very Soft

***3) Crack Spacing**

1	More than 30cm
2	10–30cm
3	3–10cm
4	1–3cm
5	Less than 1cm

0 — 250 m — (Profile)

0 — 50 m — (Geologic Log)

PUNA TSANG CHHU HYDROPOWER PROJECT

GEOLOGY
POWERHOUSE
PROFILE

Fig.7.7

LOCATION	DATE	DESCRIPTION	BY

REVISION

SHEET NO. OF

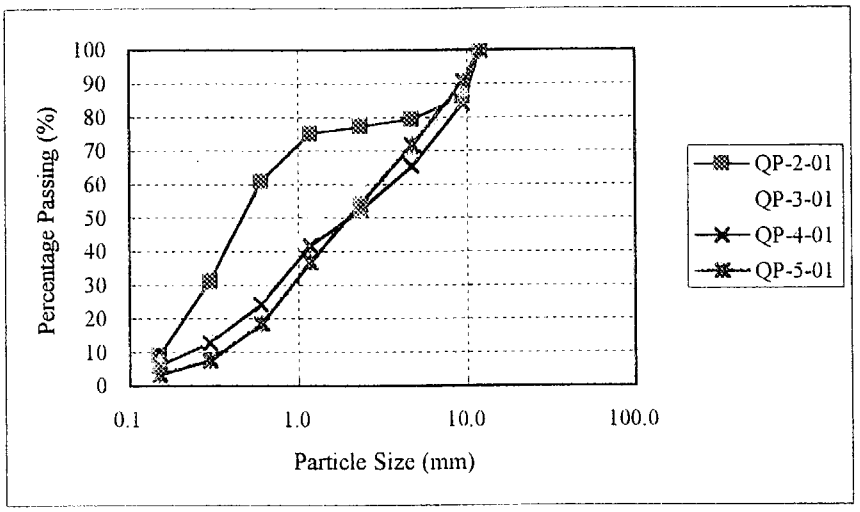

Fig. 7.8 Particle Size Distribution

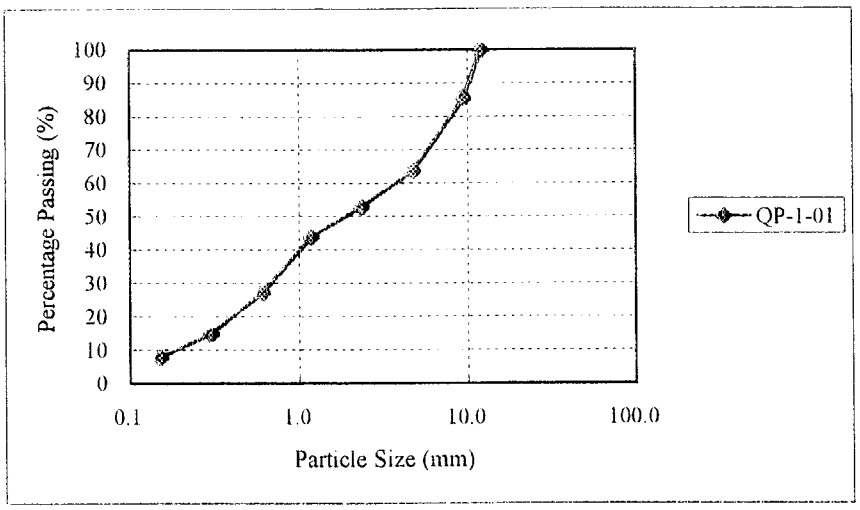

Fig. 7.9 Particle Size Distribution of River Deposits

CHAPTER 8

SEISMICITY

CONTENTS

8. SEISMICITY

8.1 Outline

The Kingdom of Bhutan is tectonically located in the eastern part of the Himalayan orogenic belt. Since the area (about 47,000 km^2) is as small as the Kyushu Island of Japan, it is necessary to understand seismotectonic situation of this country within the Himalayan region for the purposes of evaluating seismicity in this country. Likewise, when assessing earthquake hazards in the Kingdam of Bhutan, it is important to investigate the effect of earthquakes occurring in the surrounding regions, as well as those within the country.

From viewpoints of the plate tectonics, major Himalayan tectonics was formed primarily by subduction of the Indian continent below the Eurasian plate since the Eocene period (ca. 40Ma). After colliding, the Indian continent has continued to move northward on the rate of about 5cm/year until now, and this movement has caused remarkable mountain-building and high seismicity in the central and eastern Asia. Also this movement caused striking bending structures, called the syntaxes, at the western (Pakistan) and eastern (Myanmar) ends of the Himalayas (Fig. 8.1).

There is an argument that, after the collision, very low-angle underthrusting of the Indian plate beneath the Tibetan lithosphere become the main mode of movement between the two continents, in addition to the north-south crustal shortening of those continents. This movement is called the continental subduction. The Himalayan foothills has been frequently struck and damaged with great earthquakes (M>8) of low-angle thrust type which are caused by rupturing a larger detachment surface due to the continental subduction (Fig. 8.2).

Recent seismicity in the Himalayas (Fig. 8.3) is the highest in a zone 50km wide in the Lesser Himalaya, with a concentration of earthquake-epicenters just south of the Main Central Thrust (MCT). Focal mechanisms are low-angle thrust type in general and, rarely, strike-slip type, which are consistent with the slip-sense of active faults. Epicentral concentration in the vicinity of MCT (Fig.8.3) does not mean the recent reactivation of the MCT itself, but may represent seismicity at a deeper part associated with activity of the detachment surface connecting with the Main Boundary Fault (MBF) and Himalayan Frontal Fault (HFF) of the Himalayan Front. Dips of the fault plane inferred from focal mechanisms show very low-angle slip of 5 degrees north in the southern (Lesser Himalaya) side, and, rather high-angle slip of about 30 degrees north in the northern (Greater Himalaya) side. Seeber and Armbruster (1981) proposed, based on that seismicity, a seismotectonic model as shown in Fig.8.4. According to Molner (1980), underthrusting rate of the India beneath the Himalayas is up to 1.8 cm/year.

In addition, earthquakes of normal-fault type focal mechanism occur beneath the Indian plains and the Tibetan plateau. Of these, earthquakes beneath the Indian plains at about 20 km depth have the tensile force direction normal to the Himalayas, and they are probably the result of bending of the Indian plate under the loading of the Himalayan accretionary pile. On the other hand, the tensile force direction of normal-fault type earthquake in the Tibetan plateau are parallel to the Himalayas (Fig.8.5), and are considered to represent the effect of push off of some blocks in the Tibetan plateau.

Though the current seismicity in the Kingdom of Bhutan is not so active as compared with other regions of Himalayas, there are found considerable seismic activity around the country, especially both in eastern borderlands, western Sikkim and eastern Nepal. There are found also in this country a tendency of epicentral concentration in the vicinity of the MCT.

As shown in Fig. 8.3, recent Himalayan seismicity is considerably vigorous. But, according to the seismic records of the recent couple of decades, earthquakes with magnitude greater than 7 have occurred more frequently in the border region among India, Myanmar and China, 300 to 500km apart from the Kindom of Bhutan.(Fig.8.6)

In Fig.8.2, years of occurrence and epicentral areas of large earthquakes, by which the Himalayan foothills were badly damaged, are shown. Among them, events of 1897, 1905, 1934 and 1950 recorded magnitude exceeding 8 that were caused by the rupture of a shallow-dipping detachment surface between the Indian plate and Himalayas. In Fig. 8.2, inferred rupture lengths of the seismic faults are shown. And the ranges of seismic intensity $\geqq$VIII of Modified Mercalli (MM) intensity scale (approximately corresponding the intensity V of the JMA scale) of those earthquakes are given in Fig.8.5. According to Seeber and Armbruster (1981), these seismic faults extend from the deeper part below the boundary between the Lesser and Greater Himalaya to the Himalayan Front (1905 event), or further southward beneath the Gangetic foredeep (1934 event). (Refer to the profiles shown in the lower part of Fig. 8.5)

8.2 Seismic Activities

Seismic activities around the project area were studied based on the earthquake record data that occurred in the Kingdom of Bhutan and surrounding countries.

Earthquake record data was based on the Earthquake Data File that were edited by NOAA (National Oceanic and Atmospheric Environmental Data Service , USA).

Total number of data is 1,476 data and they are collected in the area of R=1,000 km centering around Punatsangchhu project site.

Table 8.1 and Fig.8.7 shows distribution of magnitude and epicentral distance of seismicity data.

For evaluating earthquake hazard on a site in the Kingdom of Bhutan, it is necessary to provide a catalog of past earthquakes occurred in and around the country, and also to research on the distribution and natures of active faults, in order to assess the recurrence nature of shallow earthquakes of moderate to large magnitude. However, it is not possible, at present, to estimate, the maximum ground motion and its return period expected at a site, since the data on earthquakes and active faults are both far from sufficiency.

However, it would be possible, to a certain degree, to estimate recurrence periods of some great earthquakes such as the 1897 Western Assam (M8.7) and the 1934 Bihar-Nepal (M8.3-8.4) events, which are inferred to cause the most-serious and nation-wide damage in the Kingdom of Bhutan, as follows. Recent subduction rate of the Indian plate under the Himalayas is estimated approximately as 1.8cm/year. Let us assume that about 2/3 of above rate (1.2cm/year) is due to the great earthquakes. Since the amounts of seismic slip associated with great subduction-type earthquakes are usually around 4 to 8m, the recurrence periods are estimated as 330 to 670 years, if similar slips are also expected for the Himalayan great earthquakes. We could, therefore, say that the occurrence probability of great earthquakes (M>8) beneath the country of the Kingdom of Bhutan is rather low in the near future (within about 100 years from now), even if considering the elapsed period, about 100 years, from the occurrence time of the latest earthquake.

8.3 Design Earthquake Motion

8.3.1 Aseismic Design of Dam by Seismic Coefficient Method

According to the Japanese Design Standard of Dam, seismic coefficient method is adopted for aseismic design of dam.

This method evaluates the influence of earthquake against dam as the horizontal force and the horizontal force would be calculated by multiplying dambody weight by seismic coefficient.

In Japan, this method has been used in aseismic design of civil structures for years.

But, if it is necessary to consider the local intensive earthquake, aseismic design is desired by dynamic analysis considering the characteristics of input earthquake motion and vibration period peculiar to dam body.

In case of Punatsangchhu Project, the surrounding region of the Kingdom of Bhutan is located in the strong earthquake area.

But, dam design at the stage of Feasibility Study, seismic coefficient method would be applied, because no big earthquake observed in the vicinity of damsite.

8.3.2 Seismic Risk in the Surrounding Regions of the Kingdom of Bhutan

To determine the design seismic coefficient for dam, the degree of seismic risk in Indian area including the Kingdom of Bhutan was studied.

Available seismic risk map for Indian area was prepared in 1986 by Bureau of Indian Standards (IS 1893-1984). Fig.8.8 shows the seismic risk map for Indian area which classifies the area into 5 Zones according to the degree of risk. And the Kingdom of Bhutan is located in IV~V zone. (Strong earthquake area)

According to Modified Mercalli (MM) intensity scale, inferred seismic intensity in the region is VIII~IX (approximately corresponding the intensity little less than V~VI).

According to Japanese design seismic coefficient for dam design, coefficient 0.12~0.15 would be applied for concrete gravity dam in strong earthquake area.

8.3.3 Estimation of Maximum Acceleration at the Damsite

(1) Analysis Method

The estimation of the maximum ground acceleration at the Punatsangchhu damsite by statistical probability analysis was performed to determine the design seismic coefficient. The seismicity data used in this study are those compiled by NOAA. The number of earthquakes which occurred within the radius of 1,000 km from the site during the period from 1897 to 1987 is 1,476. Of previously proposed attenuation models which express maximum ground acceleration A (gal), in terms of earthquake magnitude M and epicentral distance R (km), distance D (km) five models shown below are used in this study.

$\text{Log } A = 3.090 + 0.347\ M - 2\ \text{Log } (R+25)$ proposed by C. Oliveira[1] ..... ①

$\text{Log } A = 2.674 + 0.278\ M - 1.301\ \text{Log } (R+25)$ proposed by R.K. McGuire[2] ..... ②

$\text{Log } A = 2.041 + 0.347\ M - 1.601\ \text{Log } R$ proposed by L. Esteva and E. Rosenblueth[3] ..... ③

$\text{Log } A = 2.308 + 0.411\ M - 1.637\ \text{Log } (R+30)$ proposed by T. Katayama[4] ..... ④

$\text{Log } (A/640) = (D+40)(-7.6+1.724M-0.1036M^2)/100$ proposed by S.Okamoto ..... ⑤

The maximum ground acceleration for several return periods were estimated with the third-type asymptotic distribution based on the theory of Extreme Values.

Estimation were made with the data in the period 1897-1987 by taking an equal time interval of one year.

(2) Results of Seismic Risk Analysis at the Damsite

The distributions of magnitudes and epicentral distances regarding seismological data used in the seismic risk analysis at the damsite (89°55' east longitude, 27°23' north latitude) are given in Table 8.1 and Fig.8.7. The number of earthquakes yearly from 1897 to 1987 are given in Table 8.2, while the estimated values of maximum accelerations in the earthquakes with the greatest effects on the site in each of the years are given in Table 8.3.

The seismic risk analysis results based on the statistical probability theory technique concerning the damsite are shown in Fig.8.9 to 8.13.

(3) Maximum Accelerations assumed for the Damsite

The maximum accelerations at the ground surface assumed for the damsite can be put together in Table below from the previously-mentioned seismic risk analysis.

As can be comprehended from the tables, the results of estimation of maximum acceleration vary greatly depending on the attenuation equation applied. Especially, the maximum acceleration from the equation by S.Okamoto is extremely big, but the simple average value is 70 gal (100 years probability) and 158 gal (1,000 years probability).

Since such uncertainties exist in the seismic risk analysis, and as evaluations are on the conservative side, the simple average value including the value by S.Okamoto was considered as the assumed maximum acceleration for damsite.

In effect, 158 gal is to be taken as the maximum acceleration at the ground surface during earthquake for the damsite.

Maximum Accelerations expected at the Punatsangchhu Damsite

Attenuation Equation	Return Period (Year)				
	50	100	200	500	1,000
Oliveira's Equation	10	12	13	14	14
McGuire's Equation	44	47	49	51	52
Esteva & Rosenblueth's Equation	8	9	9	9	9
Katayama's Equation	23	25	27	28	29
Okamoto's Equation	166	259	374	548	688
Average	50	70	94	130	158
Probability	0.98	0.99	0.995	0.998	0.999

(Gal)

8.3.4 Design Horizontal Seismic Coefficient used in Aseismic Design

(1) Design Horizontal Seismic Coefficient of Ground at Project site

Regarding the relationship between the maximum horizontal acceleration of earthquake motion and the design horizontal seismic coefficient, the following equation will generally be valid.

$$Kh = R \times Amax / 980 \quad \text{.....} ⑥$$

where, Kh: Design horizontal seismic coefficient
R: Conversion factor
Amax: Maximum horizontal acceleration of earthquake motion (gal)

Design horizontal seismic coefficient of the above equation is what is called effective seismic coefficient or equivalent seismic coefficient, and the following proposals have been made in research in Japan.

1) $Kh = (0.35 \sim 0.42)\ Amax/980$ (effective value of steady sine wave) ..... ⑦
2) $Kh = 0.33\ (Amax/980)^{1/3}$ (Noda[5], 1975) ..... ⑧
3) $Kh = 0.072 + 0.332\ (Amax/980)$ (Matsuo[6], 1984) ..... ⑨
4) $Kh = (0.13 \sim 0.34)\ Amax/980$ (Hakuno[7], 1984) ..... ⑩

5) Kh = (0.50~0.60) Amax/980 (Watanabe[8], 1984) ..... ⑪

In the Technical Guide of Aseismic Design of Nuclear Power Plants[9] published in 1987, the following equation is proposed as a result of overall evaluation and taking into account these cases of study.

Kh = (0.40~0.60) Amax/980 ..... ⑫

The concept of effective seismic coefficient (equivalent seismic coefficient) was derived so that the largeness of stresses produced in ground and structures by earthquake motions will be equivalent for cases of handling dynamically (dynamic analysis by input of earthquake motion) and for cases of handling statically (static analysis using design seismic coefficient). The conversion factor which will be required for calculating effective seismic coefficient (equivalent seismic coefficient) is thought to be largely dependent on the frequency characteristics of design input earthquake motions. That is, for an earthquake motion with long-period components predominant, a large value (for example; 0.6) should be taken for the conversion factor. And for an earthquake motion with short-period components predominant, a small value (for example; 0.4) can be taken for the conversion factor.

As described before, the maximum acceleration assumed at the damsite is to be 158 gal. Consequently, applying Eq. ⑫, the design horizontal seismic coefficient of ground at the damsite will be Kh=0.06~0.10.

Since the frequency characteristics of earthquake motions during earthquakes at the site cannot necessarily be estimated distinctly at the present time, it is judged to be reasonable to take the design horizontal seismic coefficient of ground at the damsite as 0.15 for an evaluation on the conservative side.

(2) Design Horizontal Seismic Coefficient for Dam

Regarding the design horizontal seismic coefficient for dam, as shown in Table below, the same value as the design horizontal seismic coefficient of ground is to be adopted for rockfill dam and concrete gravity dam. For concrete arch dam, a value twice the design horizontal seismic coefficient of ground is to be adopted.

Design Horizontal Seismic Coefficient for Dam

Dam Type	Design Horizontal Seismic Coefficient
Rock Fill Dam	0.15
Concrete Gravity Dam	0.15
Concrete Arch Dam	0.30

(3) Afterward

The determination of optimum configuration and cross section of a dam, and the basic stability evaluation of the dam during earthquake are normally made according to the seismic coefficient method. The design seismic coefficient to be used in the seismic coefficient method, is evaluated considering a conversion factor for the maximum acceleration of earthquake motion assumed for the site. The value of the conversion factor can be thought to depend on the frequency characteristics of the earthquake motions assumed. It is desirable to ascertain the seismic stability of the dam by dynamic analysis at the stage of detailed design. Namely, the appropriateness of the design seismic coefficient would be verified by comparison of dynamic and static analysis.

[References]

(1) Oliveira, C.; Seismic Risk Analysis, EERC 74-1, Earthquake Engineering Research Center, University of California, Berkeley (1974), 1-102.

(2) McGuire, R.K.; Seismic Structural Response Risk Analysis incorporating Peak Response Regressions on Earthquake Magnitude and Distance, Mass. Inst. Tech. Dep. Civ. Eng., R74-51 (1974).

(3) Esteva, L. and Rosenblueth, E.; Espectos de Temblores a Distancias Moderadas y Grandes, Proc. Chilean Conference on Seismology and Earthquake Engineering, vol. 1, University of Chile (1963).

(4) Katayama, T.; Fundamentals of Probabilistic Evaluation of Seismic Activity and Seismic Risk (in Japanese), SEISAN-KENKYU (Monthly Journal of Institute of Industrial Science, University of Tokyo), 27-5 (1975), 1-11.

(5) Noda, S., Kambe, T., and Chiba, T.; "Seismic Coefficient of Gravity-type Quaywall and Ground Acceleration," Report of Port and Harbour Technical Research Institute, Ministry of Transport, Vol. 14, No. 4, PP.67-111, 1975

(6) Matsuo, M., and Itabashi, K.; "Study on Evaluation of Aseismicity of Slopes and Soil Structures," Transactions of the Japan Society of Civil Engineers, No. 352, III-2, Dec. 1984.

(7) Hakuno, M., and Morikawa, O.; "A Simulation concerning Earthquake Acceleration and Failure of Structures," Transactions of the Japan Society of Civil Engineers, No. 344, I-1, PP.299-302, Apr. 1984.

(8) Watanabe, H., Sato, S., and Murakami, S.; "Evaluation of Earthquake-Induced Sliding in Rockfill Dams," Soil and Foundation, Vol. 24, No. 3, PP1-14, Sept. 1984.

(9) Japan Electric Association, "Technical Guide to Aseismic Design of Nuclear Power Stations," 1987.

Table 8.1 Distribution of Magnitude and Epicentral Distance of Seismicity Data

	0<=D<50	<100	<200	<300	<400	<500	<600	<700	<800	<1000	1000<=	Total
0<M<3.0	0	0	0	0	0	0	0	0	0	0	0	0
<3.5	0	0	0	0	0	0	0	1	0	1	0	2
<4.0	0	0	0	0	1	2	5	5	0	6	0	19
<4.5	1	0	3	13	9	13	30	37	29	54	0	189
<5.0	0	1	13	40	35	32	176	124	87	123	0	631
<5.5	3	1	8	25	13	13	47	67	33	85	0	295
<6.0	0	1	4	8	7	7	16	20	8	15	0	86
<6.5	1	1	7	8	10	14	14	34	12	46	0	147
<7.0	0	0	1	10	3	6	7	14	9	24	0	74
<7.5	0	0	0	0	9	3	0	4	7	4	0	27
<8.0	0	0	0	0	2	1	0	1	0	0	0	4
8.0<=	0	0	1	0	0	0	0	1	0	0	0	2
Unknown	0	0	0	0	0	0	0	0	0	0	0	0
Total	5	4	37	104	89	91	295	308	185	358	0	1476

D: Epicentral Distance (km)

M: Magnitude

Table 8.2 Number of Earthquakes for the Punatsangchhu Damsite in a Year during the period from 1897 to 1987

Year	N	Sum of N	Year	N	Sum of N
1897	1	1	1943	2	111
1898	0	1	1944	5	116
1899	0	1	1945	0	116
1900	0	1	1946	5	121
1901	0	1	1947	4	125
1902	0	1	1948	1	126
1903	0	1	1949	0	126
1904	0	1	1950	28	154
1905	0	1	1951	13	167
1906	2	3	1952	4	171
1907	0	3	1953	6	177
1908	2	5	1954	5	182
1909	0	5	1955	17	199
1910	0	5	1956	11	210
1911	0	5	1957	4	214
1912	0	5	1958	4	218
1913	5	10	1959	8	226
1914	2	12	1960	5	231
1915	4	16	1961	11	242
1916	1	17	1962	1	243
1917	0	17	1963	20	263
1918	3	20	1964	34	297
1919	0	20	1965	40	337
1920	2	22	1966	42	379
1921	1	23	1967	33	412
1922	0	23	1968	34	446
1923	3	26	1969	22	468
1924	3	29	1970	23	491
1925	0	29	1971	35	526
1926	3	32	1972	27	553
1927	2	34	1973	37	590
1928	0	34	1974	34	624
1929	2	36	1975	49	673
1930	8	44	1976	69	742
1931	7	51	1977	54	796
1932	7	58	1978	59	855
1933	5	63	1979	58	913
1934	10	73	1980	83	996
1935	7	80	1981	57	1053
1936	5	85	1982	72	1125
1937	0	85	1983	48	1173
1938	9	94	1984	70	1243
1939	2	96	1985	79	1322
1940	5	101	1986	82	1404
1941	8	109	1987	72	1476
1942	0	109			

Table 8.3 Maximum Accelerations of the Year at the Punatsangchhu Damsite during the period from 1897 to 1987 (1/2)

(gal)

Year	Attenuation Equation				
	Oliveira's Eq. ACC.	McGuire's Eq. ACC.	Esteva & Rosenblueth's Eq. ACC.	Katayama's Eq. ACC.	Okamoto's Eq. ACC.
1897	15.56	71.87	14.52	56.43	63.50
1898	0.00	0.00	0.00	0.00	0.00
1899	0.00	0.00	0.00	0.00	0.00
1900	0.00	0.00	0.00	0.00	0.00
1901	0.00	0.00	0.00	0.00	0.00
1902	0.00	0.00	0.00	0.00	0.00
1903	0.00	0.00	0.00	0.00	0.00
1904	0.00	0.00	0.00	0.00	0.00
1905	0.00	0.00	0.00	0.00	0.00
1906	0.57	7.32	0.75	2.81	0.01
1907	0.00	0.00	0.00	0.00	0.00
1908	1.04	10.85	1.24	4.60	0.18
1909	0.00	0.00	0.00	0.00	0.00
1910	0.00	0.00	0.00	0.00	0.00
1911	0.00	0.00	0.00	0.00	0.00
1912	0.00	0.00	0.00	0.00	0.00
1913	0.62	7.94	0.83	3.20	0.02
1914	0.31	4.87	0.45	1.68	0.00
1915	3.30	23.20	3.35	11.93	6.67
1916	0.49	7.05	0.71	2.86	0.01
1917	0.00	0.00	0.00	0.00	0.00
1918	3.13	23.32	3.32	12.62	5.92
1919	0.00	0.00	0.00	0.00	0.00
1920	0.28	4.36	0.39	1.37	0.00
1921	1.41	12.52	1.52	5.12	0.42
1922	0.00	0.00	0.00	0.00	0.00
1923	3.89	25.84	3.87	13.64	9.58
1924	2.40	18.06	2.45	8.27	2.43
1925	0.00	0.00	0.00	0.00	0.00
1926	0.38	5.30	0.50	1.75	0.00
1927	0.58	7.20	0.74	2.63	0.01
1928	0.00	0.00	0.00	0.00	0.00
1929	0.58	6.70	0.68	2.21	0.01
1930	5.76	33.34	5.48	18.68	18.51
1931	0.75	9.23	1.00	3.97	0.05
1932	2.31	16.44	2.24	6.74	1.54
1933	4.11	23.91	3.76	10.69	6.58
1934	4.34	30.60	4.64	19.07	10.30
1935	3.71	23.51	3.54	11.17	16.17
1936	1.50	12.42	1.53	4.76	0.41
1937	0.00	0.00	0.00	0.00	0.00
1938	1.46	12.09	1.48	4.56	0.33
1939	0.89	9.66	1.07	3.89	0.10
1940	1.29	11.57	1.38	4.53	0.26
1941	4.02	25.71	3.90	13.10	15.15
1942	0.00	0.00	0.00	0.00	0.00

Table 8.3 Maximum Accelerations of the Year at the Punatsangchhu Damsite during the period from 1897 to 1987 (2/2)

(gal)

Year	Attenuation Equation				
	Oliveira's Eq. ACC.	McGuire's Eq. ACC.	Esteva & Rosenblueth's Eq. ACC.	Katayama's Eq. ACC.	Okamoto's Eq. ACC.
1943	2.50	19.53	2.66	9.74	3.28
1944	0.43	6.00	0.58	2.14	0.00
1945	0.00	0.00	0.00	0.00	0.00
1946	0.74	9.24	1.00	4.03	0.05
1947	2.56	20.59	2.81	10.91	3.66
1948	0.21	3.68	0.32	1.11	0.00
1949	0.00	0.00	0.00	0.00	0.00
1950	1.54	15.96	1.99	8.72	0.54
1951	3.24	24.40	3.49	13.73	6.29
1952	2.43	19.62	2.65	10.09	3.19
1953	0.53	6.63	0.67	2.32	0.00
1954	8.00	36.85	7.06	18.12	22.90
1955	46.08	115.86	51.05	71.50	191.86
1956	1.17	10.30	1.21	3.65	0.12
1957	0.56	6.73	0.68	2.40	0.01
1958	2.63	17.74	2.50	7.33	2.13
1959	2.08	15.47	2.05	6.31	1.17
1960	7.05	33.70	6.23	16.09	18.18
1961	0.42	5.42	0.52	1.71	0.00
1962	0.34	4.89	0.45	1.55	0.00
1963	0.99	9.31	1.05	3.27	0.07
1964	20.24	69.66	18.17	40.93	83.38
1965	3.41	21.34	3.19	9.40	4.35
1966	1.48	10.49	1.35	3.33	0.17
1967	2.59	17.22	2.43	6.88	2.16
1968	3.37	19.01	3.00	7.05	2.85
1969	12.68	43.94	12.35	18.59	28.78
1970	1.16	9.80	1.13	3.72	0.09
1971	1.42	10.07	1.29	2.94	0.14
1972	2.32	14.23	2.07	4.63	0.87
1973	0.98	8.54	0.97	2.64	0.04
1974	0.91	7.63	0.87	2.40	0.02
1975	1.55	10.94	1.42	3.36	0.21
1976	1.06	9.29	1.07	3.07	0.09
1977	1.08	8.63	1.02	2.51	0.05
1978	0.67	6.39	0.67	1.76	0.00
1979	1.21	9.32	1.13	2.76	0.08
1980	7.61	35.56	6.72	17.26	19.66
1981	12.21	43.41	11.62	18.68	39.97
1982	4.53	21.44	4.03	7.89	11.91
1983	0.90	7.75	0.87	2.23	0.02
1984	1.05	8.89	1.03	2.77	0.05
1985	5.82	24.64	5.38	8.37	17.47
1986	1.61	11.48	1.49	3.68	0.40
1987	1.05	8.26	0.98	2.31	0.05

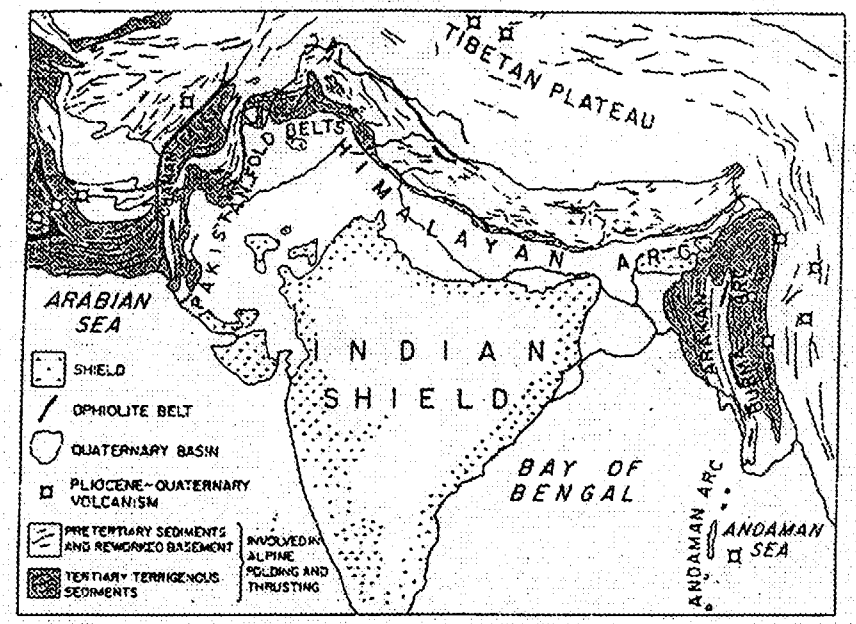

Regional setting of the Himalayan arc, along which the Indian shield is subducting northward. Tectonic features based on Ganasser [1964, plate I]; recent volcanic centers according to Katsui [1971].

Fig. 8.1 Regional Setting of the Himalayan Arc

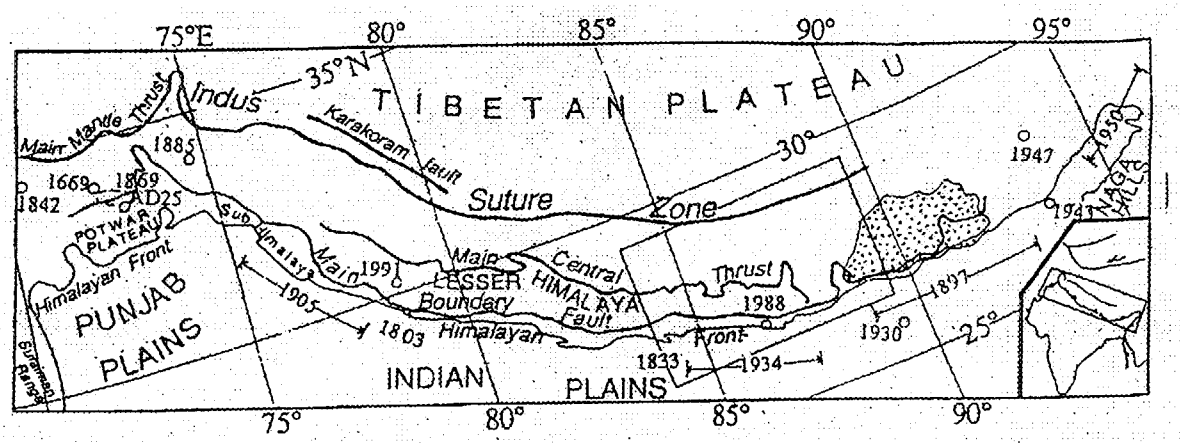

Major subdivisions of the Himalaya. Tethyan Himalaya and High Himalaya lie between Indus Suture Zone and Main Central thrust. Dates identify large earthquakes that have affected the Himalayan foothills. The earthquakes of 1897, 1905, 1934, and 1950 were $M \geq 8$. Based on earthquakes of the last two centuries, seismic gaps occur between the 1803 and 1833 earthquakes, between the 1869 and 1905 earthquakes, and possibly between the 1934 and 1897 events and between the 1897 and 1950 events.

Fig. 8.2 Major Subdivisions and Earthquakes of the Himalaya

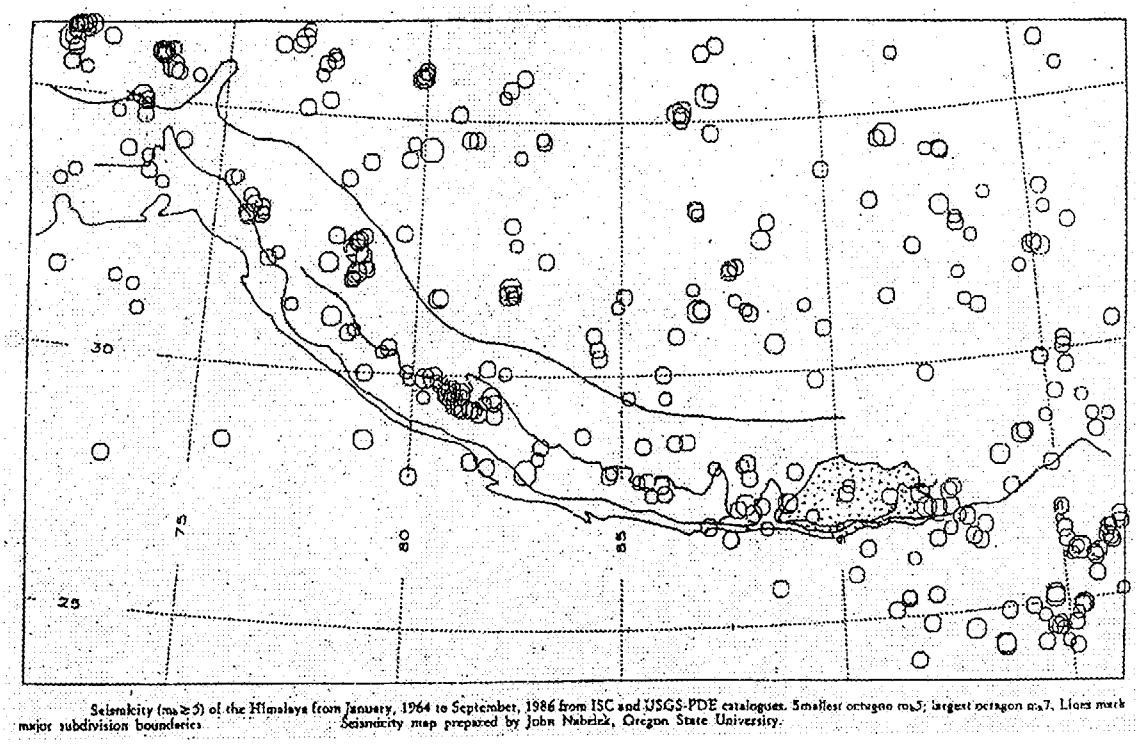

Seismicity ($m_b \geq 5$) of the Himalaya from January, 1964 to September, 1986 from ISC and USGS-PDE catalogues. Smallest octagon $m_b 5$; largest pentagon $m_b 7$. Lines mark major subdivision boundaries. Seismicity map prepared by John Nabelek, Oregon State University.

Fig. 8.3 Seismicity of the Himalaya from 1964 to 1986

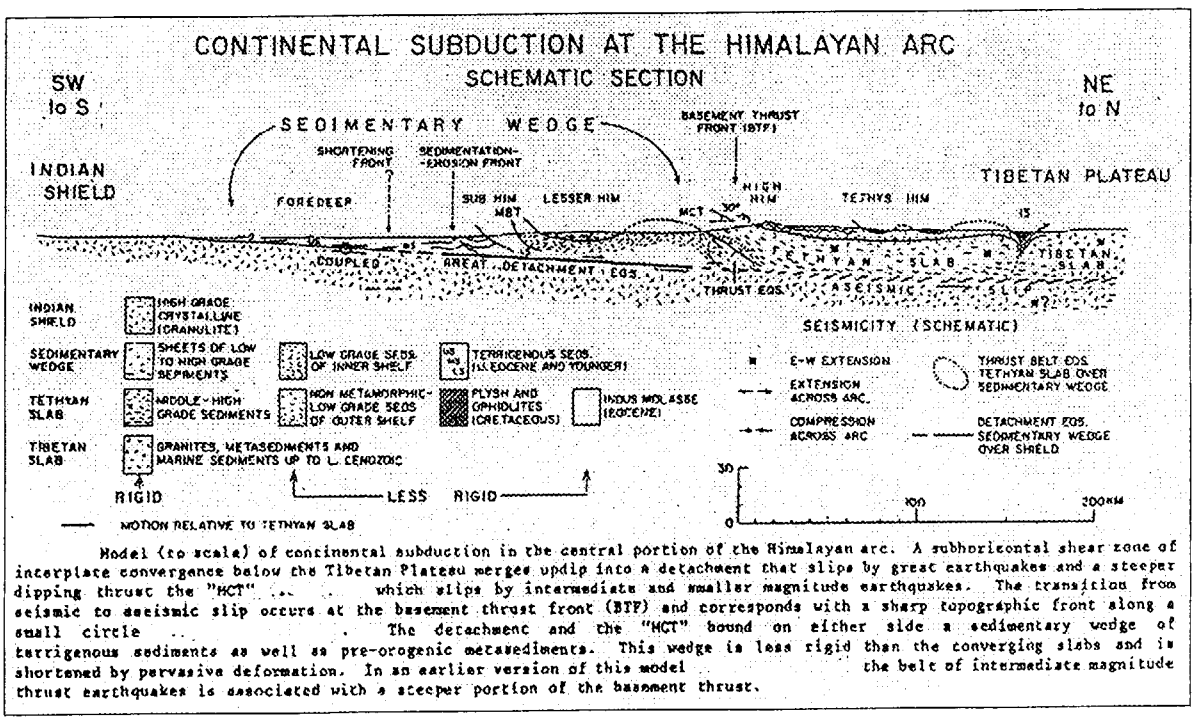

Model (to scale) of continental subduction in the central portion of the Himalayan arc. A subhorizontal shear zone of interplate convergence below the Tibetan Plateau merges updip into a detachment that slips by great earthquakes and a steeper dipping thrust the "MCT" ... . which slips by intermediate and smaller magnitude earthquakes. The transition from seismic to aseismic slip occurs at the basement thrust front (BTF) and corresponds with a sharp topographic front along a small circle ... . The detachment and the "MCT" bound on either side a sedimentary wedge of terrigenous sediments as well as pre-orogenic metasediments. This wedge is less rigid than the converging slabs and is shortened by pervasive deformation. In an earlier version of this model the belt of intermediate magnitude thrust earthquakes is associated with a steeper portion of the basement thrust.

Fig. 8.4 Model of Continental Subduction of the Himalayan Arc

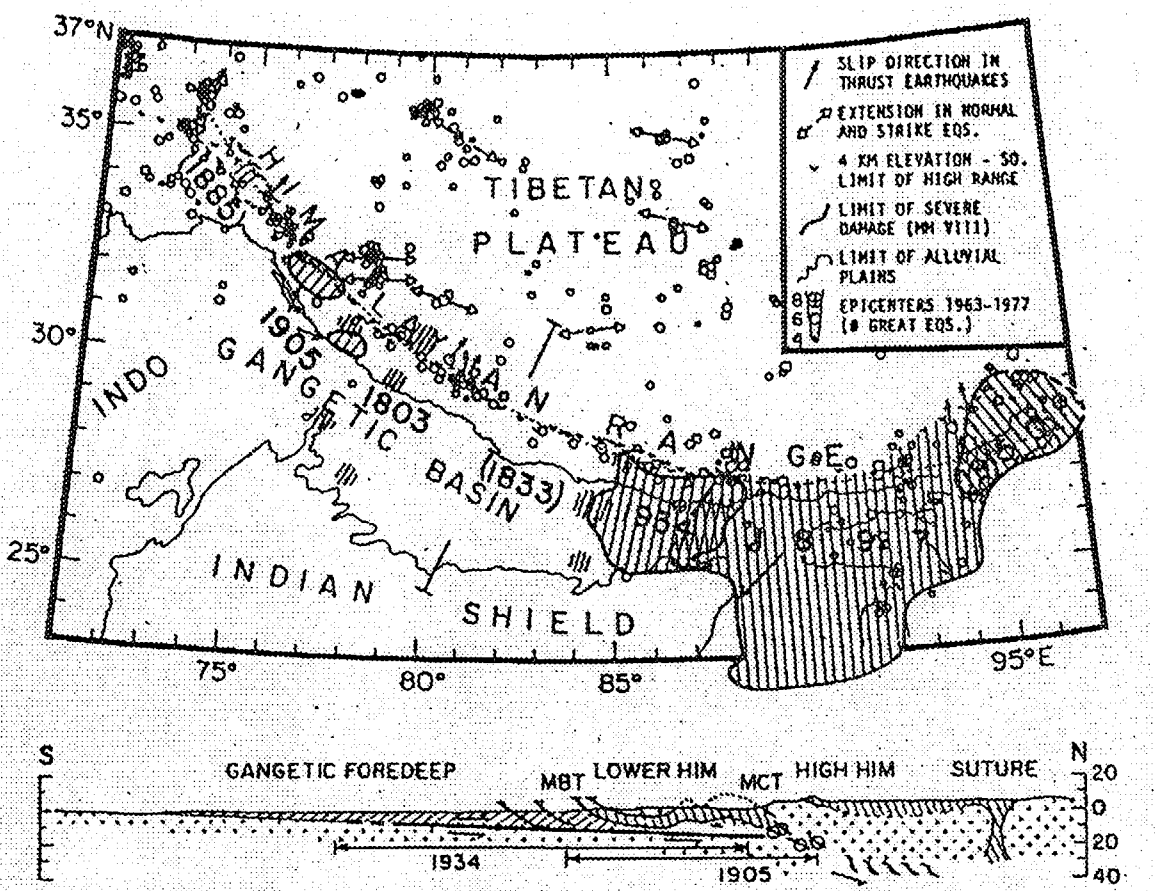

Epicentral map of the Himalaya (NOAA data, 1963-1977; only epicenters determined with 20 or more P arrival-times; size of circle proportional to magnitude) and intensity VIII contours of possible great Himalayan earthquakes (intensity ≥ VIII for each earthquake is shaded with lines perpendicular to the arc, pre 1897 shaded areas may be intensity < VIII). Representative fault plane solutions (Molnar et al., 1977) are indicated by arrows, single arrows = slip direction of thrusting events, pairs of arrows = tension axes of normal faulting events. The sharp topographic front of the High Himalaya (thresholds of 4 km elevation) correlates with the belt of moderate magnitude thrust earthquakes. This morphotectonic feature (STF , fits precisely a small circle (dotted line) over the central 2/3 of the Himalayan arc. The cross section (below) is for the central portion of the arc (location is indicated on map) and contains the hypocenters (projected along the arc) and fault dip (northward component only) of the three earthquakes near 81°E and the earthquake near 88°E for which depth and fault plane solution are well-constrained by body-wave modelling. Depth and slip direction of well-constrained earthquakes at the eastern and western terminus of the arc fit the same pattern.

Fig. 8.5 Epicentral Map of the Himalaya and Large Earthquake

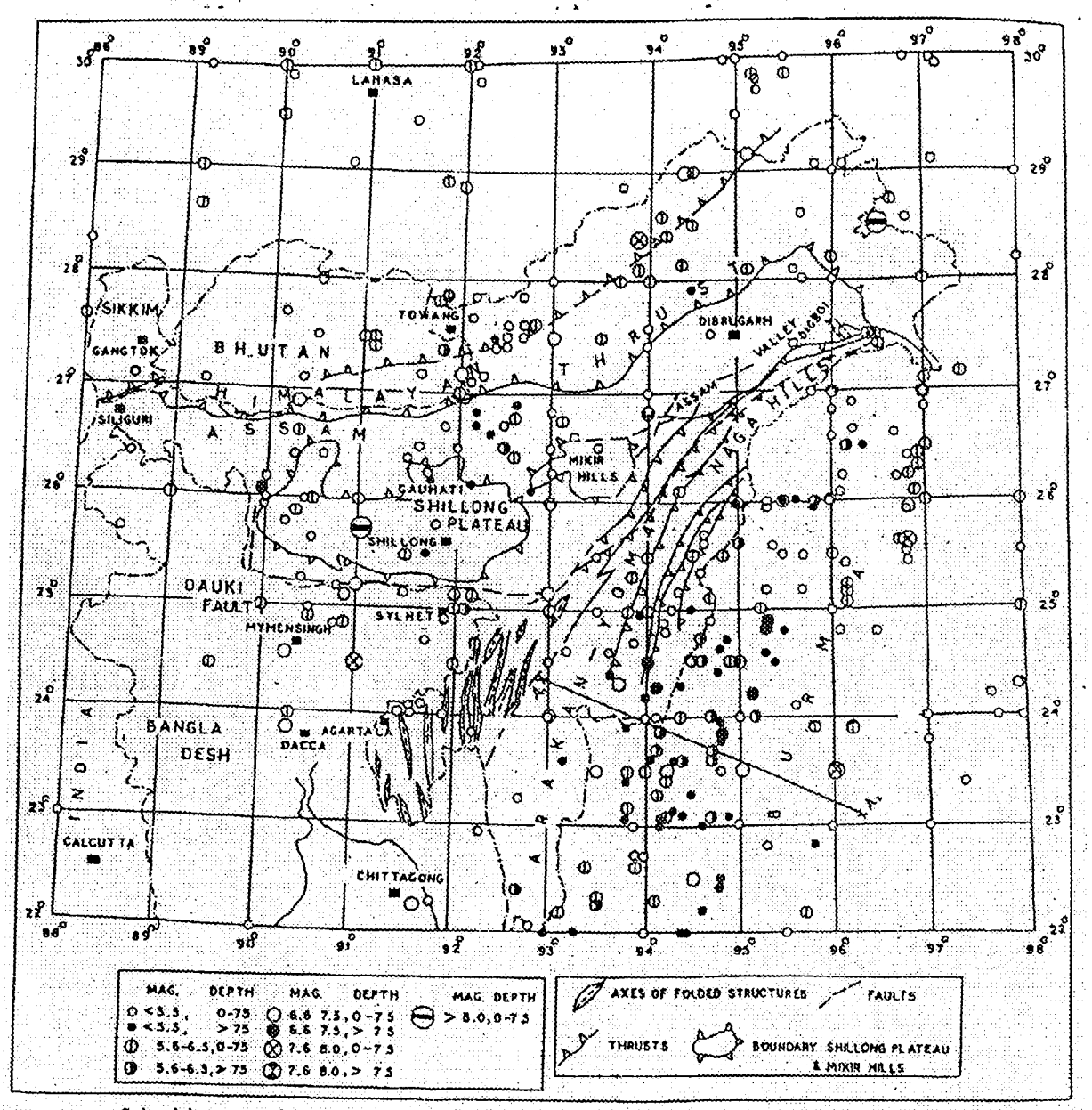

Seismicity map of northeast India and adjoining areas of northern Burma and Bangla Desh for the period 1890–1970.

Fig. 8.6 Seismicity Map of Northeastern India and adjoining Areas of Burma and Bangla Desh

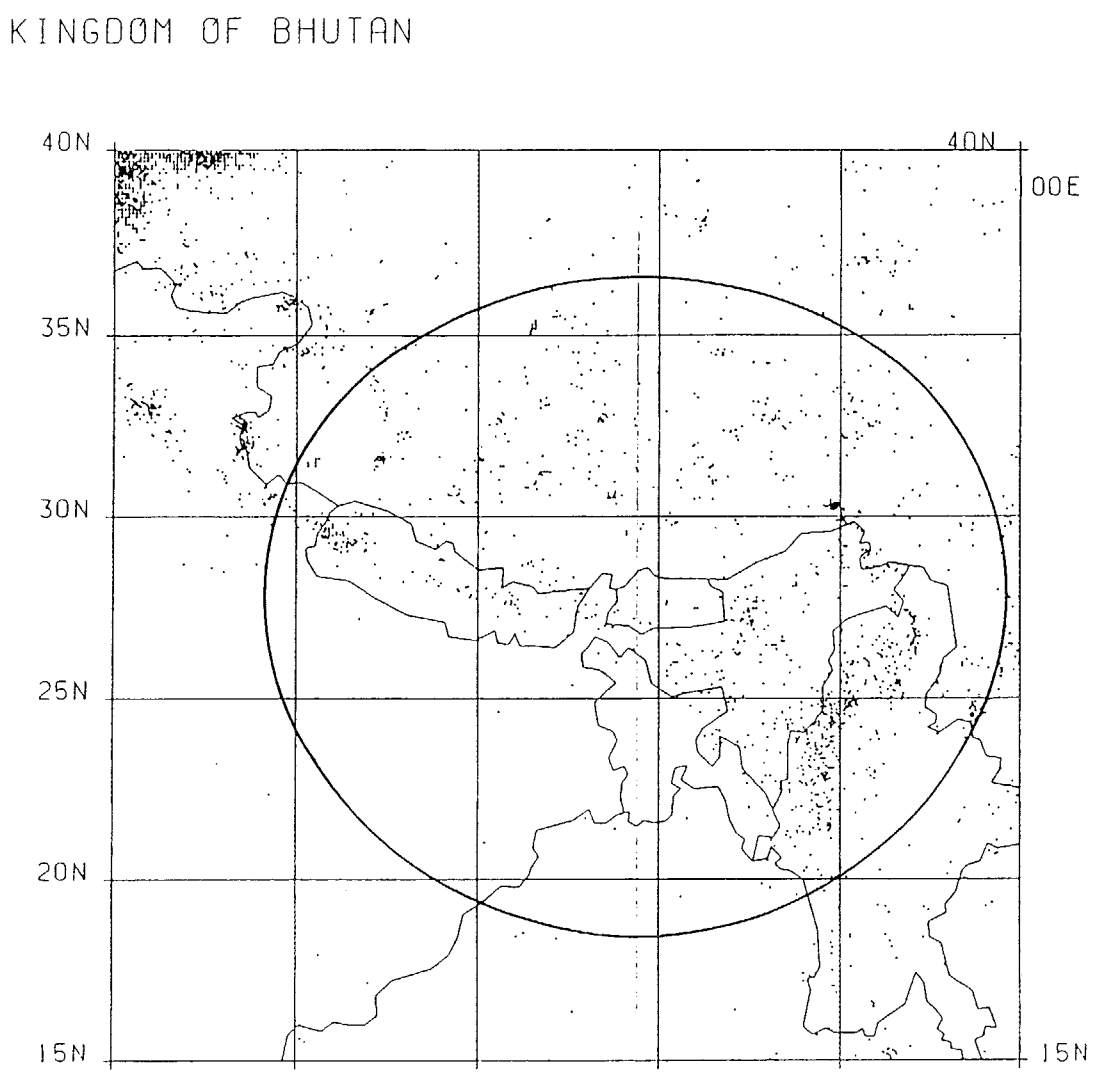

Fig. 8.7 Data for Seismicity Analysis (1897-1987)

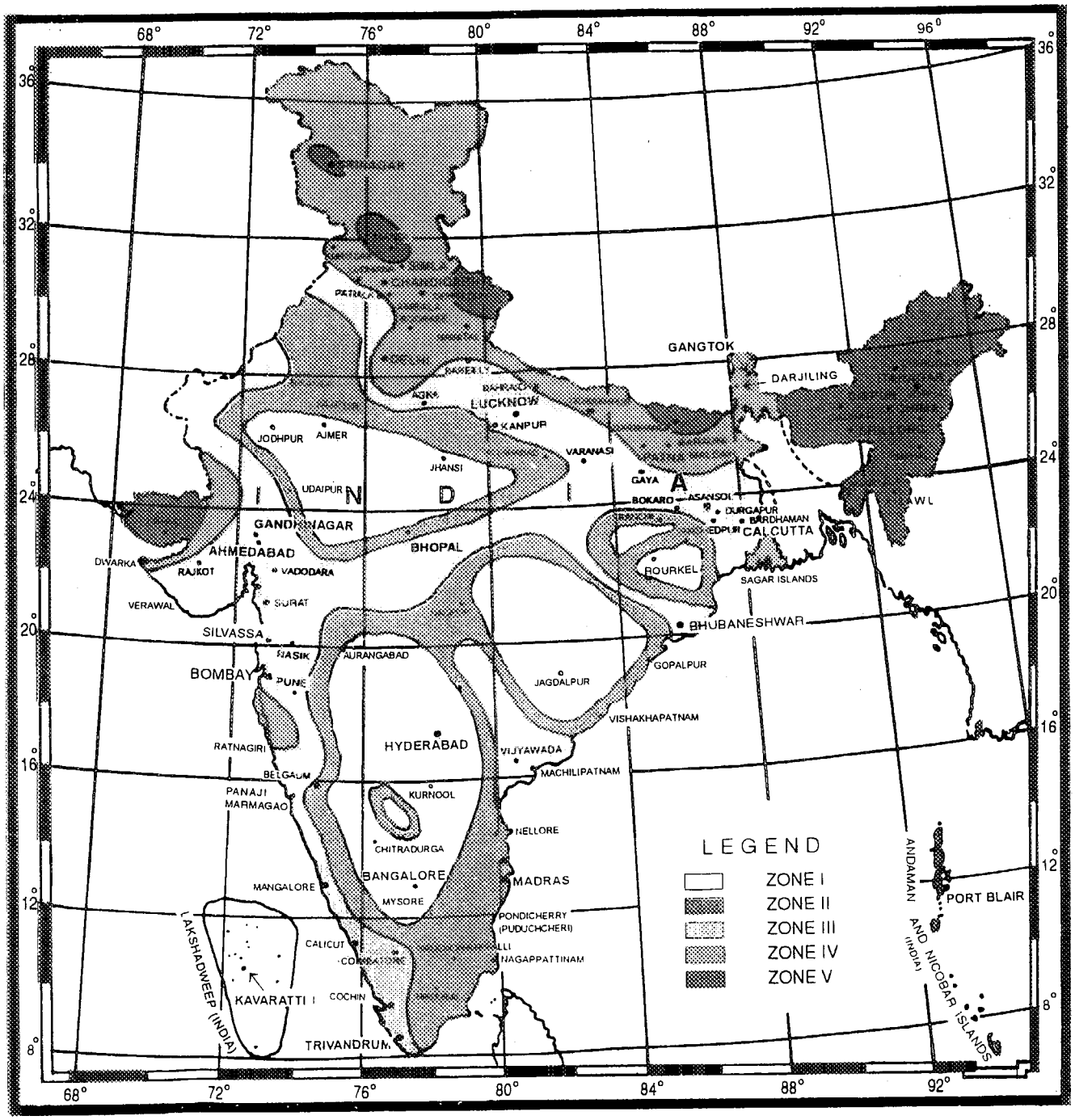

Fig. 8.8 Seismic Risk Map for India (1986)

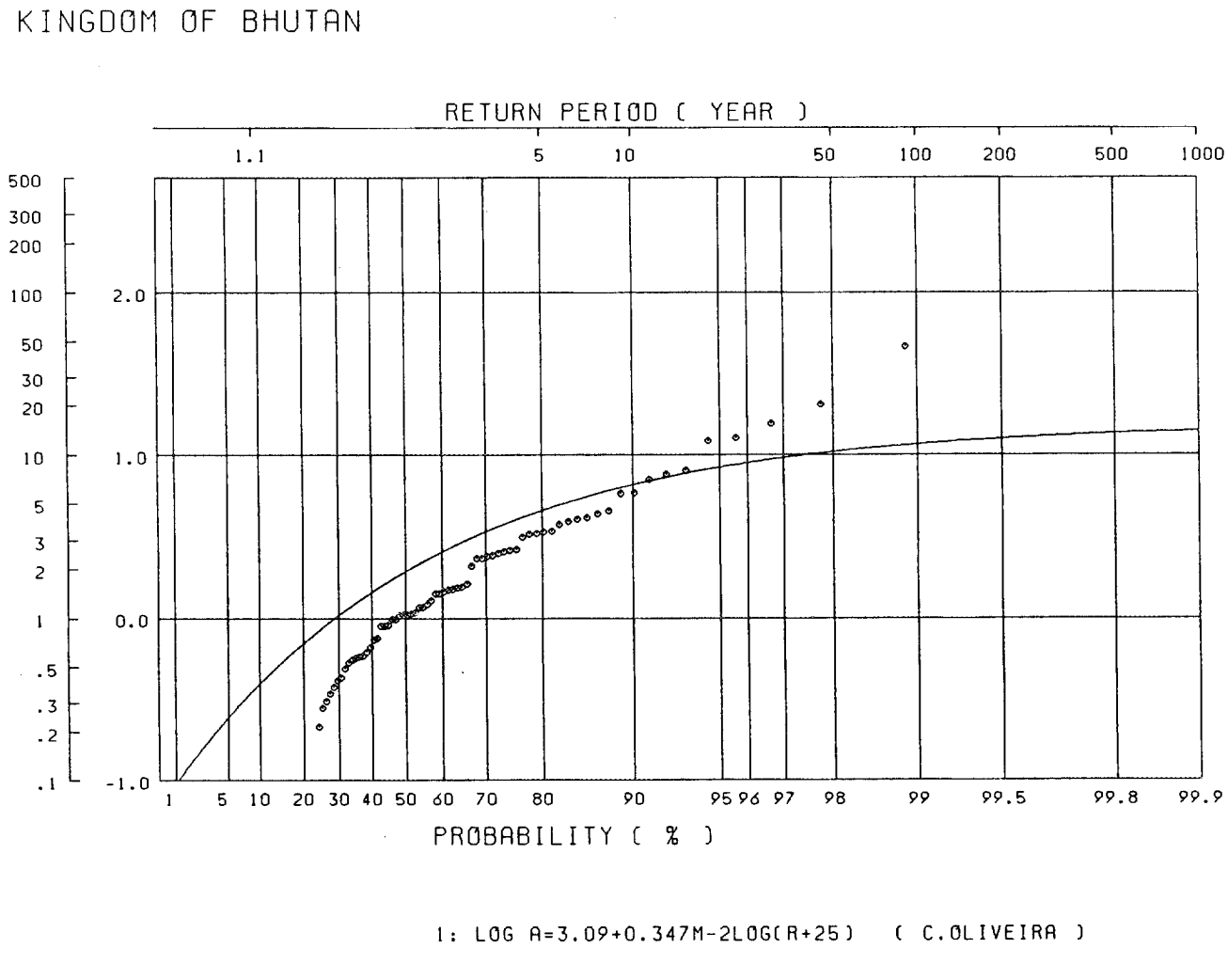

Fig. 8.9 Maximum Acceleration for Return Period at the Punatsangchhu Damsite estimated by C.Olivera's Equation

KINGDOM OF BHUTAN

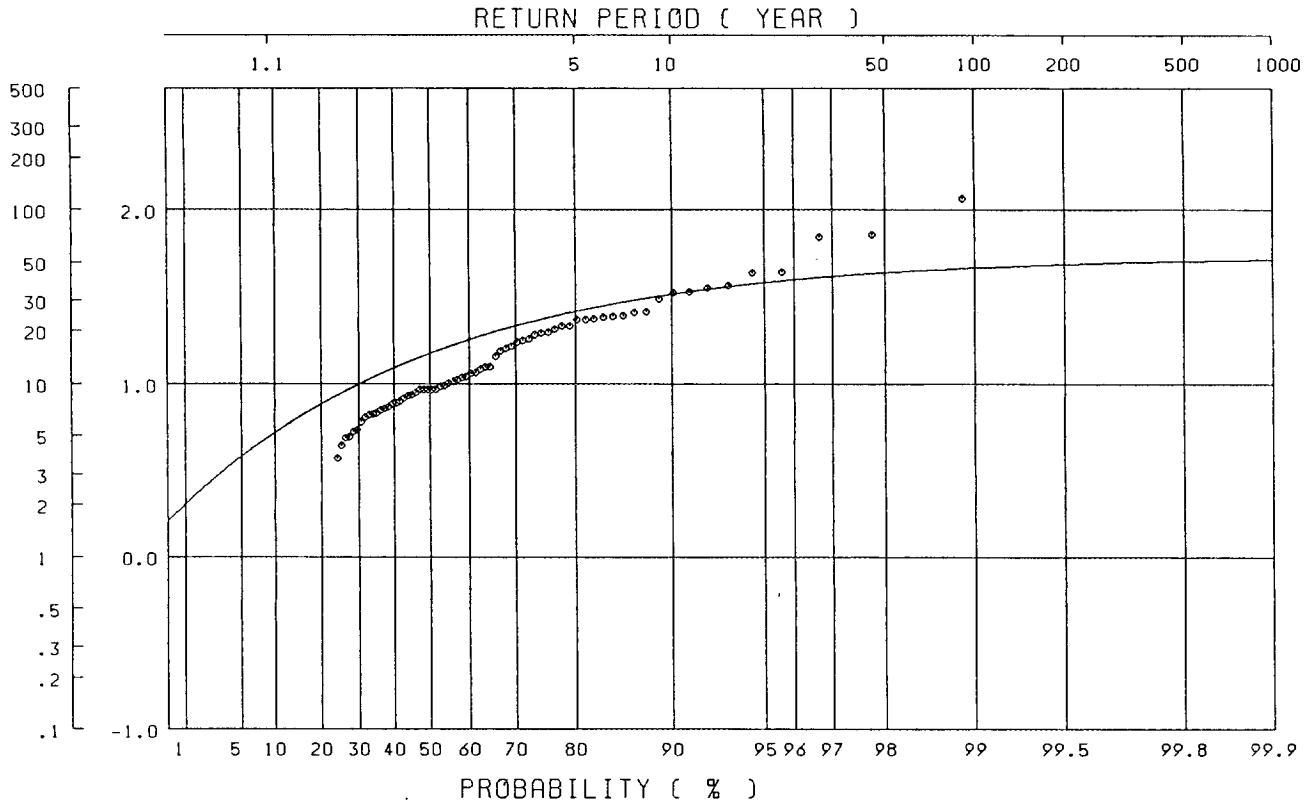

2: LOG A=2.674+0.278M-1.301LOG(R+25)

(R.K.MCGUIRE)

Fig. 8.10 Maximum Acceleration for Return Period at the Punatsangchhu Damsite estimated by R.K.McGuire's Equation

KINGDOM OF BHUTAN

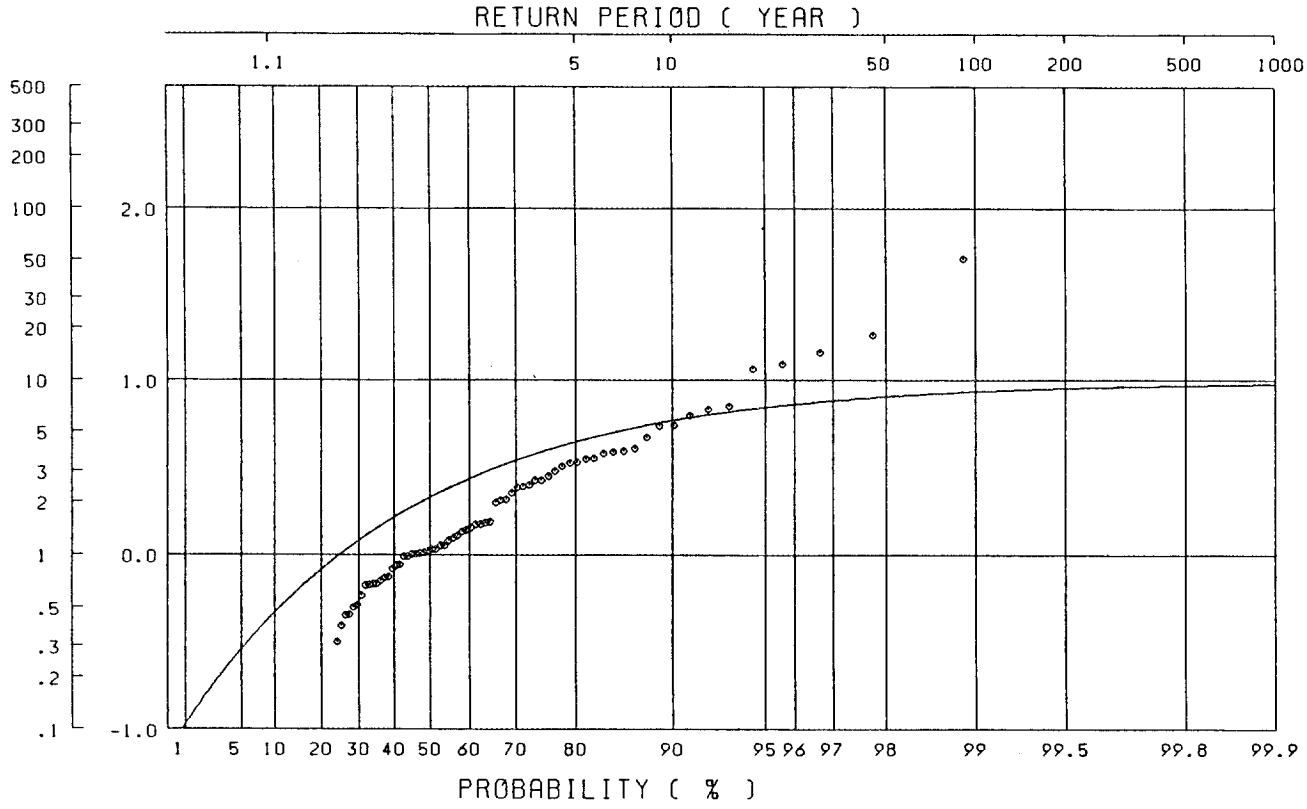

3: LOG A=2.041+0.347M-1.6LOG(R)

(L.ESTEVA & E.ROSENBLUETH)

Fig. 8.11 Maximum Acceleration for Return Period at the Punatsangchhu Damsite estimated by L.Esteva & Rosenblueth's Equation

KINGDOM OF BHUTAN

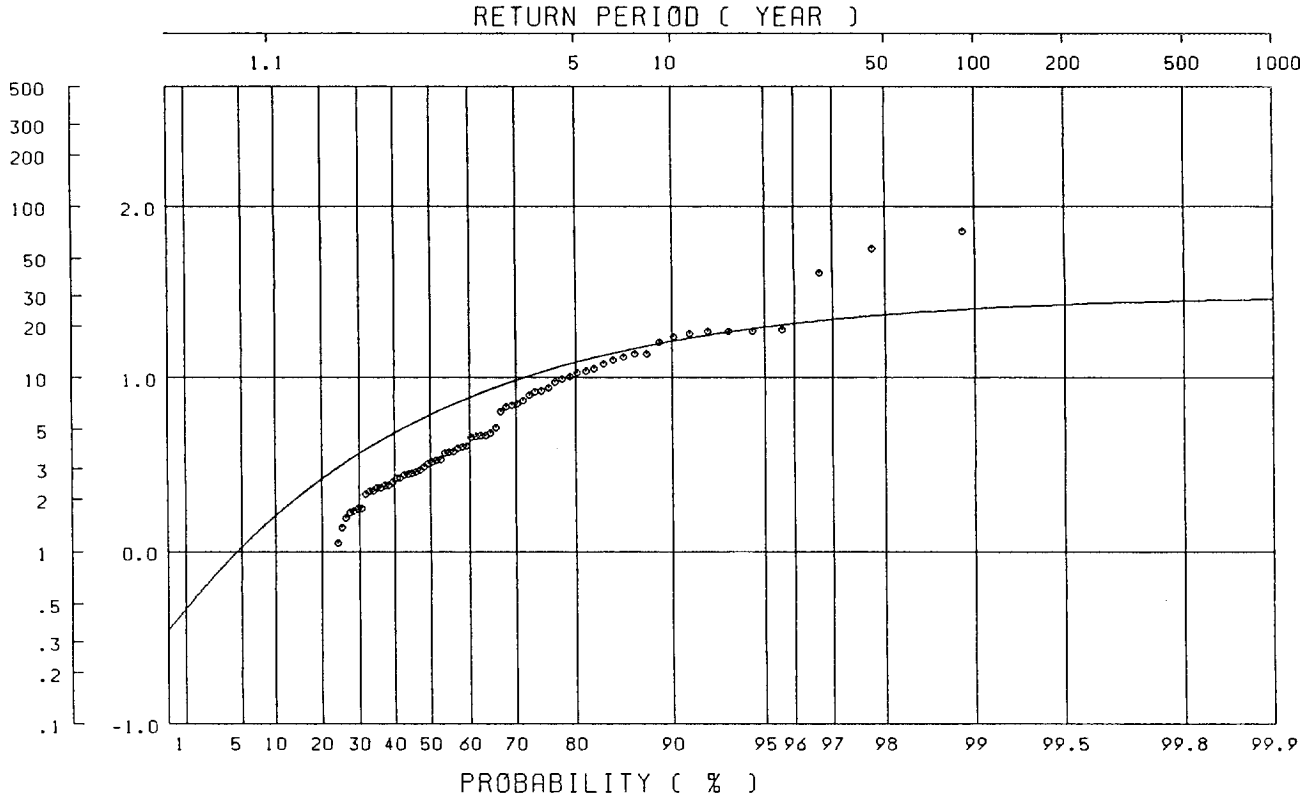

4: LOG A=2.308+0.411M-1.637LOG(R+30)

(T.KATAYAMA)

Fig. 8.12 Maximum Acceleration for Return Period at the Punatsangchhu Damsite estimated by Katayama's Equation

KINGDOM OF BHUTAN

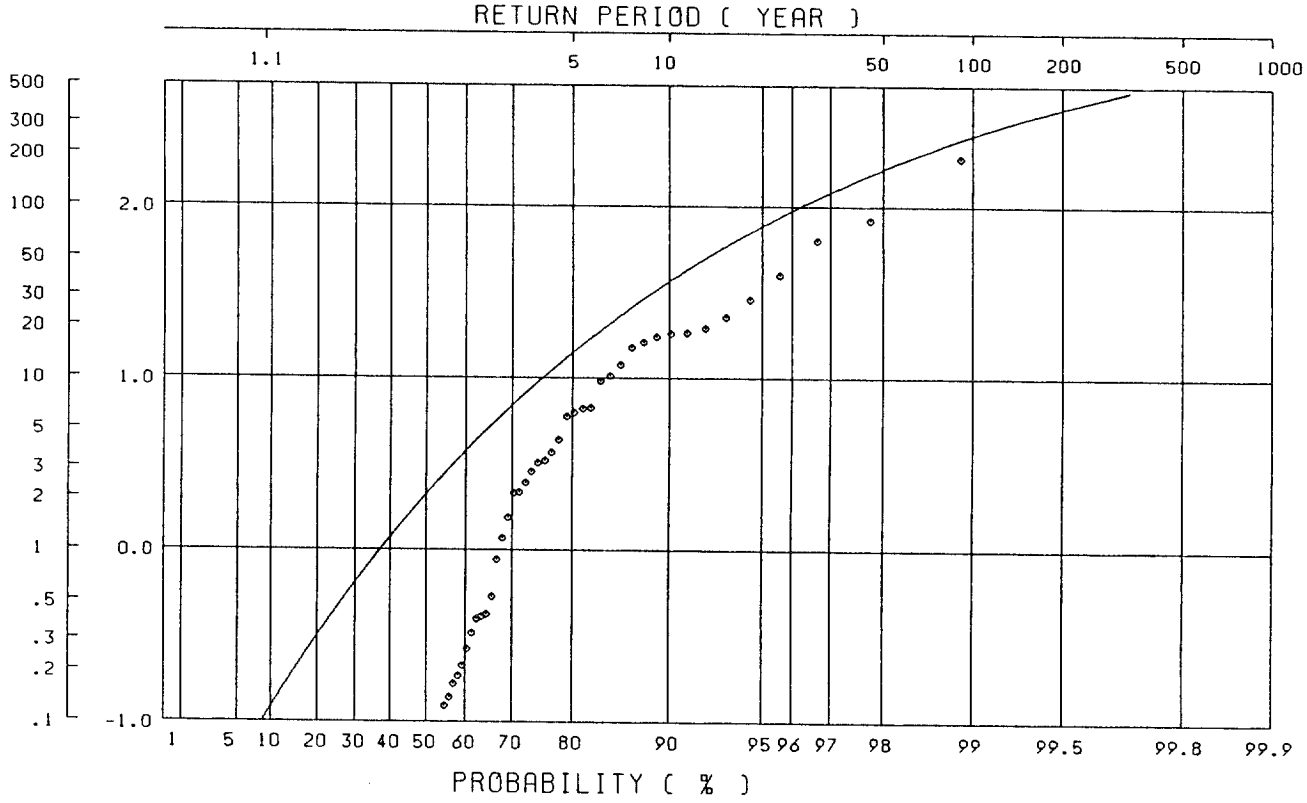

5: LOG(A/640)=(D+40)(-7.6+1.724M-0.1036M**2)/100

(S.OKAMOTO)

Fig. 8.13 Maximum Acceleration for Return Period at the Punatsangchhu Damsite estimated by S.Okamoto's Equation

CHAPTER 9

DEVELOPMENT PLAN

CONTENTS

9. DEVELOPMENT PLAN

9.1 Review of Existing Development Plan

9.1.1 Power System Master Plan and Pre F/S

The Bhutan Power System Master Plan (hereinafter referred to as the Master Plan) was formulated during the years 1990 to 1993 with financial assistance from UNDP and NORAD.

In this Master Plan, development plans for 25 projects in the whole country were formulated. The four most attractive projects, including the Punatsangchhu Project (Project 3.120) and Project 3.230B, Pre F/S studies, were carried out as a part of the Master Plan. (see Fig. 9.1)

① Punatsangchhu Project stage 1 (760 MW Project 3.120)
② Punatsangchhu Project stage 2 (650 MW Project 3.230B)
③ Mangdechhu Project (265 MW Project 4.020)
④ Kholongchhu Project (290 MW Project 5.150B)

9.1.2 Punatsangchhu Hydro Power Development Plan

Punatsangchhu is a 320 km long river which begins in the Himalayan mountain ranges, flowing southward in the mid-west part of the Kingdom of Bhutan, confluent with the Bramaphtra in India. .Upstream, the Mochhu and the Phochhu meet at the EL.1200 m point near Punakha.

In the river basin, there are seven projects (total capacity 1,894 MW) proposed in the Master Plan, and Project 3.120 (760 MW) and Project 3.230B (650 MW) in Pre F/S. Both projects are located midstream in the Punatsangchhu. The generation method of Project 3.120 is the dam and waterway type, and the damsite is proposed at a point about 10 km downstream from Wangdue Phodrang, located downstream of the conjunction point of the two rivers. The powerhouse site is to be about 8 km further downstream. And, similarly, the dam and powerhouse of Project 3.230B are arranged in succession to the upper Project 3.120 like a cascade.

The climate around the project area is generally divided into a wet season (June to September) and a dry season (October to May). Annual average rainfall in the area is about 700~900 mm, but this area is abundant with water resources. Annual average river discharge is 290 m^3/s (Wangdi Rapids GS: 1992 to 1999) and discharge in the dry season would be expected to be more than 60 m^3/s. The riverbed gradient is fundamentally steep and, especially midstream around the project area, is very steep. (average 1/20~1/30)

Table 9.1 and Fig. 9.2 show the general plan of the two projects in Punatsangchhu.

9.1.3 Review of Existing Development Plan

The midstream of the Punatsangchhu, where Project 3.120 and Project 3.230B are planned, has a relatively steep riverbed gradient. The damsite of Project 3.120 coincides with the marginal point of the riverbed gradient, and provides a good topographical condition for planning a dam and waterway type hydro power project, having a regulating reservoir in place upstream of the dam and a waterway downstream for headrace.

The waterway route of Project 3.120 is to pass in the left side of the mountain, considering the plane curvature of the river. About 6.4 km of headrace tunnel would lead the water to the underground powerhouse that is located just upstream of the relatively big tributary flowing from the left side of river at a point about 8 km downstream from the dam.

That left side tributary would be the downstream boundary for the location of the powerhouse. In other words, Project 3.120 is using the maximum headrace between the upstream marginal point of the river bed gradient and the downstream tributary.

Meanwhile, Project 3.230B is planned in succession to upper Project 3.120 like a cascade, and the waterway route is arranged in the right side of the mountain, considering the plane curvature of the river. About 11.5 km of headrace tunnel, similarly, would lead the water to the underground powerhouse that is located about 14 km downstream from the dam.

Therefore, the layouts for their dam and powerhouse are reasonable from the point of view of using headrace, because both projects are planned in an area where we can make use of a steep riverbed gradient. The daily regulations of river flow that would enable peak generation with a small capacity reservoir in the dry season, are also reasonable from the point of view of effective use of river flow.

As well, peak generation by daily regulation coincides with the change of electric demand, and this benefit would contribute to increasing the worth of electricity for export. Therefore, their daily regulations are also reasonable from the point of view of operations.

9.2 Comparative Study of Alternative Development Plan

The development plan of Project 3.120 in Pre-F/S was formulated during the years 1992 to 1993 by a Norwegian consultant under the grant aid from UNDP and NORAD. Table 9.1 shows the generation features in Pre-F/S.

However, the F/S 1st Study Work in the Kingdom of Bhutan was executed in December, 1998, and has continued to the 6th Study Work.

So far, the fundamental survey requirements such as the collection of related data and documents, reconnaissance site survey, and sub contract work for topographical, geological and environmental investigations are completed.

Based on the result of the survey, the development plan has been proposed, after the comparative studies for generation layout, generation features and more were carried out.

The result of the comparative study, including the study for alternatives, is described below.

9.2.1 Fundamental Idea in the Study of Development Plan

The most important point in the study of the development plan is the economy of the project, and it is important to decrease the investment cost as much as possible for exporting the electricity. With both projects having very long tunnels (Project 3.120 : L≒6.4km, Project 3.230B : L≒11.5km), it can be said that the economy of the project depends especially on how the tunnel construction costs would be decreased. On this point, the length of the tunnel is the key to the project, and it can be said that the tunnel layout would decide the project layout.

In the case of a change from the original layout for Project 3.120, there is still no possibility that the position of the powerhouse would be shifted downstream of the original position considering the existence of the left side tributary (Pazachhu). That means that a change of layout for Project 3.120 would not influence Project 3.230B. There is, though, the possibility that the position of the powerhouse would be shifted upstream. In this case, a comparative study for alternatives would be made from the point of view of economy and necessary funds for construction.

On the other hand, since the catchment area of the left side tributary (Pazachhu) is big enough to act as an intake basin for Project 3.230B, it seems that the dam should be located downstream of the tributary. So, the original layout of Project 3.230B would be unchanged even if there would be left unused headrace between the two projects.

As mentioned before, the planning study for F/S of Project 3.120 would be made considering the change of layout and features of generation for the improvement of the economy of the original project of the Pre F/S, and, in this case, the study of Project 3.120 would be made independently from Project 3.230B.

9.2.2 Basic Matter for Study

(1) Topographical Map

At the stage of Pre-F/S, a 1/50,000 map (made in 1964) was mainly used for study, but for the area of the dam and powerhouse, 1/2,000 and 1/2,500 maps, newly surveyed, were partly used.

As well, in addition to obtaining a new 1/50,000 map (made in 1997) in the 1st Study Work, a 1/10,000 map was made in March,.1999, and a 1/5,000 map in January, 2000. The development plan has been re-studied according to the level of accuracy of the map.

Mapping work for the 1/1,000 map was finished in March, 2000, and that was used for a feasibility design of the adopted optimum development plan.

(2) Area Capacity Curve of Dam Reservoir

Fig.9.3 shows the Area Capacity Curve of the Dam Reservoir based on the 1/5,000 map.

According to the preliminary design of the dam, fundamentally, flushing of sediment material in the reservoir would be made by opening spillway gates at the dam crest. An effective reservoir capacity necessary for daily regulation should be guaranteed above the assumed sediment level considering the raise of the sediment level until level with the gate sill. In the Area Capacity Curve, the revised curve which shows the effective reservoir capacity decreased by sediment volume was also calculated and studied.

(3) River Flow Discharge

1) Low river flow

River flow discharge has been measured at Wangdi Rapids GS and was used for the estimation of river flow at the damsite. At present, a total of eight years data is available (1992~1999). Calculation of firm discharge was made using that data.

Firm Discharge: Firm discharge was defined as 95% (for more than 347 days a year) guaranteed discharge against the daily duration curve. (Qf=64.0 m^3/s: parallel average)

2) Flood discharge

Discharge design for care of the river was decided by the flood probability calculation (Gumbel method) based on the high river flow discharge data at the same GS. (QF=1,470 m^3/s: 5 years probability)

Flood discharge design for the spillway was also decided by taking the discharge estimated from PMF (QF=13,900 m^3/s) based on the analysis by GLOF and PMF.

(4) Reservoir Operation Plan

The daily regulation method was selected so as to enable peak generation according to the pattern of daily energy demand.

Generation features related to the reservoir operation plan are described below.

Peaking time (Tp)	:	Peaking time required in the balance of electric demand and supply, Tp = 4 hr, was assumed considering the real daily peak operation of the existing Chhukha Power Plant in the dry season (Fig. 9.4)
Maximum discharge (Qmax)	:	Maximum discharge would be set based on the peaked discharge for firm discharge (Qmax = Qf x 24hr/4hr, Tp = 4hr)
Firm peak output (Pfp)	:	Firm peak output is guaranteed within the peaking period (95% probability, Tp = 4hr)
Normal water level (NWL)	:	Intake water level in normal conditions, middle of draw down of reservoir (NWL = (HWL+LWL)/2)
Firm・Secondary energy (Ef·Es)	:	Firm energy is the energy during the peaking period and secondary energy the rest of the time. (Tp=4hr)

9.2.3 Method of Comparative Study

(1) Method of Comparative Study

Alternative plans for the optimization study of the development plan were made based on the method of comparative study below. Fig. 9.5 shows the flow chart of the development plan study.

1) Study of generation method・layout

- A dam and waterway type with daily regulating reservoir is the reasonable generation method suitable to the characteristics of the river, and study of no other alternative generation method is necessary.
- In case of a complete run-off river type that has no regulating reservoir, output of the power plant changes according to river discharge, and firm output would be very small

(Pf ≒ Pmax × 1/6). It follows that, the benefit of the power plant would decrease because of the decrease of kW value.

- Therefore, as far as we presuppose to construct a competitive power plant as the plant for exporting energy, it is not necessary to study the complete run-off river type.
- The proposed damsite is located in a reasonable position from a topographical and geological point of view, and study of no alternative damsite is necessary.
- Therefore, the dam axis was fixed at the stage of the development plan study, and the comparative study of the dam axis was made at the feasibility design stage.
- The proposed powerhouse is located at the furthest downstream position, considering the existence of the left side tributary (Pazachhu). Alternative sites for the powerhouse would be set upstream of the proposed position. The type of powerhouse selected would be an underground powerhouse, similarly.
- The proposed headrace tunnel (L=6,400m) is long, and its construction cost is a high percentage of the total cost. Therefore, it would be necessary to check the economy of an alternative layout case in which the powerhouse is shifted to an upstream position to lower tunnel construction cost.

2) Study of generation scale

- Maximum discharge is set based on the peak discharge for firm discharge assuming the required peaking time for demand is four hours. However, it would be necessary to check the economy of an alternative generation scale by changing Qmax.
- The dam height is set to guarantee the least reservoir capacity for daily regulation, set more than 70 m from the existing river bed by Area Capacity Curve considering sedimentation level. Therefore, it would not be necessary to check the economy of an alternative generation scale by changing the dam height, because a steep riverbed gradient would provide enough headrace.

(2) Economic Comparison by BC method

The method used for the evaluation of alternative development plans is the benefit cost method (BC method), considering that an alternative thermal power plant would be built without the Punatsangchhu Project, and taking the cost of a thermal power plant as the benefit of the project.

An alternative thermal power plant was assumed to have been constructed in the eastern part of India, supposed to mainly transmit the electricity of the Punatsangchhu Project.

A combination coal-fired thermal power plant and gas turbine was selected as an alternative thermal power plant. B-C was used as the fundamental index for judging the economy of the project. C is the equalized annual cost for hydro power, and B is considered the equalized cost of alternative thermal power that has same power ability as hydro power.

In addition to the index (B/C, B-C) from BC method, the present tariff for an existing power station was used as another index. (1.5 Nu/kWh in 1999) The generation features of an alternative thermal power plant for comparison study are listed in Table.9.2.

1) Annual cost (C)

The equalized annual cost of Punatsangchhu hydro power consists of depreciation, interest and operation-maintenance cost. This is estimated by multiplying the annual cost factor by the investment cost.

Equalized cost (C) = Depreciation + Interest + Operation-Maintenance Cost = Annual cost factor × Investment cost

Depreciation + Interest = Investment cost × Capital recovery factor

Capital recovery factor = $i(1+i)^n/((1+i)^n-1) = 0.10$

n : service life 50 years

i : discount rate 10%

Operation and Maintenance cost (rate to investment cost): 2%

Annual cost factor = 0.10 + 0.02 = 0.12 (12%)

Equalized cost (C) = 12% × Investment cost

2) Benefit (B)

The benefit of Punatsangchhu hydro power is summarized according to the fixed cost (Depreciation + Interest + Operation · Maintenance Cost) and Variable Cost (Fuel + Operation · Maintenance Cost) of an alternative thermal power plant and kW value. kWh value were calculated as shown in Table.9.2.

Effective power output and effective energy used in calculating the benefit are given according to the conditions below.

Effective power output: Effective power output at the receiving end is expressed by the equation below. This equation reduces station service rate by 0.3%, forced outage rate by 0.3%, scheduled outage rate by 2.0% and transmission loss rate by 3.0% from firm peak output.

Effective power output = (1-0.003)×(1-0.003)×(1-0.02)×(1-0.03) × Firm peak output

Effective energy: Effective energy at the receiving end is expressed by the equation below. This equation reduces station service rate by 0.3%, forced outage rate by 0.3%, scheduled outage rate by 2.0% and transmission loss rate by 2.0% from the average annual energy for an 8 year period.

Effective energy = (1-0.003)×(1-0.003)×(1-0.02)×(1-0.02)×Average annual energy

Benefit of hydro power would be calculated below.

B = Effective power output × kW value + Effective energy (firm) × kWh value (firm) + Effective energy (secondary) × kWh value (secondary)

= Effective power output × 147.45 $/kW + Effective energy (firm) × 0.017$/kWh + Effective energy (secondary) × 0.014$/kWh

(3) Estimation of Construction Cost

The condition for cost estimation is described below.

- Investment cost for project construction consists of preparatory works (relocation of existing road, access road, camp facility), civil works, hydraulic equipment, electro-mechanical equipment, transmission line, contingency, engineering- administration cost, land acquisition and interest during construction.
- Unit price for civil works, hydraulic equipment and cost of electro-mechanical equipment was roughly estimated based on the actual cost of other similar projects collected in the Kingdom of Bhutan. However, a part of the cost was estimated using costs in foreign countries including Japan. (cost estimation base in 2000)
- Quantities of civil works are roughly calculated based on the 1/5,000 map and the contingency rate was assumed 20% for preparatory and civil works cost, 10% for hydraulic equipment, electro-mechanical equipment and transmission line cost.
- Rate for engineering-administration cost was assumed 15% for preparatory and civil works cost, 10% for hydraulic equipment, electro-mechanical equipment and transmission line cost.
- As the investment cost at the development plan study stage, land acquisition cost and interest during construction were ignored and classification between local and foreign currency was not made, all was based on foreign currency.

(4) Energy Calculation

The reservoir operation method is to have a daily peak regulation for desired peaking time by using effective reservoir capacity. The capacity is based on firm discharge that is expected to arise with at least 95% probability. Daily energy calculations were made on the conditions below.

1) Calculation condition

①	River discharge at damsite	:	Qdam = QGS × 5,796km^2/5,640km^2 (1992~1999 year: daily)
②	River maintenance discharge from dam	:	Qm = 6.0m^3/s (every time)
③	Desired peaking time	:	Tp = 4 hr
④	Maximum discharge	:	Qmax
⑤	Effective head	:	He = normal water level − tail water level − head loss = NWL − TWL − hl = (HWL+LWL)/2 − TWL − hl
⑥	Installed capacity	:	Pmax = 9.8 × Qmax × He × η TG = 9.8 × Qmax × He × 89%

2) Energy calculation

①	Discharge for generation (Firm)	:	Qpf = (Qdam − 6) × 24/Tp (upper limit Qmax)
②	Discharge for generation (Secondary)	:	Qps = ((Qdam − 6) × 24 − Qpf × Tp)/(24 − Tp) (upper limit Qmax)
③	Overflow discharge from dam	:	Qo = ((Qdam − 6) × 24 − Qpf × Tp − Qps × (24 − Tp))/24
④	Output	:	P = 9.8 × Qpf (or Qps) × He × η TG
⑤	Energy (Firm)	:	Ef = P × Tf = P × 4hr (Tf = Tp)
⑥	Energy (Secondary)	:	Es = P × Ts = P × (24 − 4)hr
⑦	Firm peak output	:	Pfp (Peak output that is guaranteed with 95% probability)

9.2.4 Comparative Study of Alternative Development Plan

(1) Study of Generation Scale and Layout

Alternative development plans were prepared based on the idea described in 「**9.2.3 Method of Comparative Study**」 The table below shows study cases for comparative study. Fig. 9.6 shows generation layouts for study cases.

Generation type (dam and waterway type) and dam axis position were fixed for all cases. However, three powerhouse positions (upstream, middle, downstream) were checked and a comparative study of maximum discharge (Qmax : 200~375m^3/s) was made for each powerhouse position.

Study Cases for Comparative Study

	HWL (EL m)	Qmax (m^3/s)	Power House Position
Case 1~5	1,161	375,348,300,250,200	Downstream
Case 6~10	〃	〃	Middle stream
Case 11-15	〃	〃	Upstream

Table 9.3 and Fig. 9.7 shows the comparative study results

Every study case had relatively good economical results (B－C: 9.36~71.94 × $10^6$$, B/C: 1.13~1.64, unit construction cost per kWh: 1.06~1.35 Nu/kWh). Results of the comparative study for alternatives are summarized below.

- As to the powerhouse position, Cases 1~5 are more economical than the others.

  It seems to be more advantageous to make use of the full headrace as much as possible by putting the powerhouse downstream.

- It seems to be more advantageous to increase maximum discharge against the given reservoir capacity. However, it is presupposed that at least 4 hr is required for peaking time and study cases in which maximum discharge is greater than 348 m^3/s (Case 2) have less benefit because firm peak output would drop in the dry season and kW benefit decreases.

(2) Study of Peaking Time

The above-mentioned comparative studies were all made assuming peaking time at 4 hours.

Furthermore, comparative studies of peaking time were made for three cases (Case 1~3) including the selected optimum development plan case. (See Fig. 9.8)

The result of the study is that smaller peaking time gives better economy.

However it was judged reasonable to take peaking time at 4 hours because the existing Chhukha hydro power plant uses 4~5 hours operation in the dry season.

9.3 Optimum Development Plan

From an overall point of view, the development plan shown in the Table below (Case 2: Qmax=348 m^3/s, Pmax=884 MW) seems to be the optimum one, from the results of the comparative study above.

Punatsangchhu Hydro Power Project

Reservoir and Structures		
Reservoir effective volume		$4.24 \times 10^6 m^3$
Reservoir area		$0.53\ km^2$
Dam height (from foundation)		140 m
Dam volume		$924{,}000\ m^3$
Headrace tunnel length		6,860 m × 2
Headrace diameter		7.40 m
Underground powerhouse (B×H×L)		20 m × 38 m × 114 m
Development Plan		
Maximum discharge	Qmax	$348\ m^3/s$
Effective head	He	291.3 m
Installed capacity	Pmax	884 MW (147 MW × 6)
Annual Average Energy	E	4,395 GWh

Table 9.1 Power System Master Plan (Pre F/s)

Item	Unit	Project3.120	Project3.230B
Reservoir			
Catchment area	km^2	5797	6199
Annual mean inflow aveQdam	m^3/s	253.8	272.7
HWL	m	1110	823
LWL	m	1093	811
Available drawdown depth hd	m	17	12
Gross storage capacity Vg	10^6m^3	4.55	4.90
Effective storage capcity Ve	10^6m^3	2.80	3.00
Dam			
Type		Concrete Gravity	Concrete Gravity
Crest length Bcrest	m	160	200
Dam height from thalweg hdam	m	40	42
Dam height from foundation Hdam	m	58	54
Dam volume Vdam	m^3	84000	147000
Spillway			
Type of gate		Radial gate	Radial gate
Number of gate		3(high level) ,1(low level)	2(high level) ,4(low level)
Size of gate	m	B9.5×H9.5 , B12×H12.5	B10.5×H14 , B10.1×H8
Intake			
Type		Horizontal	Horizontal
Number of intake		3	3
Settling basin			
Type		Underground	Underground
Number of Settling basin		9	9
Headrace tunnel			
Type & Shape		Dtype/pressure	Dtype/pressure
Number of tunnel		1	1
D×L	m	B11.5×H16.2×L6400	B11.5×H16.2×L11500
Surge tank			
Type & Shape		Chamber type	Chamber type
Number of surge tank		1	1
Penstock			
Type & Shape		Embedded type	Embedded type
Number of penstock		5	5
D×L	m	D3.5×L390	D3.5×L365
Powerhouse			
Type & Shape		Underground	Underground
Number of unit		5	5
Size of powerhouse	m	B13×H32×L95	B13×H32×L95
Tailrace tunnel			
Type & Shape		Dtype/pressure	Dtype/pressure
Number of tunnel		1	1
D×L	m	B11.5×H16.2×L250	B11.5×H16.2×L350
Outlet			
Type		Horizontal	Horizontal
Number of outlet		1	1
Development plan		dam & waterway	dam & waterway
NWL	m	1110	823
TWL	m	830	563
Gross head Hg	m	280	260
Effective head He	m	270	252
Peaking time Tp	hr	4	4
Maximum discharge Qmax	m^3/s	324	325
Installed capacity Pmax	MW	760	690
Turbine type		Francis	Francis
Firm output Pf(continuous)	MW	125	135
Firm energy Ef	GWH	1125	1120
Secondary energy Es	GWH	2180	2100
Total energy Etotal	GWH	3305	3220
Construction period	year	7	9
Project cost(including transmission)	$10^6$$	506.3	573.8
Cost per KWH(at delivery point)	Usc/kwh	2.17	2.65

Table. 9.2 Alternative Thermal Power Plant for Comparison Study

Item	Unit	Coal Fired		Gas Turbine	
Installed Capacity	MW	900		100	
Annual Usage	hr	4900 (pf=56.0%)		2000 (pf=22.8%)	
Capital Cost	$/kW	900		380	
Service Life	Year	25		15	
Construction Period	Year	5		2	
Capital Recovery Factor		0.1102		0.1315	
Coal Consumption	kg/kWh	0.54		-	
Coal Cost	$/t	22.5		-	
Fuel Consumption	MJ/kWh	-		11	
Fuel Cost	$/GJ	-		6.4	
Discount Rate	%	10		10	
Annual Cost		Fixed Cost	Variable Cost	Fixed Cost	Variable Cost
Capital Recovery	$10^6$$	89.26 (*1)	0	5.00 (*5)	0
O&M・Administration Cost	$10^6$$	32.40 (*2)	8.10 (*3)	0.91 (*6)	0.23 (*7)
Fuel Cost	$10^6$$	0	53.58 (*4)	0	14.08 (*8)
Total	$10^6$$	121.66	61.68	5.91	14.31

Annual Cost at Receiving End		
kW Cost	$/kW	147.45 (*9)
Firm kWh Cost	$/kWh	0.017 (*10)
Secondary kWh Cost	$/kWh	0.014 (*11)

Adjustment Factor for kW & kWh

		Thermal Power Plant				Hydro Power Plant	
		Coal		Gas			
		kW	kWh	kW	kWh	kW	kWh
Transmission Loss Rate	%	0.0	0.0	0.0	0.0	3.0	2.0
Station Service Rate	%	8.0	9.0	5.0	5.0	0.3	0.3
Forced Outage Rate	%	3.0	-	10.0	-	0.3	0.3
Scheduled Outage Rate	%	8.0	-	8.0	-	2.0	2.0

kW adjustment factor (for Coal) = (1-0.03)x(1-0.003)x(1-0.003)x(1-0.02)/((1-0.08)x(1-0.03)x(1-0.08))
= 1.151

kW adjustment factor (for Gas) = (1-0.03)x(1-0.003)x(1-0.003)x(1-0.02)/((1-0.05)x(1-0.1)x(1-0.08))
= 1.201

kWh adjustment factor (for Coal) = (1-0.02)x(1-0.003)x(1-0.003)x(1-0.02)/(1-0.09)
= 1.049

kWh adjustment factor (for Gas) = (1-0.02)x(1-0.003)x(1-0.003)x(1-0.02)/(1-0.05)
= 1.005

(*1) : $900000x900x0.1102 = 89.26x10^6$

(*2) : $900000x900x0.05x0.8 = 32.40x10^6$

(*3) : $900000x900x0.05x0.2 = 8.10x10^6$

(*4) : $900000x4900x0.54x22.5/1000 = 53.58x10^6$

(*5) : $100000x380x0.1315 = 5.00x10^6$

(*6) : $100000x380x0.03x0.8 = 0.91x10^6$

(*7) : $100000x380x0.03x0.2 = 0.23x10^6$

(*8) : $100000x2000x11x6.4/1000 = 14.08x10^6$

(*9) : $(121.66x10^6+5.91x10^6)/(900000/1.151+100000/1.201) = 147.45$ $/kW (2000 base)

(*10) : $(61.68x10^6+14.31x10^6)/(900000x4900/1.049+100000x2000/1.005) = 0.017$ $/kWh (2000 base)

(*11) : $(61.68x10^6)/(900000x4900/1.049) = 0.014$ $/kWh (2000 base)

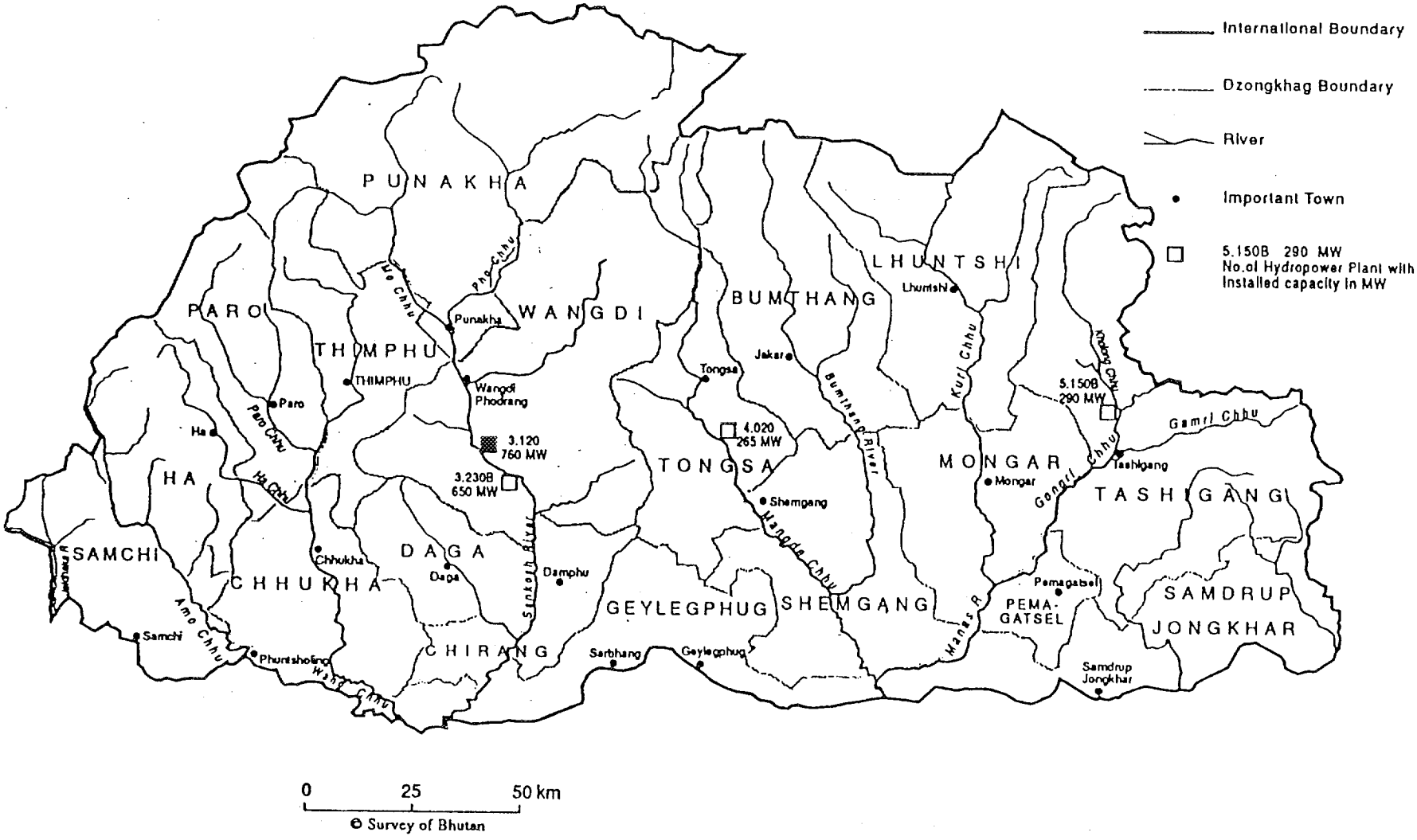

Fig. 9.1 Power System Master Plan in the Kingdom of Bhutan

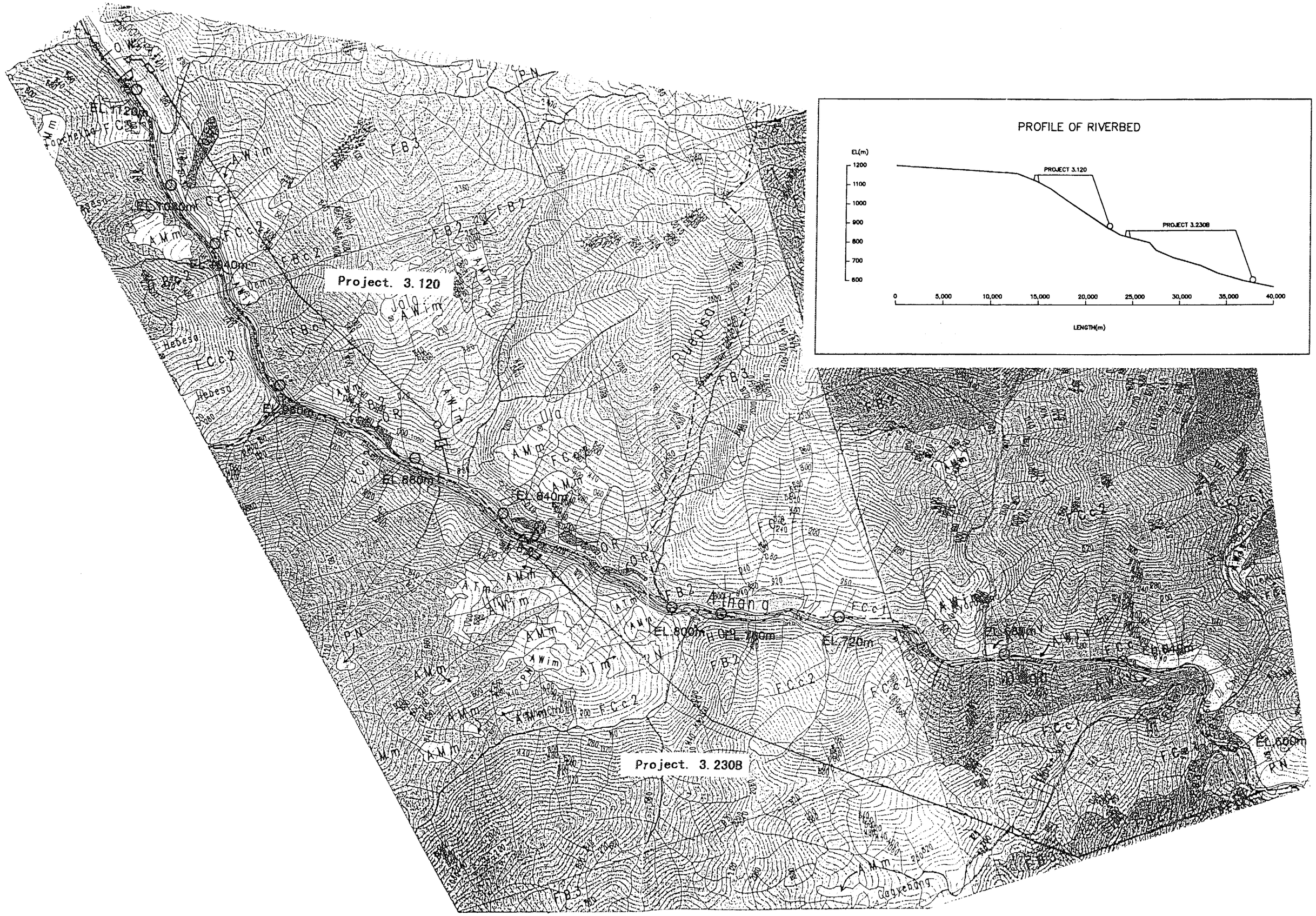

Fig. 9.2 Hydroelectric Power Development Project in Punatsangchuu

Table.9.3 Comparison Table for Alternative Development Plan

Item	Unit	Case1	Case2	Case3	Case4	Case5	Case6	Case7	Case8	Case9	Case10	Case11	Case12	Case13	Case14	Case15
Reservoir																
HWL	ELm	1,161	1,161	1,161	1,161	1,161	1,161	1,161	1,161	1,161	1,161	1,161	1,161	1,161	1,161	1,161
LWL	ELm	1,147	1,147	1,151	1,153	1,153	1,147	1,147	1,151	1,153	1,153	1,147	1,147	1,151	1,153	1,153
Available drawdown depth hd	m	14	14	10	8	8	14	14	10	8	8	14	14	10	8	8
Sedimentation level SWL	ELm	1,142	1,142	1,142	1,142	1,142	1,142	1,142	1,142	1,142	1,142	1,142	1,142	1,142	1,142	1,142
Gross storage capacity Vg	10^6m^3	12.59	12.59	12.59	12.59	12.59	12.59	12.59	12.59	12.59	12.59	12.59	12.59	12.59	12.59	12.59
Effective storage capcity Ve	10^6m^3	4.24	4.24	3.46	2.91	2.91	4.24	4.24	3.46	2.91	2.91	4.24	4.24	3.46	2.91	2.91
Dam																
Type	-	C.G	C.G	C.G	C.G	C.G	C.G	C.G	C.G	C.G	C.G	C.G	C.G	C.G	C.G	C.G
Crest length Bcrest	m	260	260	260	260	260	260	260	260	260	260	260	260	260	260	260
Dam height from thalweg hdam	m	74	74	74	74	74	74	74	74	74	74	74	74	74	74	74
Dam height from foundation Hdam	m	140	140	140	140	140	140	140	140	140	140	140	140	140	140	140
Dam volume Vdam	10^3m^3	924	924	924	924	924	924	924	924	924	924	924	924	924	924	924
Headrace																
Type	-	circular	circular	circular	circular	circular	circular	circular	circular	circular	circular	circular	circular	circular	circular	circular
Inner diameter D(v=4m/s)	m	7.7	7.4	6.9	5.6 , 6.9	5.6	7.7	7.4	6.2 , 7.6	6.3	4.6 , 6.5	6.9 , 8.5	6.7 , 8.2	6.9	6.3	4.6 , 6.5
Tunnel length L	m	2x6840	2x6860	2x6900	2x6950	2x7110	2x6100	2x6120	2x6160	2x6190	2x6410	2x3870	2x3860	2x3920	2x3960	2x4150
Penstock(main part)																
Type	-	shaft	shaft	shaft	shaft	shaft	shaft	shaft	shaft	shaft	shaft	shaft	shaft	shaft	shaft	shaft
Inner diameter D(v=7m/s)	m	5.8	5.6	5.2	4.2 , 5.2	4.2	5.8	5.6	4.6 , 5.7	4.7	3.4 , 4.9	5.2 , 6.3	5.0 , 6.1	5.2	4.7	3.4 , 4.9
Penstock length L	m	2x451	2x453	2x459	2x455	2x452	2x389	2x391	2x399	2x385	2x398	2x350	2x350	2x359	2x363	2x366
Power house																
Position	-	downstream	downstream	downstream	downstream	downstream	middle	middle	middle	middle	middle	upstream	upstream	upstream	upstream	upstream
Number of unit	unit	6	6	6	5	4	6	6	5	4	3	5	5	4	4	3
Tailrace(main part)																
Type	-	circular	circular	circular	circular	circular	circular	circular	circular	circular	circular	circular	circular	circular	circular	circular
Inner diameter D(v=4m/s)	m	7.7	7.4	6.9	5.6 , 6.9	5.6	7.7	7.4	6.2 , 7.6	6.3	4.6 , 6.5	6.9 , 8.5	6.7 , 8.2	6.9	6.3	4.6 , 6.5
Tunnel length L	m	2x381	2x381	2x381	2x361	2x342	2x224	2x224	2x204	2x184	2x182	2x717	2x717	2x698	2x698	2x695
Development plan																
NWL	ELm	1,154	1,154	1,156	1,157	1,157	1,154	1,154	1,156	1,157	1,157	1,154	1,154	1,156	1,157	1,157
TWL	ELm	845	845	845	845	845	890	890	890	890	890	935	935	935	935	935
Gross head Hg	m	309	309	311	312	312	264	264	266	267	267	219	219	221	222	222
Effective head He	m	291.8	291.3	292.6	292.4	290.3	248.7	248.3	249.6	249.5	247.6	207.7	207.4	209.0	209.3	208.0
Loss of head hl	m	17.2	17.7	18.4	19.6	21.7	15.3	15.7	16.4	17.5	19.4	11.3	11.6	12.0	12.7	14.0
Peaking time Tp	hr	4.0	4.0	4.0	4.0	4.0	4.0	4.0	4.0	4.0	4.0	4.0	4.0	4.0	4.0	4.0
Maximum discharge Qmax	m^3/s	375	348	300	250	200	375	348	300	250	200	375	348	300	250	200
Installed capacity Pmax	MW	954	884	766	638	506	813	754	653	544	432	679	630	547	456	363
Firm peak output Pf	MW	887	871	766	638	506	756	743	653	544	432	631	620	547	456	363
Firm energy Ef	Gwh	1,383	1,288	1,118	931	739	1,179	1,098	954	794	631	984	917	798	666	530
Secondary energy Es	Gwh	3,201	3,107	2,951	2,731	2,441	2,728	2,648	2,517	2,330	2,082	2,278	2,212	2,108	1,955	1,749
Total energy Etotal	Gwh	4,584	4,395	4,069	3,662	3,180	3,907	3,746	3,471	3,124	2,713	3,262	3,129	2,906	2,621	2,279
Economic evaluation																
Project cost (price in 2000 year)	$10^6$$	974	932	858	777	705	897	864	795	726	659	804	779	723	666	610
Unit construction cost per kw (*1)	$/kw	1,021	1,054	1,120	1,219	1,393	1,103	1,146	1,218	1,334	1,525	1,184	1,236	1,322	1,461	1,680
	Nu/kw	40,843	42,171	44,802	48,741	55,706	44,114	45,822	48,724	53,350	61,007	47,375	49,453	52,867	58,425	67,208
Unit construction cost per kwh (*2)	$/kwh	0.03	0.03	0.03	0.03	0.03	0.03	0.03	0.03	0.03	0.03	0.03	0.03	0.03	0.03	0.03
	Nu/kwh	1.07	1.07	1.06	1.07	1.11	1.15	1.16	1.15	1.17	1.22	1.24	1.25	1.25	1.28	1.35
B1(kw value)	$10^6$$	123.58	121.35	106.72	88.89	70.50	105.33	103.52	90.98	75.79	60.19	87.91	86.38	76.21	63.53	50.58
B2(kwh value)	$10^6$$	65.23	62.43	57.58	51.61	44.62	55.59	53.21	49.12	44.03	38.07	46.41	44.45	41.12	36.94	31.98
B/C	-	1.62	1.64	1.60	1.51	1.36	1.50	1.51	1.47	1.38	1.24	1.39	1.40	1.35	1.26	1.13
B-C	$10^6$$	71.92	71.94	61.35	47.21	30.56	53.33	53.08	44.65	32.75	19.19	37.83	37.36	30.58	20.54	9.36

*1: Unit construction cost per kw = Project cost/Pmax
*2: Unit construction cost per kwh = Project cost*Annual cost ratio / (Effective annual average energy)
= Project cost * 12% / (Annual average energy *(1-0.02)*(1-0.003)*(1-0.003)*(1-0.02))

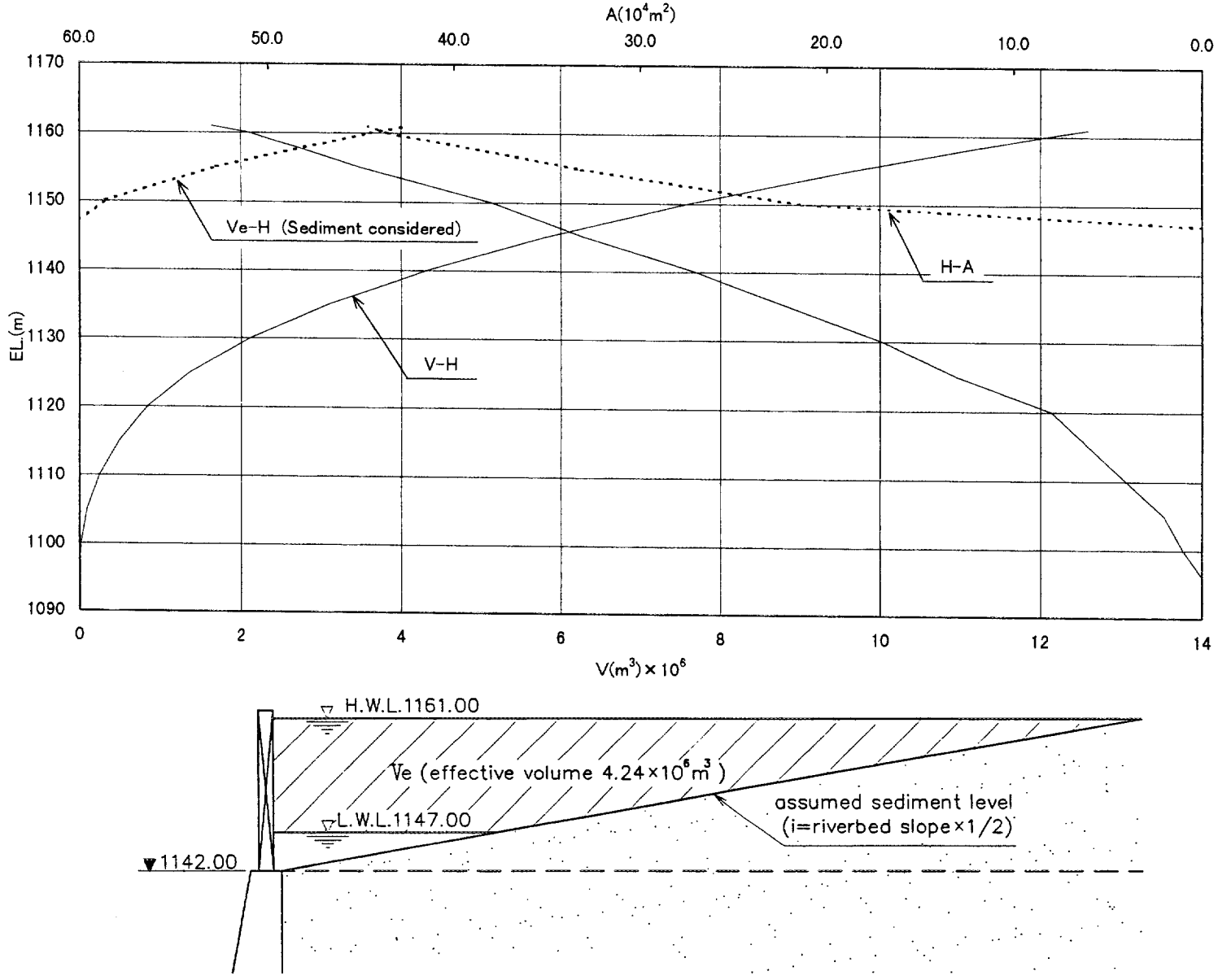

Fig. 9.3 Area-Capacity Curve of Dam Reservoir
(Original Dam Axis : Development Plan Study)

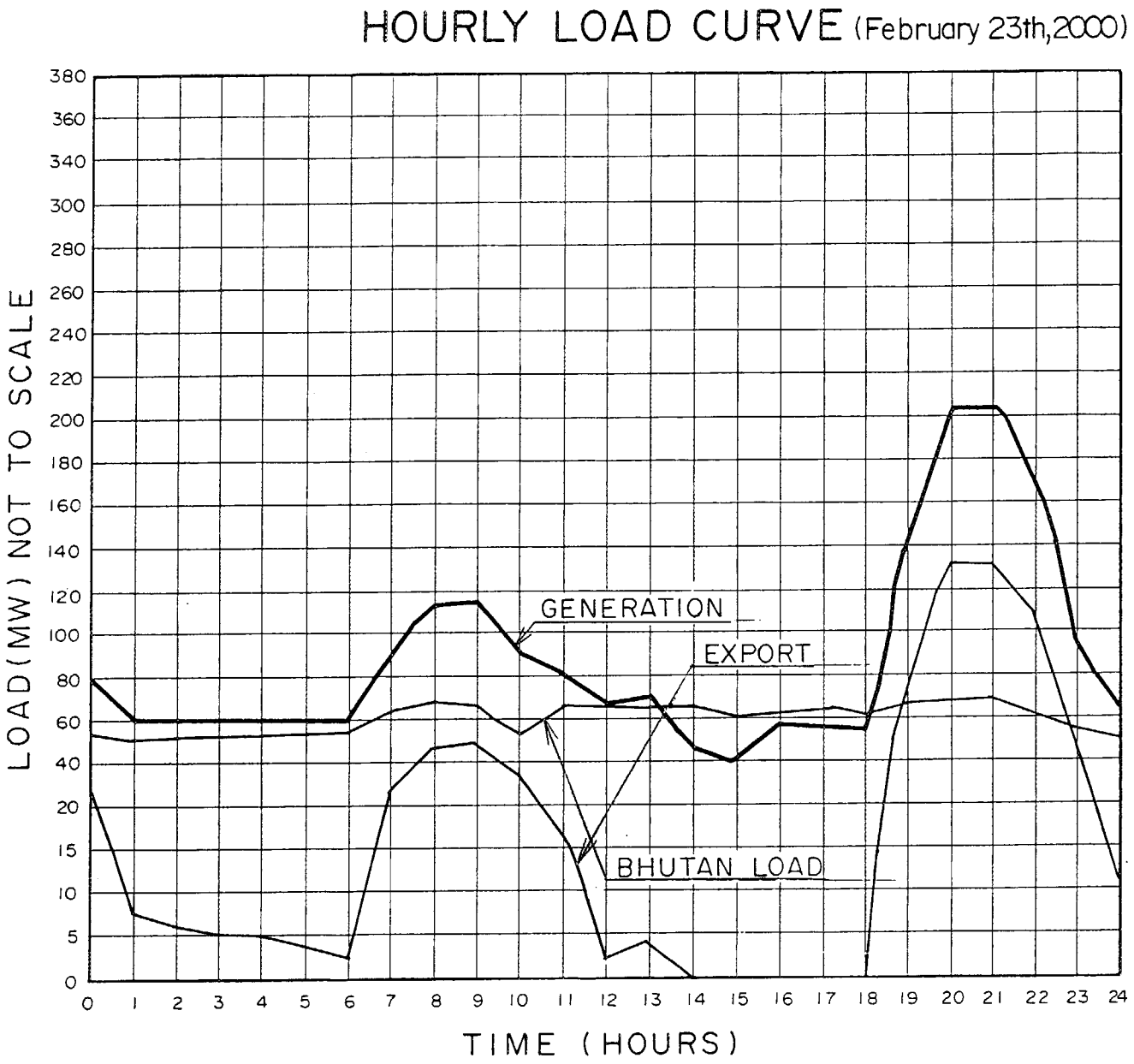

Fig. 9.4 Hourly Load Curve of Chhukha Power Plant (1/4)

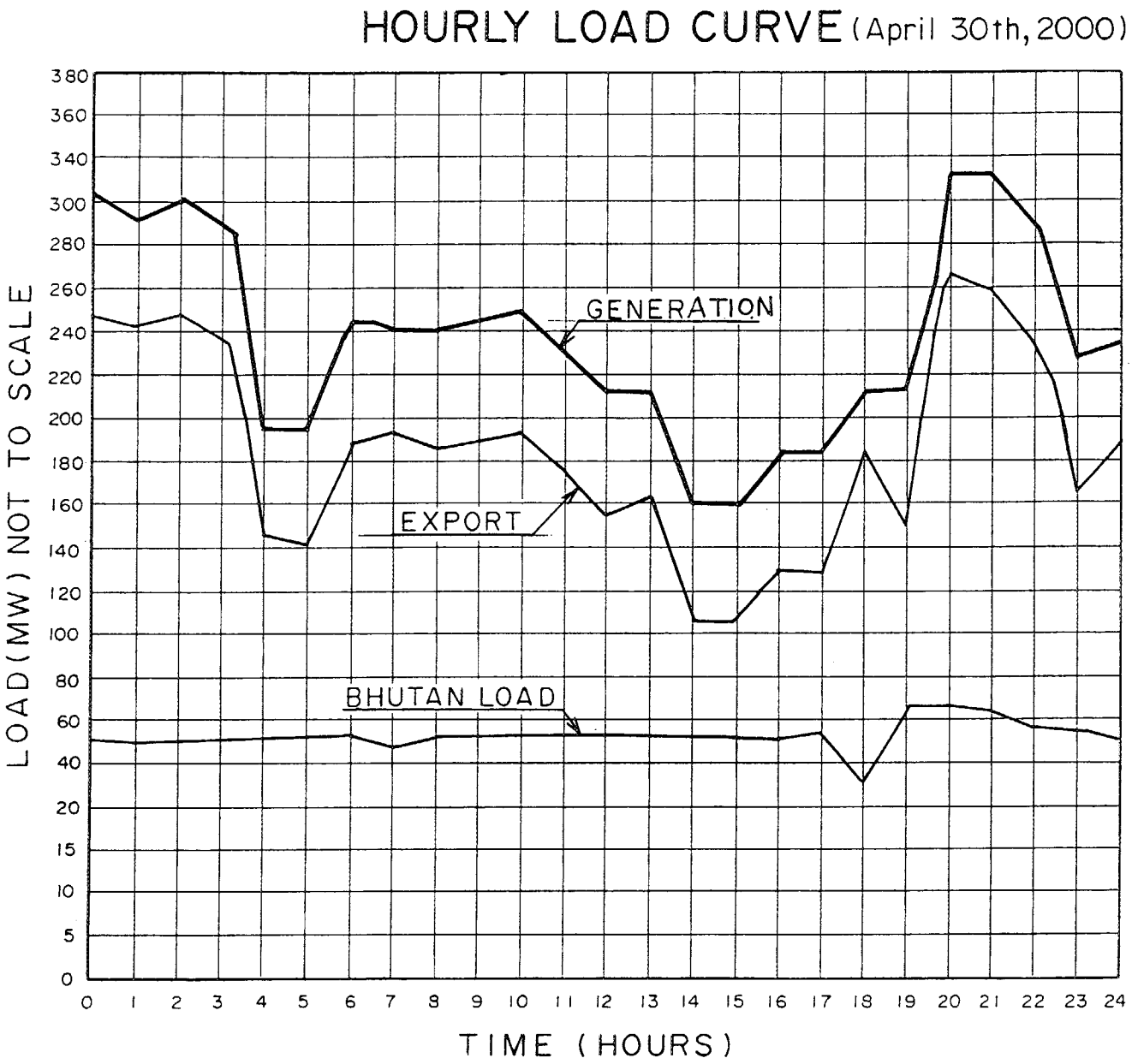

Fig. 9.4 Hourly Load Curve of Chhukha Power Plant (2/4)

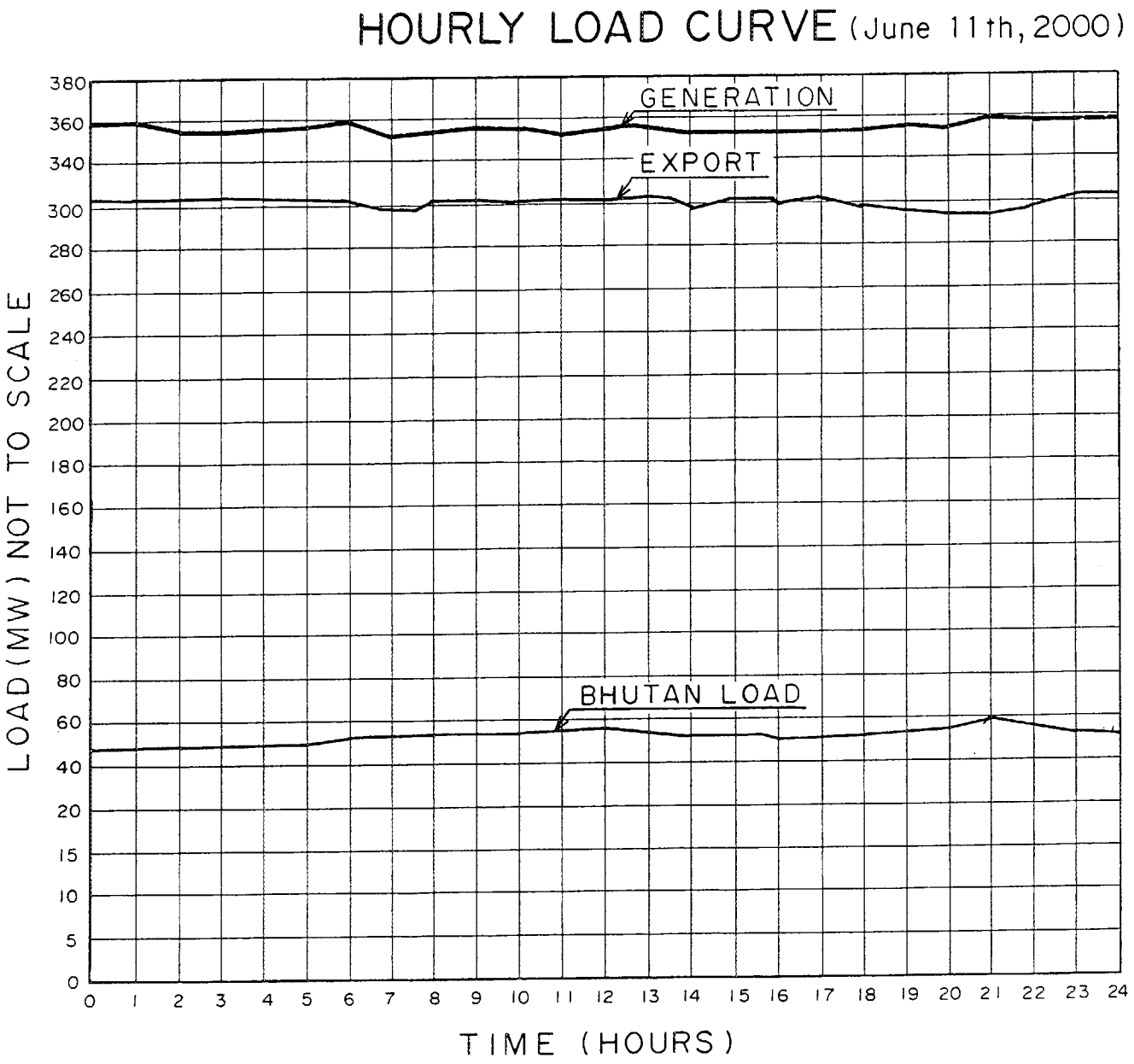

Fig. 9.4 Hourly Load Curve of Chhukha Power Plant (3/4)

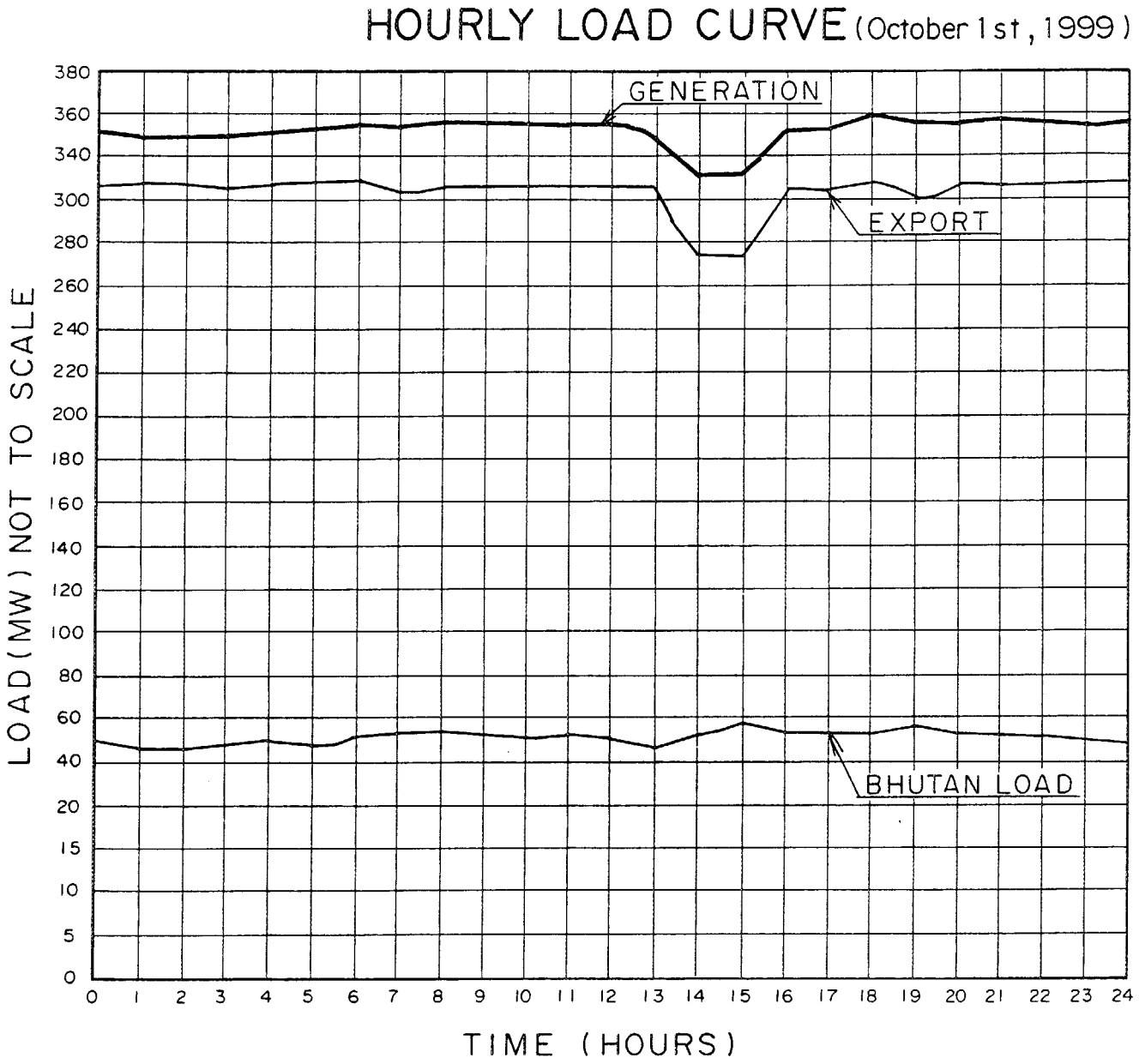

Fig. 9.4 Hourly Load Curve of Chhukha Power Plant (4/4)

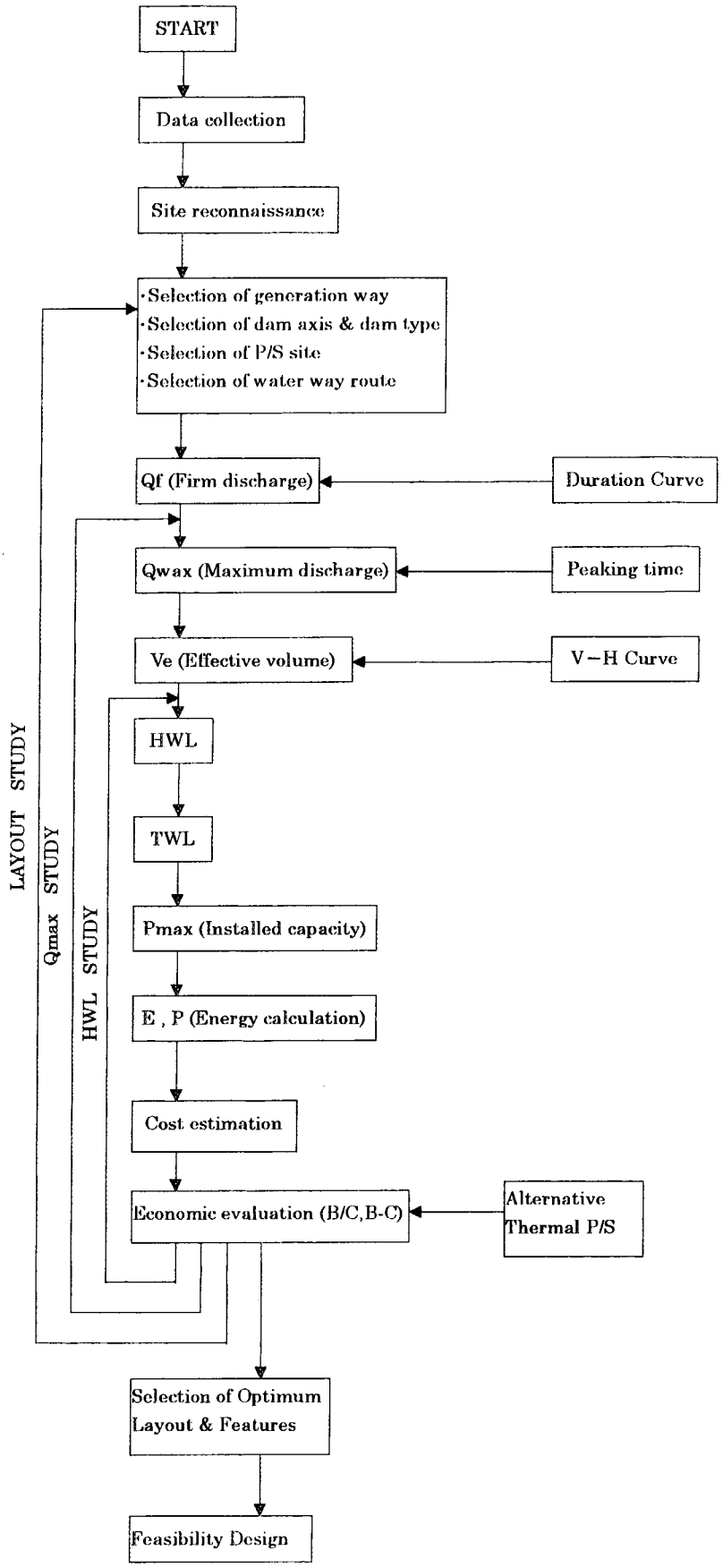

Fig.9.5 Flow Chart of Development Plan Study

Plan

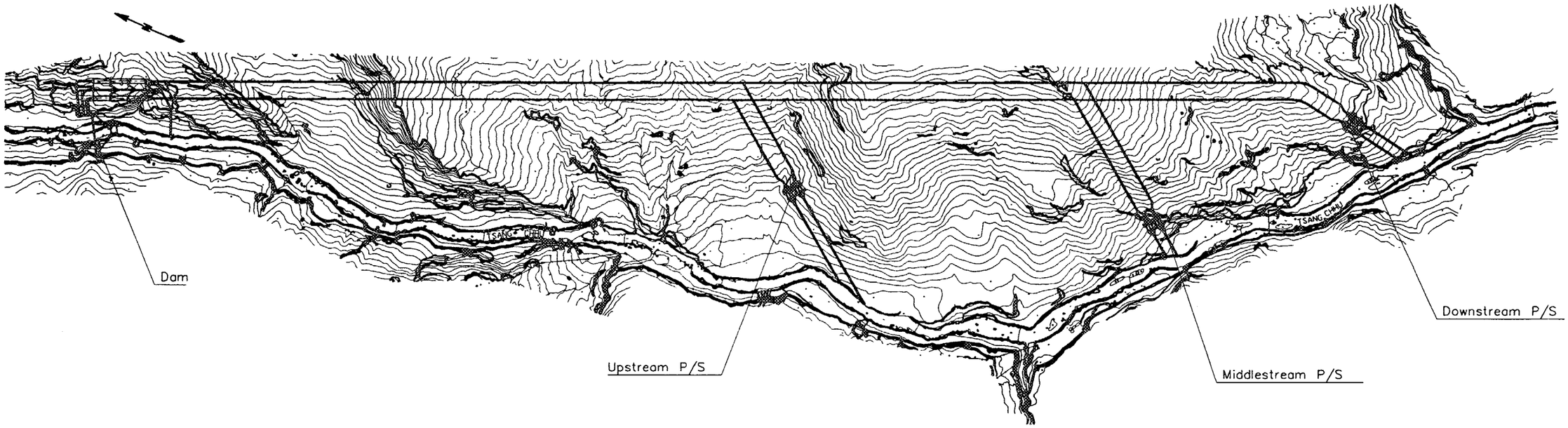

Profile

CASE 1 – 5 (Downstream P/S)

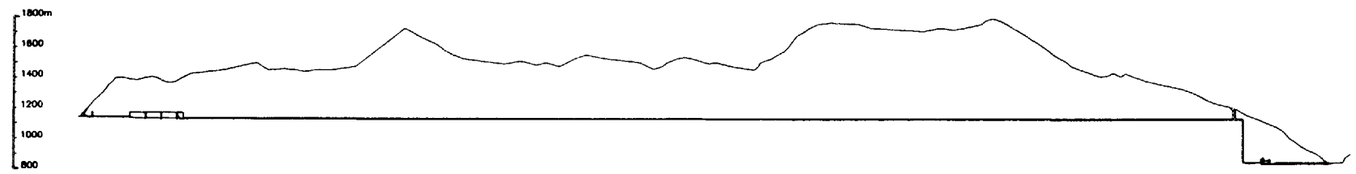

CASE 6 – 10 (Middlestream P/S)

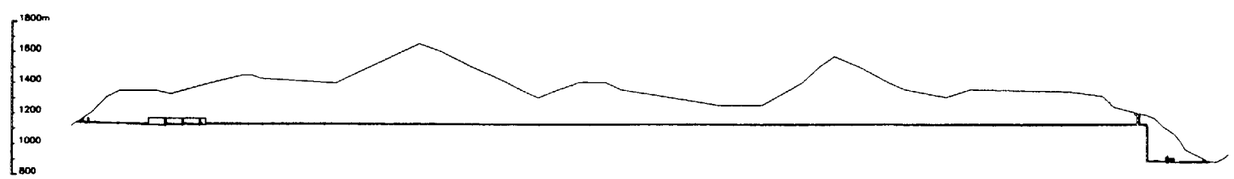

CASE 11 – 15 (Upstream P/S)

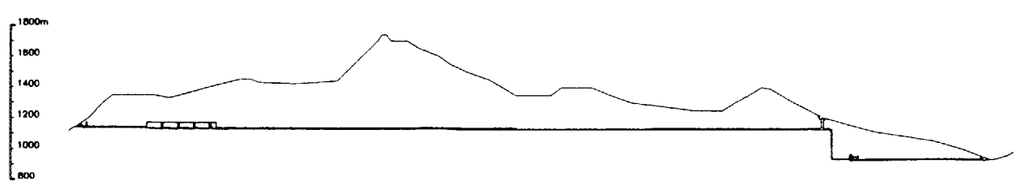

PUNATSANGCHHU HYDROPOWER PROJECT	
GENERAL LAYOUTS FOR COMPARATIVE STUDY	
Fig. 9.6	

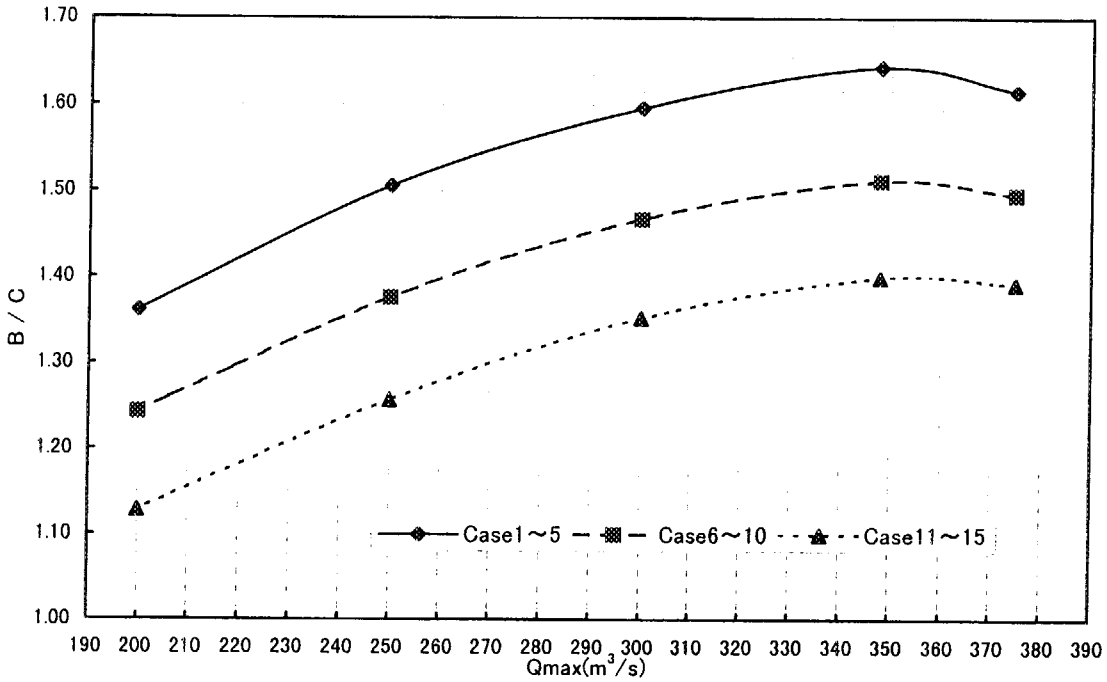

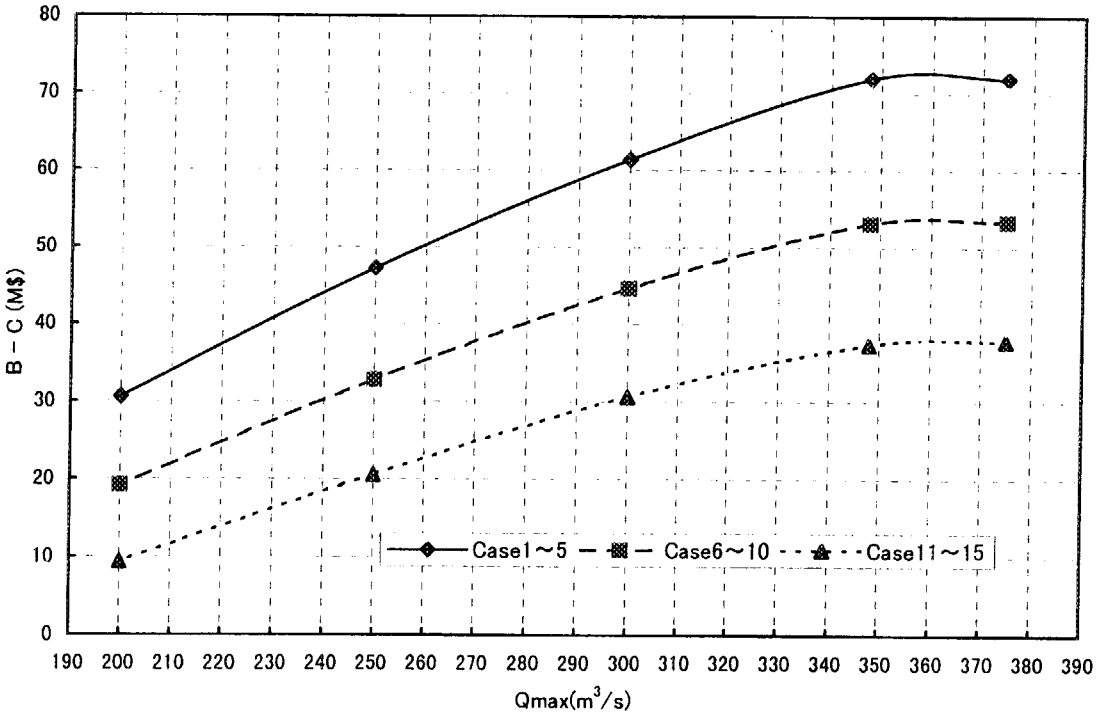

Fig. 9.7 Comparative Study of Development Scale Examination (Qmax for Case 1～15) (1/2)

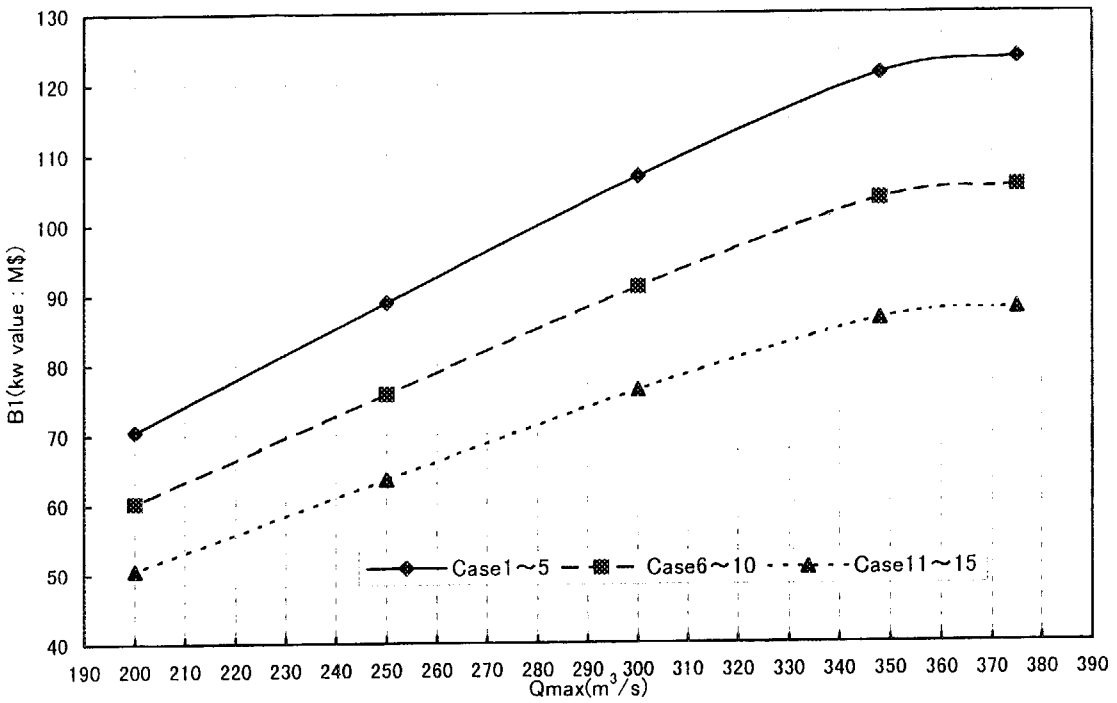

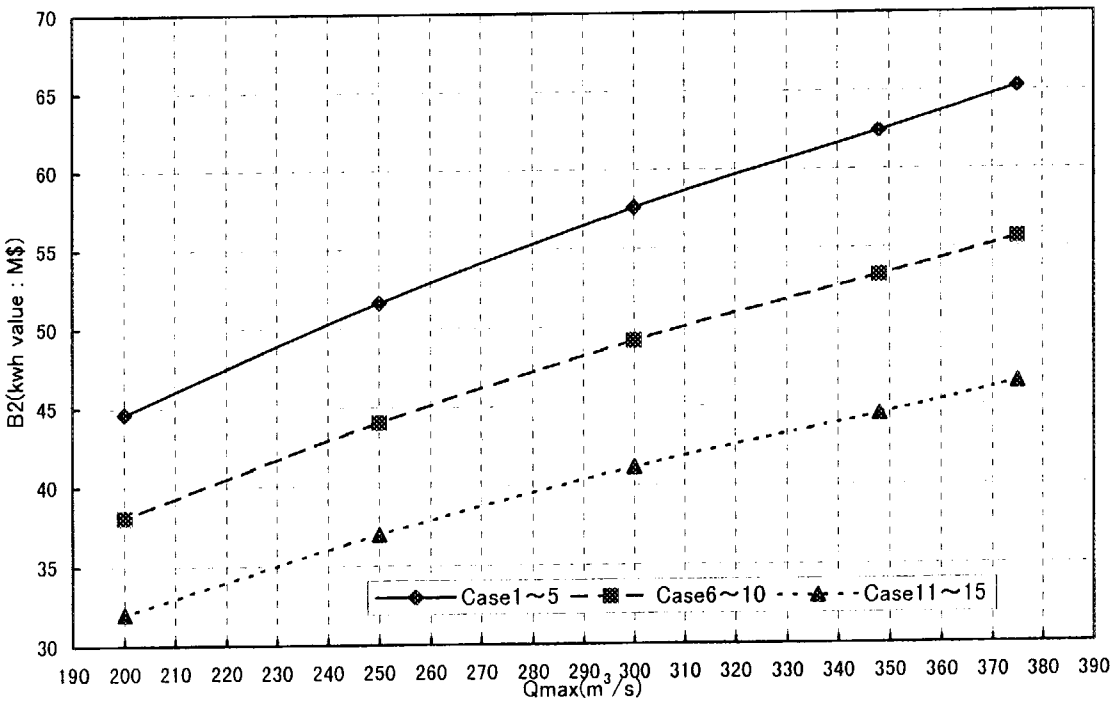

Fig. 9.7 Comparative Study of Development Scale Examination (Qmax for Case 1～15) (2/2)

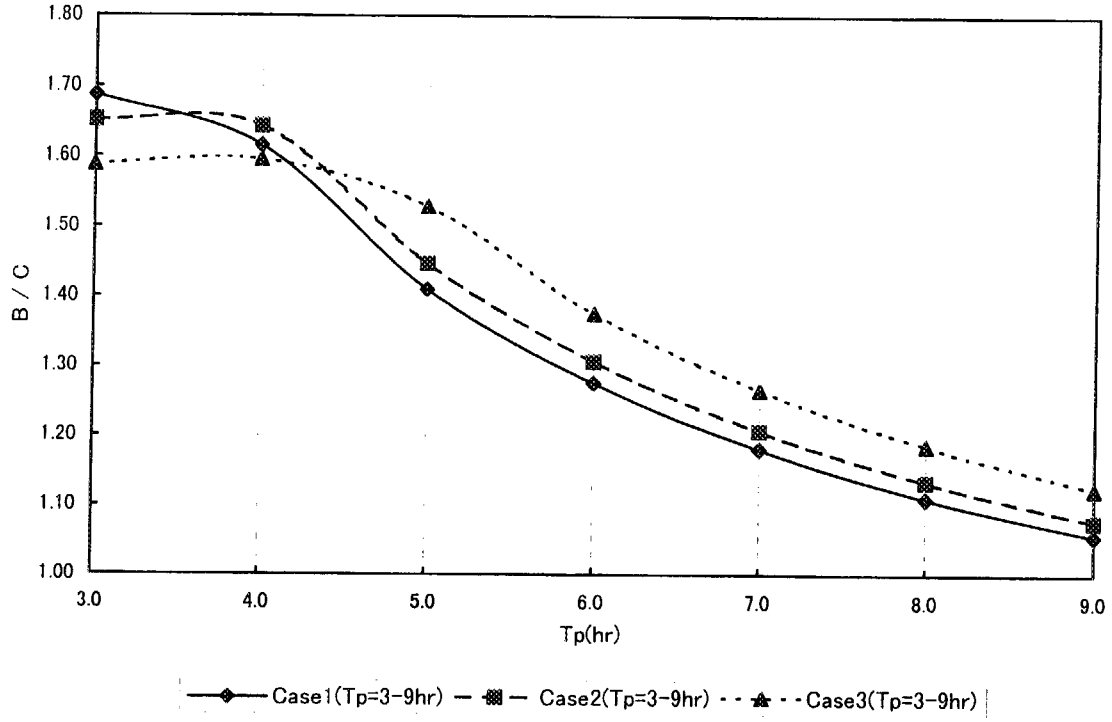

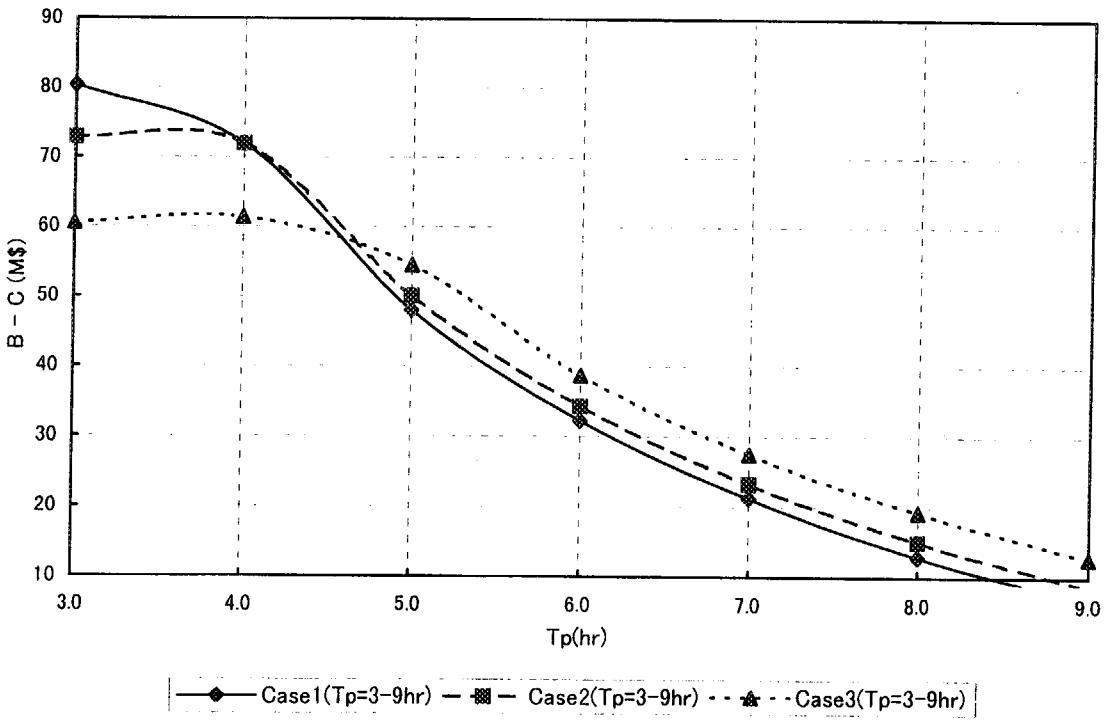

Fig. 9.8 Comparative Study of Required Peaking Time (Tp for Case 1～3)